Fall 12-2013

# Design and Synthesis of Flexible and Functional Polybenzoxazine Thin Films

Austin David Baranek
*University of Southern Mississippi*

The University of Southern Mississippi

# DESIGN AND SYNTHESIS OF FLEXIBLE AND FUNCTIONAL POLYBENZOXAZINE THIN FILMS

by

Austin David Baranek

Abstract of a Dissertation
Submitted to the Graduate School
of The University of Southern Mississippi
in Partial Fulfillment of the Requirements
for the Degree of Doctor of Philosophy

December 2013

ABSTRACT

DESIGN AND SYNTHESIS OF FLEXIBLE AND FUNCTIONAL POLYBENZOXAZINE THIN FILMS

by Austin David Baranek

December 2013

Polybenzoxazines offer the unique ability to incorporate a variety of properties and functionality into a single polymer network through simple synthetic techniques. However, within benzoxazine materials exist certain drawbacks of which brittleness is the primary issue when exploring thin film applications. This brittleness leads to poor mechanical stability and would reduce the lifetime of any device sought after. It is, however, through the simplistic nature of the benzoxazine monomer synthesis that the mechanical stability could be addressed chemically, avoiding the complications of using rubber toughening agents or plasticizers. The monomer synthesis offers tailorability of both the phenol and amine to incorporate almost any functionality into a polybenzoxazine through either commercial or synthetic sources.

In this dissertation, the modification of benzoxazine monomers using various starting materials in an effort to improve the physical properties and incorporate unique functionality into benzoxazine networks is described. In the first study, flexible benzoxazine networks were designed by first incorporating long aliphatic linkers between a diphenol to which a bisbenzoxazine monomer can be synthesized via the Mannich condensation reaction. The intent of this project is to incorporate flexibility directly into the monomer, and thus the network, creating a less brittle material without the need for additives. The second project focuses on simplifying the tailorability of these materials

by utilizing copolymers of compatible bisbenzoxazine monomers. Ultimately, copolymers of compatible monomers allow improved versatility for tailoring network properties (i.e., thermomechanical) without extensive monomer synthesis. The third and final project highlights the chemical versatility of polybenzoxazines by designing flexible networks containing quaternizable amines. Following the polymerization, modification of the network through simple alkylation chemistry affords a polyelectrolyte network capable of conducting ions. The projects mentioned above center around the versatility in both the monomer and polymer synthesis and show the potential for utilization in a variety of areas.

The University of Southern Mississippi

# DESIGN AND SYNTHESIS OF FLEXIBLE AND FUNCTIONAL POLYBENZOXAZINE THIN FILMS

by

Austin David Baranek

A Dissertation
Submitted to the Graduate School
of The University of Southern Mississippi
in Partial Fulfillment of the Requirements
for the Degree of Doctor of Philosophy

Approved:

Derek L. Patton
Director

Daniel A. Savin

Jeffrey S. Wiggins

Robson F. Storey

Charles L. McCormick

Susan A. Siltanen
Dean of the Graduate School

December 2013

# DEDICATION

This dissertation is dedicated to my family, especially to the members who are no longer with us today (RT, LT, JB).

# ACKNOWLEDGMENTS

I would first like to acknowledge my family for supporting me during graduate school. Specifically, I would like to mention my parents, Mike and Mary Baranek, and my brother Erik Baranek. I would also like to thank my close friends and roommates Chris Holley and Josh Hanna and my cousin Jesse Payant.

I would like to acknowledge my advisor Dr. Derek L. Patton for his guidance and support throughout my graduate career. His passion for science and hard work has inspired me to work hard to achieve my goals. I would also like to acknowledge my other committee members, Charles McCormick, Jeffrey Wiggins, Robson Storey, Kenneth Mauritz, and Daniel Savin for the aide and support they have given me during my time spent at USM.

I'd like to thank the PSRC staff, specifically Ms. Jody Wiggins, for helping make everything non lab-related run smoothly.

A special thanks to the Patton Research Group for making lab work exciting and for continuously challenging me to become a better researcher and person. Specifically, I would like to thank Laken Kendrick for all the hard work she has done for me over the years.

TABLE OF CONTENTS

LIST OF TABLES

Table

LIST OF ILLUSTRATIONS

Figure

LIST OF SCHEMES

Scheme

# LIST OF ABBREVIATIONS

| | |
|---|---|
| $E_a$ | activation energy |
| AEM | anion-exchange membrane |
| Å | angstrom |
| AFM | atomic force microscopy |
| BZ | benzoxazine |
| BA | butylamine |
| $CO_2$ | carbon dioxide |
| $^{13}$C-NMR | carbon-NMR |
| °C | centigrade |
| $\rho_x$ | cross-link density |
| DI | deionized |
| $\rho$ | density |
| $(CD_3)_2CO$ | deuterated acetone |
| $CDCl_3$ | deuterated chloroform |
| $CH_2Cl_2$ | dichloromethane |
| DSC | differential scanning calorimetry |
| DMEDA | dimethylethylene diamine |
| DMF | dimethylformamide |
| DMA | dynamic mechanical analysis |
| EtOH | ethanol |
| ETFE | ethylene tetrafluoroethylene |
| FEP | fluorinated ethylene propylene |

| | |
|---|---|
| FTIR | fourier transform infrared |
| FG | functional group |
| R | gas constant |
| Ge | germanium |
| $T_g$ | glass transition temperature |
| g | gram |
| gATR-FTIR | grazing angle attenuated total reflection –FTIR |
| h | hour |
| HCl | hydrochloric acid |
| $CH_3I$ | iodomethane |
| IEC | ion-exchange capacity |
| L | liter |
| E'' | loss modulus |
| $MgSO_4$ | magnesium sulfate |
| MHz | megahertz |
| MPa | megapascal |
| MCPBA | metachloroperoxybenzoic acid |
| m | meter |
| mS | millisiemens |
| min | minute |
| $M_c$ | molecular weight between cross-links |
| $N_2$ | nitrogen |
| NMR | nuclear magnetic resonance |

| | |
|---|---|
| ppm | parts per million |
| $\gamma$ | poisson's ratio |
| PBI | polybenzimidazole |
| pBZ | polybenzoxazine |
| PVA | polyvinyl alcohol |
| KBr | potassium bromide |
| KCl | potassium chloride |
| $K_2CO_3$ | potassium carbonate |
| KOH | potassium hydroxide |
| PEMFC | proton exchange membrane fuel cell |
| $^1$H-NMR | proton-NMR |
| RH | relative humidity |
| ROP | ring opening polymerization |
| rt | room temperature |
| s | second |
| $NaHCO_3$ | sodium bicarbonate |
| NaCl | sodium chloride |
| NaOH | sodium hydroxide |
| $Na_2S_2O_5$ | sodium metabisulfite |
| E’ | storage modulus |
| SPEEK | sulfonated poly(ether ether ketone) |
| T | temperature |
| TGA | thermogravimetric analysis |

| | |
|---|---|
| $H_2O$ | water |
| w/w | weight ratio |

# CHAPTER I

# INTRODUCTION

## *Phenolic Resins*

Traditional phenolic resins were first used in the early twentieth-century and are considered to be the first class of fully synthetic polymers to achieve commercial success. Phenolic materials have also found extensive commercial use in a variety of applications including adhesives, coatings, composites, dispersions, foams, foundry resins, molding compounds, plywood, and fiber board.[1-3]

While conventional phenolic resins have key advantages in the areas of thermal and chemical resistance, they have traditionally been associated with a number of shortcomings, including brittleness, volatile release upon cure, and the need for strong acid as a polymerization catalyst. Thus, conventional phenolic resins provide numerous challenges in the areas of synthesis, production, product development, and quality control.[2, 3]

## *Polybenzoxazines*

Benzoxazine monomers are heterocyclic compounds that are quickly growing in the electronics, aerospace, and other industries as an attractive alternative to traditional phenolic resins. The synthesis of benzoxazines dates back nearly 70 years with Holly and Cope first reporting the synthesis in 1944.[4] Throughout the 50's, 60's and 70's, individuals such as Burke and Schreiber significantly contributed to the fundamental understanding and exploratory implementation of benzoxazine chemistry.[5-13] However, it was not until the 1980's when Higgenbottom first developed multifunctional benzoxazine monomers, that the formation of cross-linked polybenzoxazine networks was allowed.[14-16] In the subsequent years to the present, the majority of the research focused on

understanding and exploring the capabilities of benzoxazines through a variety of synthetic and processing techniques.

Initially polybenzoxazines were thought of as being potential replacements for traditional phenolic resins since the ring-opening approach should eliminate many of the shortcomings associated with the condensation chemistry approach. Today, however, polybenzoxazines are not only considered as suitable replacements for phenolics but are a class its own, as material that can outperform epoxies and bismaleimides.[17] This is due to the numerous properties polybenzoxazines posses that extend far beyond traditional phenolic resins including: near zero shrinkage during cure, no by-product during cure, high char yield, fast development of mechanical properties relative to cure as well as a glass transition temperature ($T_g$) higher than the cure temperature, good electrical properties, and low water absorption. Additionally, with the variety of inexpensive starting material, polybenzoxazines offer a unique design flexibility unattainable to other phenolics.

Furthermore, Ishida and Allen[18] have reported that the network properties of polybenzoxazines are largely regulated by the chemical cross-linking density as well as hydrogen bonding. The role of the hydrogen bonding is of great importance in the interpretation of a variety of structure-property relationships and is also shown in the work by Ishida and Sander.[19, 20]

*Monomer synthesis*

The basic synthesis of benzoxazine monomers consists of a phenolic derivative, formaldehyde, and a primary amine shown in Scheme 1 where R and R' are open to a variety of functionalities. With the utilization of bis structure shown in the bottom of Scheme 1, both R and R' remain tailorable. Scheme 2 shows the proposed mechanism in

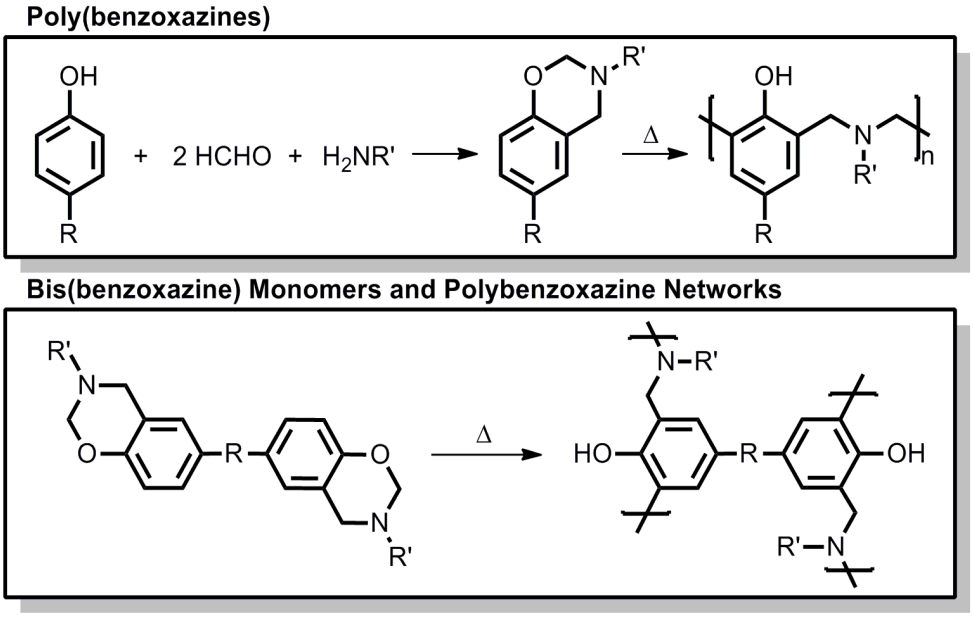


*Scheme 1*. General benzoxazine monomer synthesis and polymerization for mono and bis substituted monomers.

the formation of the oxazine ring, showing that the amine reacts with formaldehyde to rapidly generate the intermediate aminomethylol group, that can further react to form a 1,3,5-triaza compounds. With time the triaza reacts with phenol and formaldehyde to form the oxazine ring. The monomer synthesis consists of a variety of methods including homogeneous or heterogeneous solutions or even melt or high solid methods, all of which have advantages and disadvantages depending on the raw materials and the reaction conditions (temperature-time) desired. Specifically, for solution reactions, the solvent has a profound effect in the yield of forming the benzoxazine ring. The general observation is that solvents with lower dielectric constants provide the highest yield where solvents such as dioxane, chloroform, dichloromethane and xylenes are usually excellent solvents for benzoxazine synthesis.[21] Other factors that can also strongly influence the formation of the oxazine ring include the nature and position of substitutes on the phenol, reaction ratios, temperature, and the basicity of the amine. All of these must be accounted for to successfully synthesize a benzoxazine. However, other than the

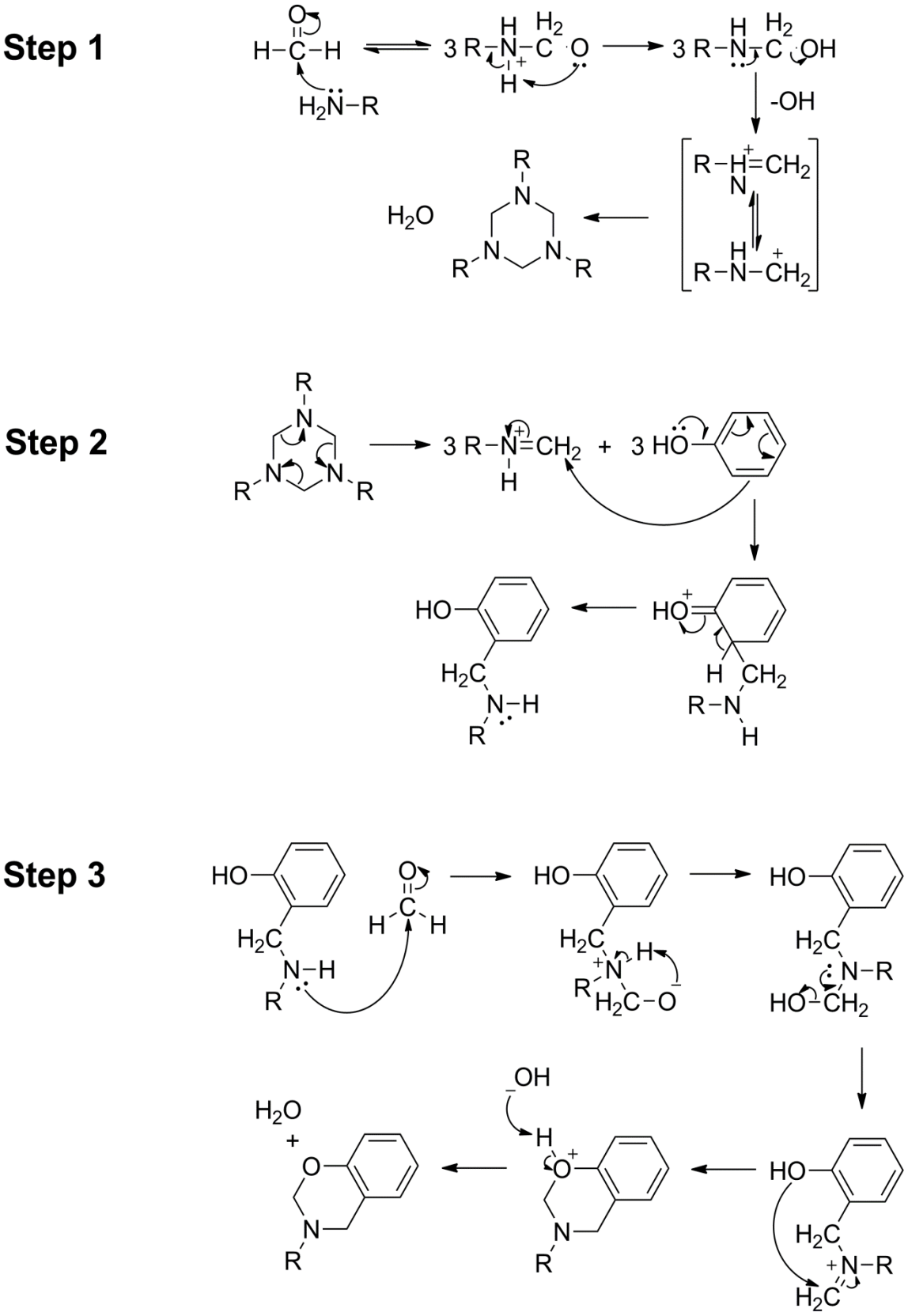


*Scheme 2*. Mechanism for benzoxazine monomer synthesis.

benzoxazine, common by-products include bis(2-Hydroxybenzyl) amine, and free bases, depending on the condensation conditions and the specific reactants used. In most cases, these impurities require removal prior to polymerization as they may greatly affect material properties or even polymerization kinetics.

The molecular design flexibility allows the opportunity to logically structure benzoxazine resins with unprecedented tailorability in polymer properties. However, the complex reaction occurring during the synthesis of the monomers makes studying them difficult. Since the beginning, great strides have been made from a controlled, laboratory synthesis of benzoxazine in homogeneous and heterogeneous solutions at modest to low concentrations to more high solid or melt systems that are much more practical for large scale synthesis

*Molecular design of benzoxazines*

This dissertation demonstrates the versatility of the benzoxazine synthesis and explores a variety of chemical structures that influence material properties and broaden functionality. The research herein investigates a variety of diphenol and amine structures to broaden the functionality of benzoxazines. Current research focuses on reducing the temperature required for cure, increasing processability, and improving the mechanical properties of the thermoset resins, all of which can be achieved through molecular design. Efforts focused on improving the mechanical properties and have drawn the most interest and included rubber toughening,[22, 23] blending with epoxies,[24, 25] polyurethanes,[26, 27] and inorganics,[28-31] monomer design,[32-35] and synthesis of side[36-39] and main-chain benzoxazine polymer precursors.[38, 40-50] Specifically, strategies that focus on the design of new monomer structures to tailor network properties take advantage of the inherent simplicity of the benzoxazine synthesis to achieve outstanding versatility in molecular

design of benzoxazine precursors.[33, 35, 48] Regardless of the approach, these strategies utilize the Mannich reaction involving inexpensive and commercially available phenols, primary amines, and formaldehyde to achieve versatility in molecular design of benzoxazine precursors affording a wide range of properties. Figure 1 shows a variety of structural features that can and have been incorporated into bisbenzoxazine monomers where the only constant feature is the benzoxazine ring itself.

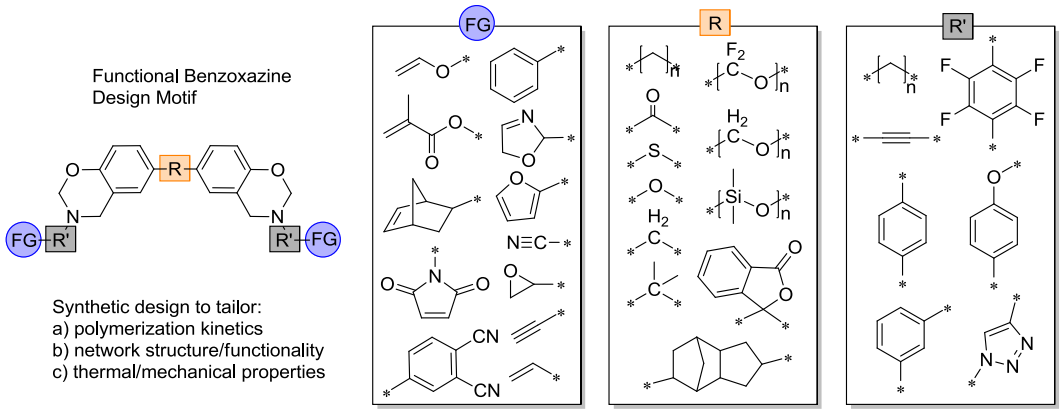


*Figure 1*. Structural features that can and have been incorporated into benzoxazine monomers.

An example by Kim and Ishida[51] showed that smaller/less restrictive amines can significantly change material properties such as volumetric expansion and water absorption. By changing the amines, the network properties are strongly affected due to interruptions in the hydrogen bonding, reducing polymer-polymer interactions. Therefore, it is believed that the physical interaction of polymer chains due to hydrogen bonding plays an important role in determining the properties of polybenzoxazines and can be drastically changed with the incorporation of different amines.[51] Allen and Ishida[33] have also explored molecular design opportunities by switching the difunctionality and making aliphatic diamine-based polybenzoxazines. Additionally, variable diamine lengths were investigated to demonstrate the feasibility of increasing the inherent flexibility of the polybenzoxazine network structure itself without using

additives. Their results show significantly more intramolecular hydrogen bonding compared to intermolecular bonding, which along with increased network flexibility is believed to be associated with the sub-100°C $T_g$ capabilities. Further thermal characterization using DSC showed better curing kinetics represented by the lower onset of polymerization (<180°C) temperature for the lowest diamine length.

*Ring Opening Polymerization (ROP)*

Polybenzoxazines derived from phenolic and amine precursors will undergo ring-opening polymerization (ROP) upon heating with the addition of a curing agent (strong acid and alkaline) or self-polymerize with the aid of phenolic impurities acting as initiators. The polymerization takes place by simply using heat to increase the rate of the ring opening reactions. Small impurities such as cationic or phenolic impurities including benzoxazine oligomers initiate polymerization. Thus, the polymerization is classified as a 'thermally accelerated/activated polymerization'.[17] Additionally, the ring opening polymerization is readily achieved by heating the purified monomer to temperatures above 150°C to open small amounts of benzoxazines thus supplying a phenolic moiety to initiate further ring opening processes. The ring opening process for benzoxazines is a form of addition polymerization in which the terminal end of the polymer acts as a reactive center, where further cyclic monomers join to form a long polymer chain. Through this process, no condensation byproducts are released in which no corrosion processes can take place on the processing equipment. In addition, this makes polybenzoxazine resins very pure.

Generally, the functionality contained in the cyclic starting material as well as the ring size has a decisive effect on the polymerization behavior.[52] In the case of benzoxazines, polymerization can occur at the *ortho* and *para* positions on the phenol.

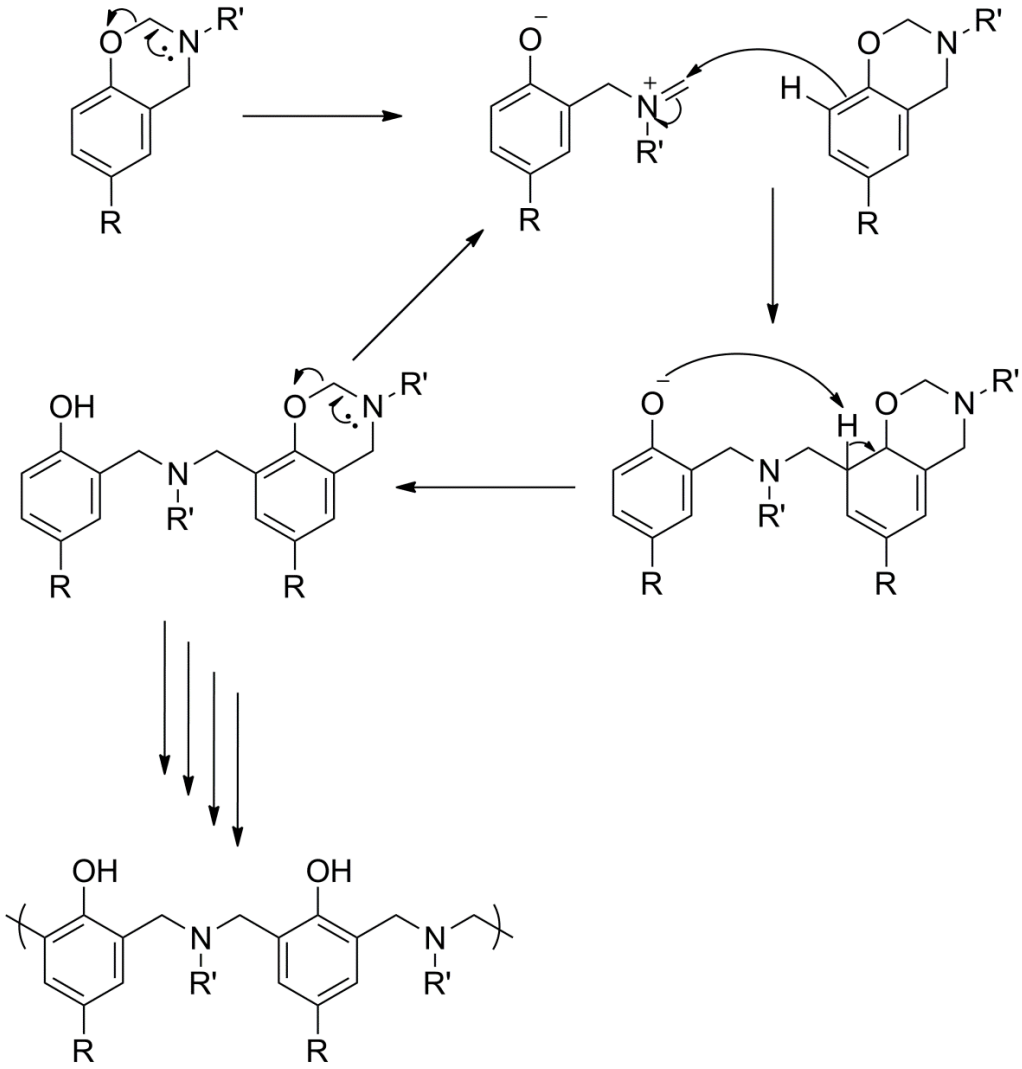


*Scheme 3*. Cationic ring opening mechanism of benzoxazine monomers.

It was demonstrated that the preferred reaction site is the position *ortho* to the hydroxyl functionality of the phenol.[5, 12] It is speculated that under no catalytic influence, the ring opening process of benzoxazines involve a cationic ring opening process described in Scheme 3.[53] It has been proposed that the reaction is initiated by the approach of the phenol to the benzoxazine via intermolecular hydrogen bonding. The initial step produces an intermediary complex, which provides the electron movement from the nitrogen atom to the hydroxyl group followed by nucleophilic aromatic substitution and proton abstraction.[11]

The network properties and curing behavior of benzoxazines are greatly influenced by molecular design. To date, numerous benzoxazine monomer derivatives have been reported with variability in both the phenol and amine as shown in Figure 1, and this list is continuously growing. In doing so, the potential applications keep expanding, and with the versatility of the monomer synthesis, should continue to expand as the continued challenges of molecular design can be overcome through benzoxazines chemistry.

*Copolymers of benzoxazines*

Besides molecular design, tailoring the properties of benzoxazine networks is also possible through copolymerizations. Initially shown by Huang and Ishida,[54] the viscosity of a difunctional benzoxazine resin was reduced by the use of monofunctional benzoxazine monomers as reactive diluents to further improve processability. Glassy state properties, such as stiffness at room temperature, were unaffected by the incorporation of the monofunctional benzoxazine. Also, the thermal stability of the monofunctional modified polybenzoxazine below 200°C was not significantly affected. However, properties sensitive to network structure were affected by the presence of the monofunctional benzoxazine. The incorporation of the monofunctional benzoxazine reduced crosslink density and produced a looser network structure which can be seen and quantified at temperatures above the glass transition temperature.

A recent example of copolybenzoxazines done by Zang et. al.[55] shows a benzoxazole-based benzoxazine monomer copolymerized with the common bisphenol A-aniline-based benzoxazine to decrease the dielectric constants and improve thermal stability. The corresponding copolybenzoxazines displayed higher thermal stability than the bisphenol-A-based benzoxazine, reaching char yields of 62% at 800 °C. Moreover,

the dielectric constants and dielectric loss of the copolybenzoxazines were low and changed slightly at room temperature in the frequency range of 0.1 Hz to 1 MHz. Additionally, the flexural modulus and flexural strength of the copolymer were increased by 66% and 41%, respectively, after the addition of 20% of the benzoxazole-based benzoxazine monomer.

Utilizing copolymers of benzoxazines allows versatile molecular design and eliminates the need for extensive synthesis to incorporate all the desired properties into a single benzoxazine network. Additionally, by copolymerizing benzoxazines with different functionality, the variety of network properties and property combinations can be achieved.

*Benzoxazines in membranes*

The benzoxazine chemistry offers one of the richest design flexibility among all classes of polymers thus leading to advances in many fields with tailored properties. However, one field that polybenzoxazines have gained little attention is in membrane technologies. Membranes have been implemented in a variety of separation devices including desalination as well as in energy generation to accommodate the growing demand for clean water and sustainable energy. The key component in all these devices is a solid electrolyte membrane capable of selectively transporting ions while acting as a barrier to other components. The performance/efficiency of the devises are therefore tied closely to the properties of the solid electrolyte membrane, and because of this, much time and money have been devoted to the research and development of these polymer materials.

Of all the different ionic membranes anion-exchange membranes, (AEMs) are of the oldest and most developed for fuel cells, being first used in the Gemini and Apollo

missions in the 1960s. However, like most ionic membranes, there is a careful balance between performance and stability for AEMs. High performance usually necessitates a high concentration of ionic charge carriers at the expense of mechanical stability by increasing swelling effects. The most common and easiest approach to stabilize an ionic membrane is to cross-link the polymers so as to immobilize polymer chains. Multi (di-, tri-, or tetra)-functional groups-containing cross-linkers have been widely adopted, and some examples include di-amines (react with halogenoalkyl groups),[56-60] di-thiol (with allyl groups),[61] di-aldehyde (with hydroxyl-alkyl groups),[62-66] tri/tetra-alkoxysilanes (with hydroxyl-alkyl or alkoxysilanyl groups),[67, 68] and tetraepoxy (with phenol groups).[69-71] Additionally, a bi-cycloalkene ring-opening with simultaneous polymerization and cross-linking was recently reported.[70, 71]

Due to the simple synthesis and the inherent thermal, mechanical, and chemical stabilities, benzoxazines have recently found use in membrane applications as a logical means to improve membrane stability. While there have been few reports of these, some recent examples that utilize benzoxazines in fuel cell applications can be found in the work of Kim[72-74] and Choi.[75] In these examples mono-, di-, or tri-functional benzoxazine monomers were used to cross-link polybenzimidazole (PBI) through the aromatic component of the PBI by grafting a thermosetting resin into a thermoplastic polymer. Once cross-linked with the benzoxazine, conductivities remained similar to neat PBI; however, the lifetime of the membrane was increased three fold.

Also, Ye et. al.[76] explored sulfonated poly(ether ether ketone) membranes cross-linked with different benzoxazine monomers with and without a sulfonic acid group. For the incorporation of the benzoxazine without the sulfonic acid group, the total concentration of sulfonic acid groups or ion-exchange capacity (IEC) decreased along

with the membrane conductivity. As for incorporating a sulfonic acid functional benzoxazine to cross-link the SPEEK, the IEC and conductivity also decreased but to lesser extremes. Overall, the cross-linking techniques mentioned above require the introduction of a separate cross-linker molecule or specific polymer structures that usually take at least two reaction-steps, increasing the process complexity as well as lowering the IEC. In addition, problems exist when the cross-linker has a distinctive molecular structure that is not compatible with the polymer chain, which can lead to poor membrane quality or make cross-linking impossible. Although this concept of a copolymer system can play a pioneering role in high-temperature PEMFCs when applied to fuel cells and components, in general certain drawbacks still exist: 1) since the benzoxazines contain no charge carrying capabilities, higher loadings would dilute the ionic component driving down efficiency; 2) the cross-linking mechanism requires aromatic functionality in the ionic polymer, limiting the versatility of polymers that can be used and; 3) the high temperature required for polymerization also limits the variety of polymers that can utilize this process

Ideally, a system composed of high ionic content as well as a self-cross-linking mechanism would provide the simplest approach to designing mechanically stable ion-exchange membranes. Instead of simply using benzoxazines as a separate cross-linker, designing an ionic network directly from a benzoxazine network would both utilize the favorable inherent thermal, mechanical, and chemical stabilities as well as eliminate the complexities with secondary cross-linking steps. However, to our knowledge, no such system exists, but promising results from Sawaryn et. al.[77] suggest that it is possible. Sawaryn et. al. designed a linear polyelectrolyte based on a monofunctional benzoxazine monomer with a pendant ionizable group (methyl imidazole). Through their

experiments, high concentrations of cationic moieties were incorporated into the linear polybenzoxazine as there were two ionizable groups per repeat unit. Characterization of these materials was limited to structural and thermal techniques – no membrane applications or properties were reported.

*Summary*

The molecular design along with the simple benzoxazine monomer synthesis allows tailorability of structural features within a polybenzoxazine network. This tailorability is made possible with the extensive library of commercially/synthetically available phenols and amines. In addition to molecular design, copolybenzoxazines can simplify tailoring properties within a benzoxazine network without extensive time and resources dedicated to designing a single monomer structure. Lastly, with the inherent properties associated with benzoxazines, these materials are beginning to reach out into membrane technologies as a means to improve the thermal mechanical stabilities; however, the full potential of these materials has yet to be realized. The molecular diversity of benzoxazines points toward the idea of designing an ionic network directly from a polybenzoxazine network to both utilize the favorable inherent thermal, mechanical, and chemical stabilities as well as to eliminate the complexities with secondary cross-linking steps.

REFERENCES


1. Ibeh, C. C. *Handbook of Thermoset Plastics (2nd Edition)*. William Andrew Publishing/Noyes: Westwood, NJ **1998**.
2. Knop, A.; Pilato, L. A. *Phenolic resins: Chemistry, application and performance—future directions*. Springer-Verlag, Berlin: **1987**.
3. Kopf, P. W. *Encyclopedia of polymer science and engineering*. Wiley: New York, 1985.
4. Holly, F. W.; Cope, A. C. *Journal of the American Chemical Society* **1944,** *66* (11), 1875-1879.
5. Burke, W. J. *Journal of the American Chemical Society* **1949,** *71* (2), 609-612.
6. Burke, W. J.; Weatherbee, C. *Journal of the American Chemical Society* **1950,** *72* (10), 4691-4694.
7. Burke, W. J.; Stephens, C. W. *Journal of the American Chemical Society* **1952,** *74* (6), 1518-1520.
8. Burke, W. J.; Kolbezen, M. J.; Stephens, C. W. *Journal of the American Chemical Society* **1952,** *74* (14), 3601-3605.
9. Burke, W. J.; Smith, R. P.; Weatherbee, C. *Journal of the American Chemical Society* **1952,** *74* (3), 602-605.
10. Burke, W. J.; Murdock, K. C.; Ec, G. *Journal of the American Chemical Society* **1954,** *76* (6), 1677-1679.
11. Burke, W. J.; Glennie, E. L. M.; Weatherbee, C. *The Journal of Organic Chemistry* **1964,** *29* (4), 909-912.
12. Burke, W. J.; Bishop, J. L.; Glennie, E. L. M.; Bauer, W. N. *The Journal of Organic Chemistry* **1965,** *30* (10), 3423-3427.

13. Schreiber, H. German Offen. 2,323,936, **1973**.

14. Higgerbottom, H. P. Polymerizable compositions comprising polyamines and poly(dihydrobenzoxazines). 4,501,864, **1985**.

15. Higgerbottom, H. P. Aqueous dispersions of polyamines and poly(dihydrobenzoxazines). 4,507,428, **1985.**

16. Higgerbottom, H. P. Process for deposition of resin dispersions on metal substrates. 4,557,979, **1985**.

17. Ishida, H.; Agag, T. *Handbook of Benzoxazine Resins*. Elsevier: Amsterdam, **2011**; Vol. 1.

18. Ishida, H.; Allen, D. J. *Journal of Polymer Science Part B: Polymer Physics* **1996,** *34* (6), 1019-1030.

19. Ishida, H.; Sanders, D. P. *Macromolecules* **2000,** *33* (22), 8149-8157.

20. Ishida, H.; Sanders, D. P. *Journal of Polymer Science Part B: Polymer Physics* **2000,** *38* (24), 3289-3301.

21. Agag, T.; Jin, L.; Ishida, H., *Polymer* **2009,** *50* (25), 5940-5944.

22. Ishida, H.; Lee, Y. H. *Polym. Polym. Compos.* **2001,** *9* (2), 121-134.

23. Jang, J.; Seo, D. *J. Appl. Polym. Sci.* **1998,** *67* (1), 1-10.

24. Ishida, H.; Allen, D. J. *Polymer* **1996,** *37* (20), 4487-4495.

25. Li, X.; Xia, Y.; Xu, W.; Ran, Q.; Gu, Y. *Polym. Chem.* **2012,** *3* (6), 1629-1633.

26. Takeichi, T.; Guo, Y. *Polymer Journal* **2001,** *33* (5), 437-443.

27. Yeganeh, H.; Razavi-Nouri, M.; Ghaffari, M. *Polym. Advan. Technol.* **2008,** *19* (8), 1024-1032.

28. Agag, T.; Tsuchiya, H.; Takeichi, T. *Polymer* **2004,** *45* (23), 7903-7910.

29. Huang, K. W.; Kuo, S. W. *Polym. Composite* **2011,** *32* (7), 1086-1094.

30. Liu, Y.; Zheng, S. *J. Polym. Sci. A: Polym. Chem.* **2006,** *44* (3), 1168-1181.

31. Wu, Y. C.; Kuo, S. W. *Polymer* **2010,** *51* (17), 3948-3955.

32. Agag, T.; Akelah, A.; Rehab, A.; Mostafa, S. *Polym. Int.* **2012,** *61* (1), 124-128.

33. Allen, D. J.; Ishida, H. *J. Appl. Polym. Sci.* **2006,** *101* (5), 2798-2809.

34. Allen, D. J.; Ishida, H. *Polymer* **2007,** *48* (23), 6763-6772.

35. Allen, D. J.; Ishida, H. *Polymer* **2009,** *50* (2), 613-626.

36. Agag, T.; Vietmeier, K.; Chernykh, A.; Ishida, H. *J. Appl. Polym. Sci.* **2012,** *125* (2), 1346-1351.

37. Ergin, M.; Kiskan, B.; Gacal, B.; Yagci, Y. *Macromolecules* **2007,** *40* (13), 4724-4727.

38. Kukut, M.; Kiskan, B.; Yagci, Y. *Des. Monomers Polym.* **2009,** *12* (2), 167-176.

39. Oie, H.; Sudo, A.; Endo, T. *J. Polym. Sci. A: Polym. Chem.* **2011,** *49* (14), 3174-3183.

40. Agag, T.; Arza, C. R.; Maurer, F. H. J.; Ishida, H. *J. Polym. Sci. A: Polym. Chem.* **2011,** *49* (20), 4335-4342.

41. Agag, T.; Geiger, S.; Alhassan, S. M.; Qutubuddin, S.; Ishida, H. *Macromolecules* **2010,** *43* (17), 7122-7127.

42. Aydogan, B.; Sureka, D.; Kiskan, B.; Yagci, Y. *J. Polym. Sci. A: Polym. Chem.* **2010,** *48* (22), 5156-5162.

43. Chernykh, A.; Agag, T.; Ishida, H. *Polymer* **2009,** *50* (2), 382-390.

44. Chernykh, A.; Liu, J.; Ishida, H. *Polymer* **2006,** *47* (22), 7664-7669.

45. Chou, C. I.; Liu, Y. L. *J. Polym. Sci. A: Polym. Chem.* **2008,** *46* (19), 6509-6517.

46. Dogan Demir, K.; Kiskan, B.; Yagci, Y. *Macromolecules* **2011,** *44* (7), 1801-1807.

47. Kiskan, B.; Yagci, Y.; Ishida, H. *J. Polym. Sci. A: Polym. Chem.* **2008,** *46* (2), 414-420.

48. Lin, C. H.; Chang, S. L.; Shen, T. Y.; Shih, Y. S.; Lin, H. T.; Wang, C. F. *Polym. Chem.* **2012,** *3* (4), 935-945.

49. Nagai, A.; Kamei, Y.; Wang, X. S.; Omura, M.; Sudo, A.; Nishida, H.; Kawamoto, E.; Endo, T. *J. Polym. Sci. A: Polym. Chem.* **2008,** *46* (7), 2316-2325.

50. Velez-Herrera, P.; Doyama, K.; Abe, H.; Ishida, H. *Macromolecules* **2008,** *41* (24), 9704-9714.

51. Kim, H. D.; Ishida, H. *The Journal of Physical Chemistry A* **2001,** *106* (14), 3271-3280.

52. Santhosh Kumar, K. S.; Reghunadhan Nair, C. P.; Ninan, K. N. *Thermochimica Acta* **2006,** *441* (2), 150-155.

53. Brunovska, Z.; Liu, J. P.; Ishida, H. *Macromolecular Chemistry and Physics* **1999,** *200* (7), 1745-1752.

54. Huang, M., T.; Ishida, H. *Polymers & Polymer Composites* **1999,** *7* (4), 233-247.

55. Zhang, K.; Zhuang, Q.; Liu, X.; Cai, R.; Yang, G.; Han, Z. *RSC Advances* **2013,** *3* (15), 5261-5270.

56. Agel, E.; Bouet, J.; Fauvarque, J. F. *Journal of Power Sources* **2001,** *101* (2), 267-274.

57. Park, J.-S.; Park, S.-H.; Yim, S.-D.; Yoon, Y.-G.; Lee, W.-Y.; Kim, C.-S. *Journal of Power Sources* **2008,** *178* (2), 620-626.

58. Hong, J.-H.; Hong, S.-K. *Journal of Applied Polymer Science* **2010,** *115* (4), 2296-2301.

59. Hong, J.-H.; Li, D.; Wang, H. *Journal of Membrane Science* **2008,** *318* (1-2), 441-444.

60. Wang, G.; Weng, Y.; Chu, D.; Chen, R.; Xie, D. *Journal of Membrane Science* **2009,** *332* (1-2), 63-68.

61. Stoica, D.; Ogier, L.; Akrour, L.; Alloin, F.; Fauvarque, J. F. *Electrochimica Acta* **2007,** *53* (4), 1596-1603.

62. Wan, Y.; Peppley, B.; Creber, K. A. M.; Bui, V. T.; Halliop, E. *Journal of Power Sources* **2008,** *185* (1), 183-187.

63. Wang, E. D.; Zhao, T. S.; Yang, W. W. *International Journal of Hydrogen Energy* **2010,** *35* (5), 2183-2189.

64. Xiong, Y.; Fang, J.; Zeng, Q. H.; Liu, Q. L. *Journal of Membrane Science* **2008,** *311* (1-2), 319-325.

65. Xiong, Y.; Liu, Q. L.; Zhang, Q. G.; Zhu, A. M. *Journal of Power Sources* **2008,** *183* (2), 447-453.

66. Yang, C.-C.; Chiu, S.-J.; Chien, W.-C.; Chiu, S.-S. *Journal of Power Sources* **2010,** *195* (8), 2212-2219.

67. Wu, Y.; Wu, C.; Xu, T.; Lin, X.; Fu, Y. *Journal of Membrane Science* **2009,** *338* (1-2), 51-60.

68. Wu, Y.; Wu, C.; Xu, T.; Yu, F.; Fu, Y. *Journal of Membrane Science* **2008,** *321* (2), 299-308.

69. Wu, Y.; Wu, C.; Varcoe, J. R.; Poynton, S. D.; Xu, T.; Fu, Y. *Journal of Power Sources* **2010,** *195* (10), 3069-3076.

70. Clark, T. J.; Robertson, N. J.; Kostalik Iv, H. A.; Lobkovsky, E. B.; Mutolo, P. F.; Abruna, H. c. D.; Coates, G. W. *Journal of the American Chemical Society* **2009,**

*131* (36), 12888-12889.

71. Robertson, N. J.; Kostalik, H. A.; Clark, T. J.; Mutolo, P. F.; Abruna, H. c. D.; Coates, G. W. *Journal of the American Chemical Society* **2010,** *132* (10), 3400-3404.

72. Kim, S.-K.; Choi, S.-W.; Jeon, W. S.; Park, J. O.; Ko, T.; Chang, H.; Lee, J.-C. *Macromolecules* **2012,** *45* (3), 1438-1446.

73. Kim, S.-K.; Kim, K.-H.; Park, J. O.; Kim, K.; Ko, T.; Choi, S.-W.; Pak, C.; Chang, H.; Lee, J.-C. *Journal of Power Sources* **2013,** *226* (0), 346-353.

74. Kim, S.-K.; Ko, T.; Choi, S.-W.; Park, J. O.; Kim, K.-H.; Pak, C.; Chang, H.; Lee, J.-C. *Journal of Materials Chemistry* **2012,** *22* (15), 7194-7205.

75. Choi, S.-W.; Park, J.; Pak, C.; Choi, K.; Lee, J.-C.; Chang, H. *Polymers* **2013,** *5* (1), 77-111.

76. Ye, Y.-S.; Yen, Y.-C.; Cheng, C.-C.; Chen, W.-Y.; Tsai, L.-T.; Chang, F.-C. *Polymer* **2009,** *50* (14), 3196-3203.

77. Sawaryn, C.; Landfester, K.; Taden, A. *Macromolecules* **2011,** *44* (19), 7668-7674.

# CHAPTER II

# OBJECTIVES

Polybenzoxazine (pBZ) resins are traditionally associated with having a high modulus and a high glass transition temperature with the major uses being related to these properties. To tailor or adjust these properties plasticizers, blends, and composite materials are generally used. However, through synthetic design, a variety of properties can be adjusted or even added to a pBZ network without the complexities associated with foreign additives. This work focuses on the synthetic versatility of BZ monomers in an effort to improve the thermal and mechanical properties for low temperature, thin film applications. The objectives of this dissertation include:

1. Synthesis and characterization of a series of flexible aliphatic-bridged bisphenol-based polybenzoxazines to improve the thermal and mechanical properties
2. Design of a solvent-free copolymerization of rigid and flexible bis-1,3 benzoxazines to allow facile tunability of polybenzoxazine network properties
3. Synthesis and characterization of quaternary ammonium functional polybenzoxazine networks for anion-exchange membrane capabilities

In the first objective (Chapter III), flexible 4, 6, 8, and 10 carbon spacers were incorporated as the core of a series of diphenols followed by the benzoxazine monomer synthesis. A variety of structure property relationships were developed as a function of the core length to support the efficacy of synthetic design to tailor polybenzoxazine properties toward thin film applications.

The second objective (Chapter IV) focuses on the simplistic nature of the ring-

opening process for benzoxazine monomers. Compatible bis-1,3 benzoxazine monomers were copolymerized, and the network properties were analyzed and predicted as a function of the weight percents of the each monomers.

For the third objective (Chapter V), quaternizable polybenzoxazine networks were synthesized using the simplistic monomer/polymer synthesis. Following a post polymerization quaternization reaction, networks with a high array of cationic moieties were created. Anion exchange capabilities (water uptake, ion-exchange capacity, ion conductivity) were examined as a function of core length and hydrophilicity.

# CHAPTER III

# FLEXIBLE ALIPHATIC-BRIDGED BISPHENOL-BASED POLYBENZOXAZINES

## Introduction

Thermoset resins derived from heterocyclic bis-1,3-benzoxazines have been vigorously investigated in recent years as attractive alternatives to traditional phenolic resins for a variety of high performance applications.[1-4] Bis-1,3-benzoxazines undergo thermally-accelerated cationic ring-opening polymerization (ROP) – in the absence of catalyst and without by-products – yielding a cross-linked polymer network comprised of a phenol and a tertiary amine bridge as the structural motif.[5, 6] Extensive hydrogen bonding between the phenol and tertiary amine give rise to many salient features observed in polybenzoxazines (pBZs), including high $T_g$, high thermal stability, low surface energy, and low water adsorption.[4, 7, 8] Furthermore, pBZs exhibit excellent dimensional stability, flame resistance, and stable dielectric constants – properties not found in traditional phenolic resins.[4] Despite these advantageous properties, there continues to be room for improving the mechanical properties and processability of BZ materials – particularly those derived from monomeric precursors. Strategies to address these shortcomings are being rapidly developed, including monomer design, rubber toughening,[9, 10] blending with epoxies,[11] polyurethanes,[12, 13] and inorganics,[14-17] and the synthesis of side[18-21] and main-chain benzoxazine polymer precursors.[22-34] Regardless of the approach, these strategies take advantage of the inherent simplicity of benzoxazine synthesis – namely a Mannich reaction involving inexpensive and commercially available phenols, primary amines, and formaldehyde – to achieve unprecedented versatility in molecular design of benzoxazine precursors.

Literature regarding molecular design of bis-1,3-benzoxazine monomers has

predominately dealt with rigid core bifunctional phenolic derivatives (i.e. bisphenol-A, Scheme 4) and mono-functional primary amines – a design strategy that provides thermosets with high $T_g$ and high thermal stability, but also imparts brittleness that plagues conventional thermosets. Alternatively, Ishida and co-workers[35-37] have shown that the inherent flexibility of pBZs can be greatly improved via monomer design, where benzoxazines based on a series of bifunctional aliphatic amine core molecules with monofunctional phenol pendent groups produced materials with improved flexural properties. Furthermore, these aliphatic BZ monomers could be processed into thin films via solvent-free processing. While Agag et al.[38] recently showed improved flexibility of bisphenol-A derived benzoxazines via incorporation of pendent aliphatic chains, strategies that attempt to integrate flexibility directly into the bisphenol motif have not been thoroughly explored.

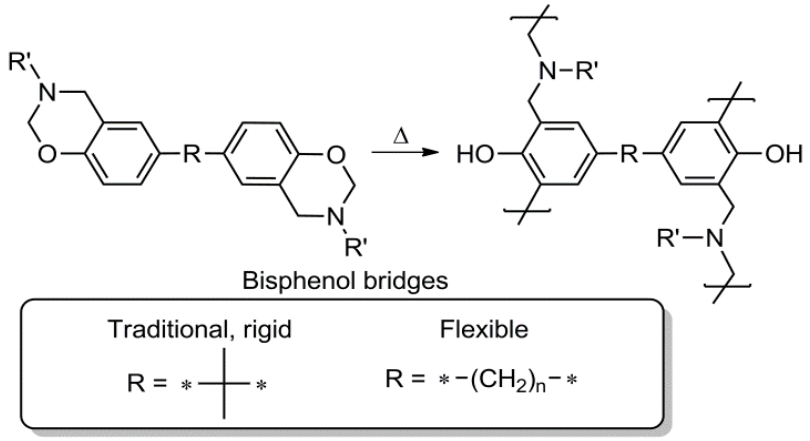


*Scheme 4***.** Thermal ring-opening polymerization of bisfunctional benzoxazines containing the traditional, rigid methylethylidene linker versus the flexible, aliphatic linkers reported in the current work.

In this paper, the synthesis of a series of novel aliphatic-bridged, bisphenol-based, benzoxazine monomers comprising from four to ten methylene unit spacers is reported. Integrating flexibility into the bisphenol component of the monomer, rather than the diamine, enables a broader design space with potential to incorporate a vast array of

commercially available primary amine derivatives as pendent moieties to the monomer structure – though for simplicity and to develop structure-property relationships related to the aliphatic bisphenol, the identity of the primary amine in the current work was kept constant. Cationic ring-opening polymerization of these monomers provides flexible pBZ thermosets with good film-forming characteristics and tuneable thermomechanical properties. The effects of aliphatic bisphenol chain length on polymerization behavior, thermomechanical transitions, and mechanical properties of the pBZ thermosets are reported.

## Experimental

### *Materials*

All reagents and solvents were obtained at the highest purity available from Aldrich Chemical Company and used without further purification unless otherwise specified. Paraformaldehyde was purchased from Acros Organics. Anhydrous potassium carbonate, magnesium sulfate, and sodium hydroxide were purchased from Fisher Scientific. The synthesis of compounds 3 – 5 was adapted from literature.[39]

### *Synthesis of aliphatic-bridged dibenzaldehyde compounds (3)*

Into a 250mL round bottom flask fitted with a condenser, 0.0287 mol of the dibromo species (1,4-dibromobutane, 1,6-dibromohexane, 1,8-dibromooctane, or 1,10-dibromodecane), 7.007 g (0.0574 mol) of 4-hydroxybenzaldehyde, and 15.8665 g (0.1148mol) of anhydrous potassium carbonate were added to approximately 100mL of dimethylformamide. The flask was set in an oil bath and refluxed at 110 °C for 48 h. The solution was cooled to room temperature, diluted with dichloromethane, and washed with water. The organic layer was dried over $MgSO_4$ and evaporated under vacuum to an off white solid. *4,4'-(butane-1,4-diylbis(oxy))dibenzaldehyde* **(3a).**(83.9% yield) $^1$H NMR

($CDCl_3$), ppm: δ=1.99 (4H, m, $CH_2$), 4.09 (4H, t, $CH_2$-O), 6.95 (4H, d, CH, aromatic) 7.78 (4H, d, CH, aromatic), 9.83 (2H, s, CH=O, aldehyde); $^{13}$C NMR ($CDCl_3$), ppm: δ=25.90 (2C, $CH_2$), 67.86 (2C, $CH_2$-O), 114.83 (4C, CH, aromatic) 130.06 (2C, C, aromatic) 132.10 (4C, CH, aromatic), 164.05 (2C, C, aromatic) 190.85 (2C, CH aldehyde). *4,4'-(hexane-1,6-diylbis(oxy))dibenzaldehyde* **(3b).** (94.5% yield) $^1$H NMR ($CDCl_3$), ppm: δ=1.52-1.92 (8H, m, $CH_2$), 4.07 (4H, t, $CH_2$-O), 6.98 (4H, d, CH, aromatic) 7.83 (4H, d, CH, aromatic), 9.88 (2H, s, CH=O, aldehyde); $^{13}$C NMR ($CDCl_3$), ppm: δ=25.76, 28.97 (4C, $CH_2$), 68.15 (2C, $CH_2$-O), 114.71 (4C, CH, aromatic) 129.81 (2C, C, aromatic) 131.96 (4C, CH, aromatic), 164.11 (2C, C, aromatic) 190.74 (2C, CH aldehyde). *4'-(octane-1,8-diylbis(oxy))dibenzaldehyde* **(3c).** (94.9% yield) $^1$H NMR ($CDCl_3$), ppm: δ=1.39-1.89 (12H, m, $CH_2$), 4.13 (4H, t, $CH_2$-O), 7.11 (4H, d, CH, aromatic) 7.87 (4H, d, CH, aromatic), 9.89 (2H, s, CH=O, Aldehyde); $^{13}$C NMR ($CDCl_3$), ppm: δ=25.88, 29.01, 29.20 (6C, $CH_2$), 68.31 (2C, $CH_2$-O), 114.71 (4C, CH, aromatic) 129.74 (2C, C, aromatic) 131.95 (4C, CH, aromatic), 164.18 (2C, C, aromatic) 190.75 (2C, CH aldehyde). *4,4'-(decane-1,10-diylbis(oxy))dibenzaldehyde* **(3d).** (92.4% yield) $^1$H NMR ($CDCl_3$), ppm: δ=1.29-1.81 (16H, m, $CH_2$), 3.98 (4H, t, $CH_2$-O), 6.94 (4H, s, CH, aromatic) 7.77 (4H, d, CH, aromatic), 9.82 (2H, s, CH=O, Aldehyde); $^{13}$C NMR ($CDCl_3$), ppm: δ=25.91, 29.00 29.27, 29.41 (8C, $CH_2$), 68.34 (2C, $CH_2$-O), 114.70 (4C, CH, aromatic) 129.68 (2C, C, aromatic) 131.91 (4C, CH, aromatic), 164.19 (2C, C, aromatic) 190.69 (2C, CH aldehyde).

*Synthesis of aliphatic-bridged diformate compounds (4)*

Into a 500 mL round bottom flask, 0.022 mol of dibenzaldehyde **(3)** was dissolved in 150-200 mL of dichloromethane, and metachloroperoxybenzoic acid (MCPBA) (14.68 g, 0.0891 mol) was added in portions to the solution. The reaction was then capped and

purged with nitrogen gas for 10 min, and then set to stir at room temperature for 3-4 h. 112 mL of a saturated sodium bicarbonate solution was added to the solution and stirred for another 2 h at room temperature. The solution was extracted with dichloromethane and washed with 10% sodium metabisulfite followed by washing with water. The organic layer was dried over $MgSO_4$ and evaporated under vacuum to give a light yellow solid. *(Butane-1,4-diylbis(oxy))bis(4,1-phenylene) diformate* **(4a).** (97.3% yield) $^1$H NMR ($CDCl_3$), ppm: δ=1.97 (4H, m, $CH_2$), 4.02 (4H, t, $CH_2$-O), 6.88 (4H, d, CH, aromatic) 7.04 (4H, d, CH, aromatic), 8.28 (2H, s, O-CH=O, formate); $^{13}$C NMR ($CDCl_3$), ppm: δ=25.93 (2C, $CH_2$), 67.84 (2C, $CH_2$-O), 115.22 (4C, CH, aromatic) 121.94 (4C, C, aromatic) 143.31 (2C, C, aromatic), 157.03 (2C, C, aromatic) 159.70 (2C, CH formate). *(Hexane-1,6-diylbis(oxy))bis(4,1-phenylene) diformate* **(4b).** (84.3% yield) $^1$H NMR ($CDCl_3$), ppm: δ=1.49-1.88 (8H, m, $CH_2$), 3.96 (4H, t, $CH_2$-O), 6.89 (4H, d, CH, aromatic) 7.03 (4H, d, CH, aromatic), 8.28 (2H, s, O-CH=O, formate); $^{13}$C NMR ($CDCl_3$), ppm: δ=25.79, 29.15 (4C, $CH_2$), 68.22 (2C, $CH_2$-O), 115.22 (4C, CH, aromatic) 121.89 (4C, C, aromatic) 143.23 (2C, C, aromatic), 157.16 (2C, C, aromatic) 159.74 (2C, CH formate). *(Octane-1,8-diylbis(oxy))bis(4,1-phenylene) diformate* **(4c).** (94.4% yield) $^1$H NMR ($CDCl_3$), ppm: δ=1.37-1.84 (12H, m, $CH_2$), 4.13 (4H, t, $CH_2$-O), 6.97 (4H, d, CH, aromatic) 7.10 (4H, d, CH, aromatic), 8.39 (2H, s, O-CH=O, formate); $^{13}$C NMR ($CDCl_3$), ppm: δ=25.93, 29.00 29.16, 29.24 (6C, $CH_2$), 68.35 (2C, $CH_2$-O), 115.21 (4C, CH, aromatic) 121.87 (4C, C, aromatic) 143.19 (2C, C, aromatic), 157.20 (2C, C, aromatic) 159.73 (2C, CH formate). *(Decane-1,10-diylbis(oxy))bis(4,1-phenylene) diformate* **(4d).** (93.3% yield) $^1$H NMR ($CDCl_3$), ppm: δ=1.30-1.83 (16H, m, $CH_2$), 4.00 (4H, t, $CH_2$-O), 6.97 (4H, d, CH, aromatic) 7.10 (4H, d, CH, aromatic), 8.39 (2H, s, O-CH=O, formate); $^{13}$C NMR ($CDCl_3$), ppm: δ=25.99, 29.00 29.20, 29.33, 29.46 (8C, $CH_2$),

68.39 (2C, $CH_2$-O), 115.21 (4C, CH, aromatic) 121.88 (4C, C, aromatic) 143.18 (2C, C, aromatic), 157.21 (2C, C, aromatic) 159.79 (2C, CH formate).

*Synthesis of aliphatic-bridged diphenol compounds (5)*

Into a 500mL round bottom flask fitted with a condenser, 0.0068mol of diformate **(4)** was added to sodium hydroxide (1.082 g, 0.0271mol) in 50 mL of ethanol and 20 mL of water, and the solution was then refluxed at 100°C for 24 h. The solution was cooled to room temperature and acidified using 3M HCl. The product precipitated and was extracted using ethyl acetate. The organic layers were combined, washed with 3M HCl, water, and dried over $MgSO_4$. The solution was filtered, and solvent was removed by rotary evaporation to give a brown solid. *4,4'-(butane-1,4-diylbis(oxy))diphenol* **(5a).** (94.9% yield) $^1$H NMR (acetone-$d_6$), ppm: δ=1.90 (4H, m, $CH_2$), 3.97 (4H, t, $CH_2$-O), 6.76 (8H, m, CH, aromatic) 7.82 (2H, s, OH); $^{13}$C NMR (acetone-$d_6$), ppm: δ=26.05 (2C, $CH_2$), 68.04 (2C, $CH_2$-O), 115.82 (4C, CH, aromatic) 116.12 (4C, CH, aromatic), 151.53 (2C, C, phenol) 151.86 (2C, C, ether). *4,4'-(hexane-1,6-diylbis(oxy))diphenol* **(5b).** (89.6% yield) $^1$H NMR (acetone-$d_6$), ppm: δ=1.48-1.82 (8H, m, $CH_2$), 3.91 (4H, t, $CH_2$-O), 6.75 (8H, m, CH, aromatic) 7.81 (2H, s, OH); $^{13}$C NMR (acetone-$d_6$), ppm: δ=25.81, 29.27 (4C, $CH_2$), 68.24 (2C, $CH_2$-O), 115.78 (4C, CH, aromatic) 116.12 (4C, CH, aromatic), 151.48 (2C, C, phenol) 151.92 (2C, C, ether). *4,4'-(octane-1,8-diylbis(oxy))diphenol* **(5c).** (92.5% yield) $^1$H NMR (acetone-$d_6$), ppm: δ=1.34-1.79 (12H, m, $CH_2$), 3.89 (4H, t, $CH_2$-O), 6.75 (8H, m, CH, aromatic) 7.81 (2H, s, OH); $^{13}$C NMR (acetone-$d_6$), ppm: δ=25.87, 29.27, (6C, $CH_2$), 68.28 (2C, $CH_2$-O), 115.75 (4C, CH, aromatic) 116.10 (4C, CH, aromatic), 151.48 (2C, C, phenol) 151.93 (2C, C, ether). *4,4'-(decane-1,10-diylbis(oxy))diphenol* **(5d).** (91.0% yield) $^1$H NMR (acetone-$d_6$), ppm: δ=1.35-1.74 (16H, m, $CH_2$), 3.88 (4H, t, $CH_2$-O), 6.75 (8H, m, CH, aromatic) 7.81 (2H, s,

OH); $^{13}$C NMR (acetone-$d_6$), ppm: δ=25.92, 29.30 29.39 (8C, $CH_2$), 68.12 (2C, $CH_2$-O), 115.33 (4C, CH, aromatic) 115.68 (4C, CH, aromatic), 151.13 (2C, C, phenol) 152.52 (2C, C, ether).

*Synthesis of aliphatic-bridged bisbenzoxazine monomers (6)*

Into a 100mL round bottom flask fitted with a condenser, 0.0033 mol of the diphenol **(5a-d),** butylamine (0.4827 g, 0.0066 mol), and paraformaldehyde (0.3964 g, 0.0132 mol) were suspended in 7.9 mL of xylene and placed in an oil bath heated to 120°C. Once at temperature, the reactants dissolved, and aliquots were taken at 5 minute intervals and observed via $^1$H-NMR to monitor the progress of the reaction. Upon completion of the reaction (~15 – 20 min), the reaction was cooled to room temperature, and the xylenes was evaporated. The crude residue was then diluted with excess ethyl acetate and stirred with basic alumina for 10 min, filtered, and evaporated under vacuum to give an off white solid. The crude benzoxazine was then recrystallized in cold ethyl acetate to afford white crystals. *1,4-bis((3-butyl-3,4-dihydro-2H-benzo[e][1,3]oxazin-6-yl)oxy)butane* **(6a).**(39.0% yield) $^1$H NMR ($CDCl_3$), ppm: δ=0.85 (6H, t, $CH_3$) 1.21-1.90 (12H, m, $CH_2$), 2.66 (4H, t, ($CH_3$)-N), 3.80 (4H, t, $CH_2$-O), 3.81 (4H, s, $CH_2$, oxazine), 4.74 (4H, s, $CH_2$, oxazine), 6.44 (2H, s, CH, aromatic) 6.62 (4H, s, CH, aromatic); $^{13}$C NMR ($CDCl_3$), ppm: δ=13.95 (2C, $CH_3$), 20.37, 26.08, 30.25 (6C, $CH_2$), 50.50 (2C, $CH_3$-N), 51.11 (2C, $CH_2$-N, oxazine), 68.00 (2C, $CH_2$-O), 82.29 (2C, $CH_2$-O, oxazine), 112.96, 114.19, 116.89, 120.80, 148.01, 152.77 (12C, aromatic). *1,6-bis((3-butyl-3,4-dihydro-2H-benzo[e][1,3]oxazin-6-yl)oxy)hexane* **(6b).**(31.2% yield) $^1$H NMR ($CDCl_3$), ppm: δ=0.85 (6H, t, $CH_3$) 1.21-1.77 (16H, m, $CH_2$), 2.67 (4H, t, ($CH_3$)-N), 3.81 (4H, t, $CH_2$-O), 3.88 (4H, s, $CH_2$, oxazine), 4.74 (4H, s, $CH_2$, oxazine), 6.43 (2H, s, CH, aromatic) 6.62 (4H, s, CH, aromatic); $^{13}$C NMR ($CDCl_3$), ppm: δ=13.86 (2C, $CH_3$),

20.36, 25.88, 29.34, 30.27 (8C, $CH_2$), 50.50 (2C, $CH_3$-N), 51.05 (2C, $CH_2$-N, oxazine), 68.35 (2C, $CH_2$-O), 82.29 (2C, $CH_2$-O, oxazine), 112.93, 114.16, 116.86, 120.79, 148.02, 152.87 (12C, aromatic). *1,8-bis((3-butyl-3,4-dihydro-2H-benzo[e][1,3]oxazin-6-yl)oxy)octane* **(6c).** (28.2% Yield) $^1$H NMR ($CDCl_3$), ppm: δ=0.92 (6H, t, $CH_3$) 1.29-1.81 (20H, m, $CH_2$), 2.72 (4H, t, ($CH_3$)-N), 3.87 (4H, t, $CH_2$-O), 3.95 (4H, s, $CH_2$, oxazine), 4.80 (4H, s, $CH_2$, oxazine), 6.50 (2H, s, CH, aromatic) 6.67 (4H, s, CH, aromatic); $^{13}$C NMR ($CDCl_3$), ppm: δ=13.96 (2C, $CH_3$), 20.37, 26.00, 29.30, 29.36, 30.27 (10C, $CH_2$), 50.51 (2C, $CH_3$-N), 51.11 (2C, $CH_2$-N, oxazine), 68.46 (2C, $CH_2$-O), 82.28 (2C, $CH_2$-O, oxazine), 112.92, 114.16, 116.86, 120.78, 148.00, 152.90 (12C, aromatic). *1,10-bis((3-butyl-3,4-dihydro-2H-benzo[e][1,3]oxazin-6-yl)oxy)decane* **(6d)**. (38.9% Yield) $^1$H NMR ($CDCl_3$), ppm: δ=0.91 (6H, t, $CH_3$) 1.27-1.80 (24H, m, $CH_2$), 2.73 (4H, t, ($CH_3$)-N), 3.87 (4H, t, $CH_2$-O), 3.95 (4H, s, $CH_2$, oxazine), 4.80 (4H, s, $CH_2$, oxazine), 6.50 (2H, s, CH, aromatic) 6.67 (4H, s, CH, aromatic); $^{13}$C NMR ($CDCl_3$), ppm: δ=13.95 (2C, $CH_3$), 20.38, 26.04, 29.36, 29.38, 29.48 30.26 (12C, $CH_2$), 50.51 (2C, $CH_3$-N), 51.11 (2C, $CH_2$-N, oxazine), 68.51 (2C, $CH_2$-O), 82.28 (2C, $CH_2$-O, oxazine), 112.92, 114.16, 116.85, 120.77, 147.98, 152.93 (12C, aromatic).

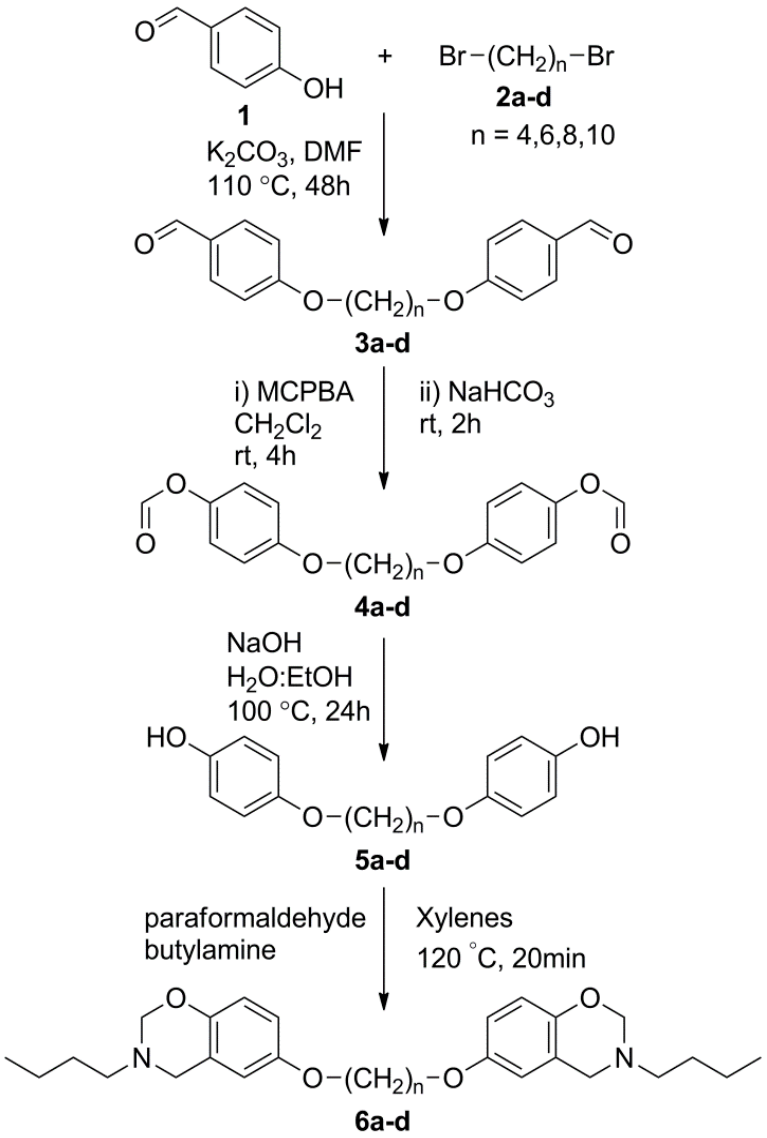


*Scheme 5*. Synthetic route for the alkyl-bridged bisbenzoxazine monomer series BZ(n)BA.

*Polybenzoxazine Film Preparation*

75-125mg of BZ(n)BA was placed in the center of a RainX® coated 75 × 50 mm glass slide and heated gently with a heat gun until the monomer was molten and all the bubbles were removed. Teflon spacers (~130µm) were inserted on the sides of a glass slide, and a second RainX® coated 75 × 50 mm glass slide was gently placed on the top making sure bubbles were excluded when 'sandwiching' the monomer. The glass slides were clamped together, and the sandwiched monomer was quickly placed in a preheated

oven at 100 °C. The thermal step cure proceeded as follows; 100°C for 1h, 140°C for 1h, 160°C for 2h and lastly 180°C for 8h. After curing, the films were removed and placed in methanol for 1h to remove any residual RainX®.

*Characterization and Measurements*

$^{1}$H-NMR and $^{13}$C-NMR measurements were performed in deuterated chloroform ($CDCl_3$) and deuterated acetone ($(CD_3)_2CO$) to determine purity of the synthesized molecules using a Varian Mercury Plus 300 MHz NMR spectrometer, operating at a frequency of 300 MHz with tetramethylsilane as an internal standard. The number of transients for $^{1}$H and $^{13}$C are 32 and 256, respectively, and a relaxation time of 5 s was used for the integrated intensity determination of $^{1}$H NMR spectra.

The ROP conversion was analyzed using a Fourier transform infrared spectroscopy in grazing-angle attenuated total reflectance mode (gATR-FTIR) using a Thermo Scientific FTIR instrument (Nicolet 8700) equipped with a VariGATR™ accessory (grazing angle 65°, germanium (Ge) crystal; Harrick Scientific). Spectra were collected with a resolution of 4 $cm^{-1}$ by accumulating a minimum of 128 scans per sample. All spectra were collected while purging the VariGATR™ attachment and FTIR instrument with $N_2$ gas along the infrared beam path to minimize the peaks corresponding to atmospheric moisture and $CO_2$. Spectra were analyzed and processed using Omnic software. Differential scanning calorimetry was also performed to monitor conversion of the ROP on a TA instruments DSC Q200 differential scanning calorimeter at a heating rate of 5 °C/min and a nitrogen flow rate of 50 mL/min. Samples were crimped in hermetic aluminum pans with lids.

Thermogravimetric analysis (TGA) was performed using a TA Instruments Q50 thermogravimetric analyzer with a platinum pan. Samples were heated at 20 °C/min from

40 °C to 800 °C under a nitrogen atmosphere. Dynamic mechanical analysis (DMA) was performed on a TA Instruments Q800 DMA in tension film mode with a heating rate of 2 °C/min from 25 °C to 200 °C at 1 Hz. Samples were prepared using the sandwich method previously described and cut into bars.

Mechanical testing was performed using a Bose Electroforce 3330®. Dog bone samples with cross-sectional dimensions 9.38 mm in length and 3 mm at the neck were secured in tensile clamps set to a gauge distance of 15 mm and were carefully centered in clamps and deformed in tensile mode. Uniaxial tensile testing proceeded in force-control mode using a ramp rate of 0.1 Newtons per second. Output was recorded through force and displacement feedback channels at a data acquisition rate of 1024 points per second. Stress (MPa) was calculated as the ratio of force at each point to the facial area of the sample between the clamps in $m^2$. Strain was determined from the change in displacement from the gauge length. Young's modulus was determined from the initial linear elastic region of the stress-strain curve.

## Results and Discussion

### *Monomer Synthesis*

The series of bisbenzoxazine monomers comprising aliphatic linkers of various lengths (6a-d; n = 4, 6, 8, 10) were prepared in four steps according to Scheme 5. The first step provided the dibenzaldehyde series (3a-d) in excellent yield following a Williamson etherification between 4-hydroxybenzaldehyde (1) and dibromoalkanes (2a-d) in the presence of anhydrous $K_2CO_3$. Subsequently, the dibenzaldehyde series was oxidized to the diformate ester derivatives (4a-d) in the presence of m-chloroperoxybenzoic acid (MCPBA), followed by hydrolysis of the formate to the corresponding diphenol series (5a-d) with good overall yields. Bisbenzoxazine

monomers (6a-d) were synthesized by the Mannich condensation of the diphenol derivatives (5a-d), butyl amine, and paraformaldehyde in xylenes at 120 °C. Among solvents evaluated for the benzoxazine synthesis, xylenes provided the products in highest yield and purity due to their high boiling point and low dielectric constant – two factors previously shown to improve the efficiency of the Mannich condensation and minimize the formation of oligomeric impurities.[40] The bisbenzoxazines were recrystallized in ethyl acetate to afford white crystals with high purity as shown by the $^{1}$H-NMR spectrum for the representative monomer 6b in Figure 2.

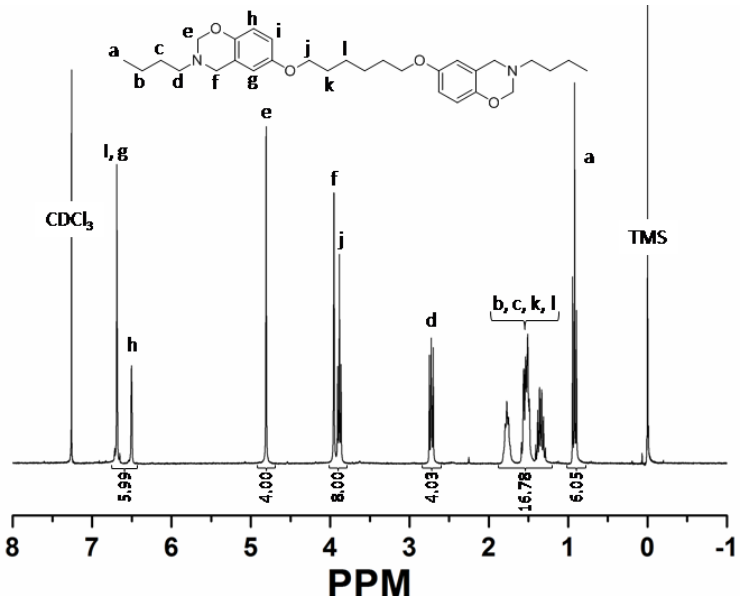


*Figure 2*. $^{1}$H NMR of bisbenzoxazine monomer BZ(6)BA (6b).

It is important to note that the current synthesis provides the first example of bisbenzoxazine monomers derived from a flexible bisphenol bridge – an approach that extends monomer design beyond the traditional but rigid bisphenol-A bridge. Complimentary to the flexible bisbenzoxazines derived from aliphatic diamines reported by Allen and Ishida,[35] this approach also enables the design of a broad range of flexible bisphenol derived benzoxazines by incorporation of any number of commercially available primary amine derivatives as pendent moieties to the monomer structure.

Hereafter, monomer abbreviations will follow as BZ(n)BA, where n equals the number of methylene repeat units in the structure.

*Cationic Ring-Opening Polymerization*

Cationic ring-opening polymerization of the monomer series BZ(n)BA was carried out according to a stepwise heating protocol of 100 °C (1h), 140 °C (1h), 160 °C (2h), and 180 °C (8h). The curing protocol was developed by considering the onset of thermal degradation obtained from TGA experiments (vide infra). Highly transparent polybenzoxazine films free from voids were prepared by sandwiching the monomer between two glass slides treated with RainX® to ensure facile removal of the film following the cure. In Appendix A, Figure A1 shows photos of pBZ(10)BA films cured in an air-circulation oven by the described sandwich method and in open atmosphere (i.e. film formed on a single glass slide). The pBZ(10)BA film cured in open atmosphere exhibit a reddish-brown color and is noticeably more brittle than the light yellow, flexible film cured by the sandwich method. This behaviour is likely due to oxidative effects of curing in open air. Similar sensitivity to cure environment of aliphatic diamine-linked benzoxazines were reported in detail by Allen and Ishida.[36] Thus, this behaviour was not investigated further. All samples for gATR-ATR, DMA, tensile tests, and TGA characterization were cut from films prepared and cured in the sandwich configuration in an air circulation oven as shown in Figure A1. The progress of the cationic ring-opening polymerization of monomers 6a-d was initially followed by gATR-FTIR. Figure 3 shows the representative FTIR spectra for the BZ(10)BA monomer (Figure 3a) and the respective polymer network (Figure 3b) following cationic ring-opening polymerization at 180 °C. The characteristic benzoxazine peaks observed for the monomer – one at 933 $cm^{-1}$ assigned to the out of plane C-H vibration of the benzene ring attached to the

oxazine ring, another at 1213 $cm^{-1}$due to C-O-C asymmetric stretch of the oxazine ring, and two peaks at 1498 $cm^{-1}$ and 804 $cm^{-1}$ assigned to the vibration of the tri-substituted benzene ring – are no longer present following the thermal cure at 180 °C. The diminished intensities of these peaks indicate high conversion is achieved for the ROP. Additionally, a new peak appears at 1479 $cm^{-1}$, corresponding to the tetra-substituted benzene ring that results from ring-opening polymerization of the benzoxazine.

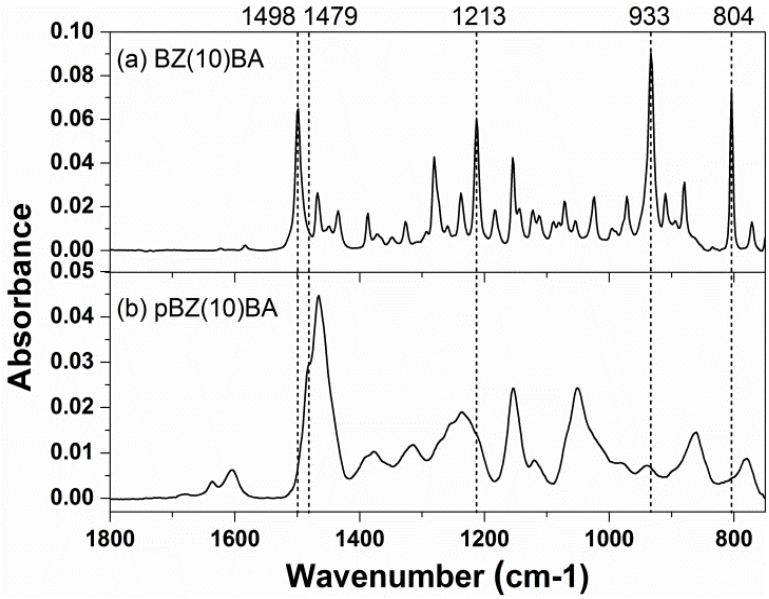


*Figure 3.* FTIR spectra of (a) BZ(10)BA monomer and (b) pBZ(10)BA polymer following cationic ring-opening polymerization at 180 °C. The results shown are representative for the monomer series.

The thermal curing behaviour of the BZ(n)BA monomer series was also studied by DSC. The DSC thermograms for the monomer series are shown in Figure 4. Monomer melting points – reported as the onset of the endothermic transition – initially decrease from 83.9 °C for BZ(4)BA to 71.5 °C for BZ(6)BA, but then increase almost linearly to 76.5 °C and 79.4 °C for BZ(8)BA and BZ(10)BA, respectively. As shown in Figure 4, the polymerization exotherms from the first heating cycle are characterized by a unimodal transition which broadens slightly as a function of aliphatic bisphenol chain length. The peak position of the polymerization exotherm is somewhat insensitive to the

structure of the monomer, but generally shifts to a higher temperature with increasing length of the aliphatic bisphenol linker. The exotherm magnitude is highest for BZ(4)BA, at 104.3 J/g and continuously decreases with longer aliphatic chain lengths to 48.5 J/g for BZ(10)BA – an expected result attributed to the dilution of the benzoxazine ring mass fraction with increasing bisphenol chain length. These observations are consistent with those reported by Allen and Ishida[36] for flexible benzoxazines derived from aliphatic diamines. Consistent with the FTIR data previously discussed, the second heating cycle (Figure 4, dashed lines) for each monomer exhibits little to no residual exotherm, indicating the ring-opening polymerization proceeds to near quantitative conversion under the DSC ramp conditions (i.e. $T_{max}$ 300 °C). A zoomed in view of the curing exotherm for BZ(4)BA can be found in Figure A2. It should be noted that the peak temperature of the cure exotherm (ca. 250 °C) coincides with the onset of degradative weight loss according to TGA (vide infra). However, we see no evidence of degradation in the second heating cycle, suggesting that the observed polymerization behaviour measured by DSC is not convoluted by degradation. This observation is likely due to the different cure environments between the DSC polymerizations (cured entirely under $N_2$) and TGA samples (cured by the sandwich method in an air circulation oven). To this end, DSC was also used to determine the extent of polymerization for oven-cured pBZ(n)BA samples prepared according to the previously described cure schedule in the sandwich configuration. Figure A2 shows the first and second heating cycles for pBZ(4)BA following an 8 h sandwich cure profile up to 180 °C in an air circulation oven, compared with the first heating cycle of monomer. The first heating run (dashed line) shows an exothermic transition beginning at 230 °C and peaking at 267 °C, which is attributed to residual cure as this is no longer observed in the second heating run (dotted line).

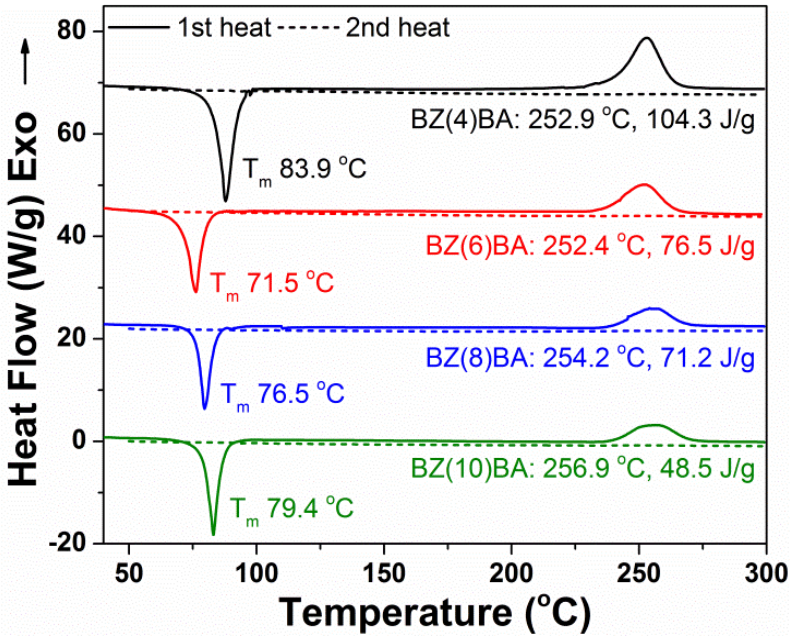


*Figure 4.* DSC thermograms for the BZ(n)BA monomer series. First (solid line) and second (dashed line) heating cycles are shown.

*Thermomechanical and tensile properties*

Thermomechanical transitions of the cured polybenzoxazine films were investigated using dynamic mechanical analysis in tension mode. The ratio E"/E' of the loss and storage moduli gives tan δ, a damping term, which relates the energy dissipation relative to the energy stored in the material upon periodic deformation. The glass transition temperature was determined from the peak maximum of the tan δ curve. Figure 5a shows the tan δ curves for the pBZ(n)BA series. As expected, the pBZ(n)BA films show a systematic decrease in $T_g$ – from 101 °C for pBZ(4)BA to 66.5 °C for pBZ(10)BA – with increasing aliphatic bisphenol chain length. Figure 5b shows the temperature dependence of the storage modulus for the pBZ(n)BA series. As shown, the sub-$T_g$ storage modulus is dependent on the length of the aliphatic bisphenol linker with the film decreasing in stiffness as the length of the linker increases from n=4 ($E'_{30°C}$ = 796 MPa) to n=10 ($E'_{30°C}$= 602 MPa). Similar trends are observed through the glass transition and into the rubber plateau region, where the rubbery storage modulus is higher

for samples with shorter aliphatic bisphenol chain lengths, although E' values for pBZ(6)BA and pBZ(8)BA essentially coincide in the rubbery plateau region. For the purpose of comparison, the crosslink density ($p_x$) of the pBZ(n)BA samples was estimated from the rubbery plateau storage modulus at $T_g$+ 40 °C according to the theory of rubber elasticity[41] (Eq. 1).

$$p_x = E'/2(1+\gamma)RT \qquad (1)$$

In equation 1 E´ is the rubbery storage modulus at temperature T, R is the gas constant, and γ is Poisson's ratio, which is assumed to be 0.5 for incompressible networks. If the sample density is known, then the molecular weight between cross-links ($M_c$) can be calculated according to Eq. 2.

$$M_c = 3\rho RT/E' \qquad (2)$$

In equation 2 ρ is sample density, determined using Archimedes' Principle in the present case. It should be mentioned that the above equations typically apply only to lightly cross-linked networks, thus the values should be taken as qualitative comparisons. As shown in Appendix A (Table A1), the calculated $p_x$ values decrease from $1.16 \times 10^{-3}$ mol $cm^{-3}$ for pBZ(4)BA to $0.786 \times 10^{-3}$mol $cm^{-3}$ for pBZ(10)BA. The decrease in the cross-link density as a function of increasing length of the aliphatic bisphenol linker is, as expected, consistent with decreasing the rigidity and increasing the distance between the reactive functional groups – a trend that is also illustrated by the calculated $M_c$ values shown in Table 1. The crosslink densities and trends for the pBZ(n)BA series also compare favourably with crosslink density values previously published for bisphenol-A based benzoxazines ($1.1\times10^{-3}$mol $cm^{-3}$to $1.7\times10^{-3}$mol $cm^{-3}$),[35, 42] where the rigidity and length of the bisphenol-A linker yields polybenzoxazine thermosets with a higher

modulus and crosslink density than the flexible pBZ(n)BA materials reported in the current work.

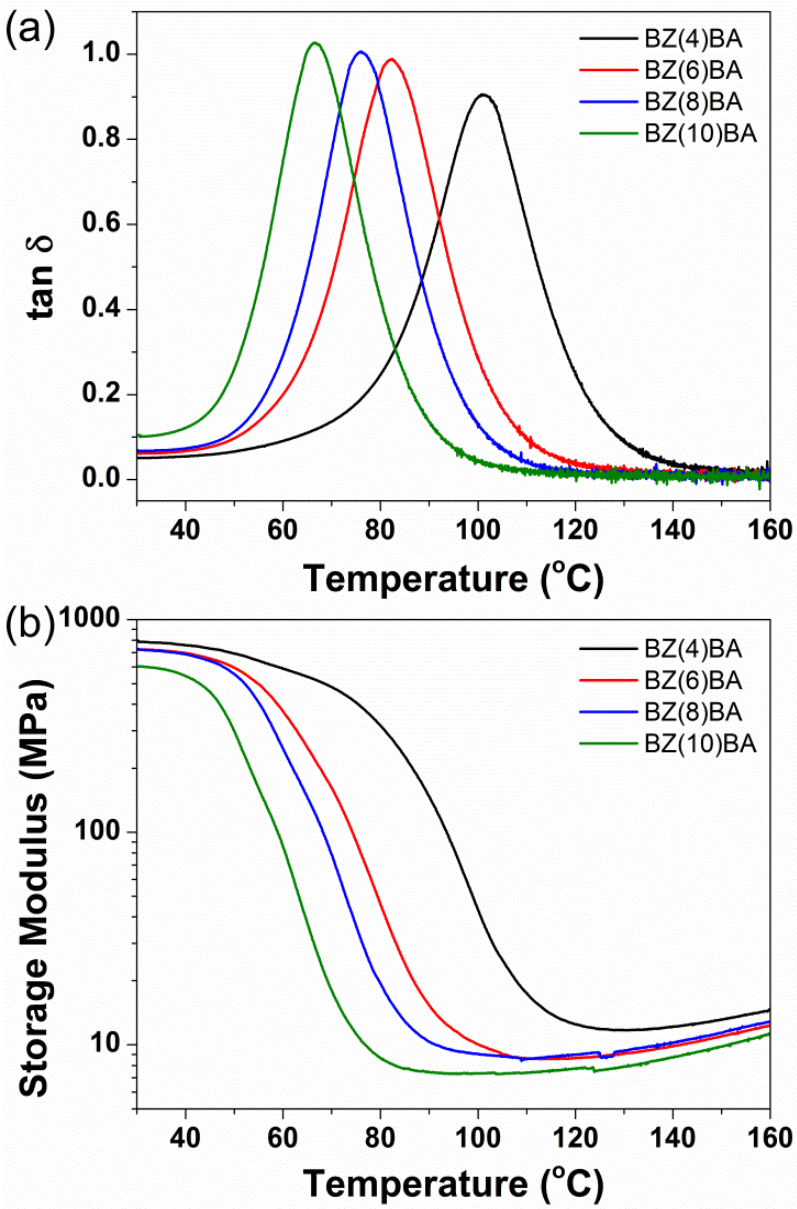


*Figure 5.* Plots of a) tan δ vs. temperature and b) storage modulus vs. temperature for the pBZ(n)BA thermoset series.

It is notable that the thermomechanical properties and crosslink densities for the pBZ(n)BA materials differ significantly from benzoxazine monomers of similar linker lengths derived from aliphatic diamines reported by Allen and Ishida.[35, 36] Namely, storage moduli, $T_g$, and crosslink densities are lower for aliphatic bisphenol linked

benzoxazines than those linked with aliphatic diamines.[42] The lower $T_g$ and storage modulus in our pBZ(n)BA materials can be attributed to the presence and conformational flexibility of the ether linkage in the aliphatic bisphenol structure, as incorporation of ether linkages is a commonly used strategy to induce similar trends in a broad range of polymeric materials,[43] including recently reported main chain benzoxazines.[34] While differences in cure profile and environment certainly also contribute, these contrasting properties highlight the ability to significantly tailor polybenzoxazine properties via small changes in monomer molecular design. Figure 6 presents the stress-strain curves obtained from the tensile tests of the pBZ(n)BA films. The data are also summarized in Table 1. The results reveal a small dependence of Young's modulus on the aliphatic bisphenol chain length, where modulus decreases from 19.5MPa for pBZ(4)BA to 13.0MPa for pBZ(10)BA. Elongation at break clearly increases as a function of increasing aliphatic bisphenol chain length, from 6.47% for pBZ(4)BA to 9.71% for pBZ(10)BA. For comparison, Young's modulus and elongation at break have been reported at 3.3 – 4.3 GPa and 1.3%, respectively, for rigid bisphenol-A based benzoxazines.[44, 45] Replacing the methylethylidene linker of bisphenol-A with more flexible aliphatic chains clearly illustrates the effect of molecular architecture and molecular weight between cross-links on tensile properties.

*Thermal stability of the polybenzoxazine thermoset*

The onset of thermal degradation plays an important role in designing an appropriate cure schedule for the aliphatic bisphenol based benzoxazines. Thermogravimetric analysis was used to characterize the thermal stability of the pBZ(n)BA thermosets. Figure 7 shows the TGA thermograms for the pBZ(n)BA series as a function of increasing aliphatic bisphenol chain length. The thermal degradation

values are summarized in Table A1. As illustrated by the 2% weight loss values ($T_d$2%), the onset of thermal degradation depends on the length of the aliphatic chain, where the highest $T_d$2%, at 206 °C, was observed for the shortest chain length system of pBZ(4)BA. pBZ(6)BA exhibited the lowest onset of degradation, whereas pBZ(8)BA and pBZ(10)BA show minimal dependence of weight loss on chain length.

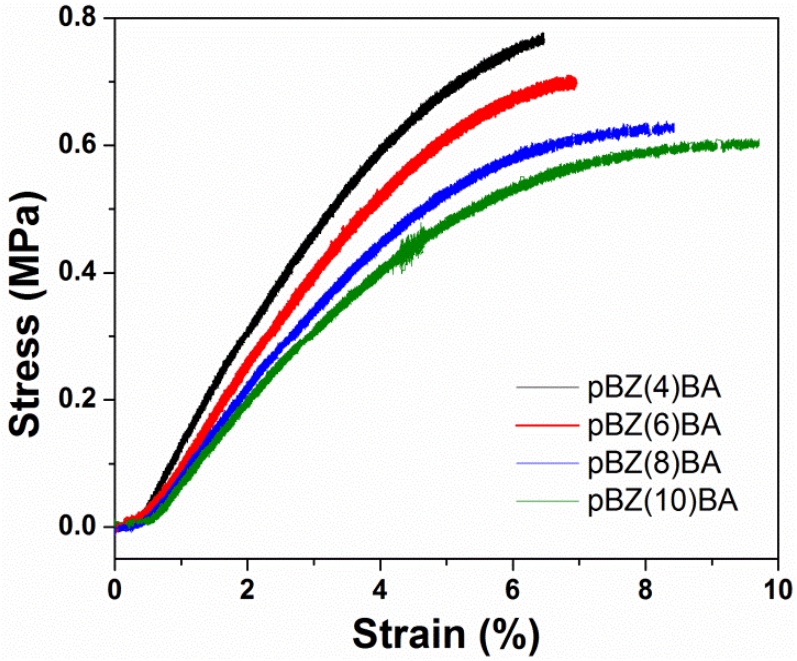


*Figure 6.* Stress-strain curves for the pBZ(n)BA series.

As expected, the char yield systematically decreases, from 19.7% for pBZ(4)BA to 14.4% for pBZ(10)BA, with increasing aliphatic chain length owing to a decrease in aromatic content in the thermoset network. From the derivative weight loss curves, the pBZ(n)BA thermosets degrade in a three step process. Without further analysis of the gaseous by-products by spectroscopic analysis, one can only speculate, based on previous observations of aliphatic amine derived benzoxazines,[46] that the lowest temperature degradation is associated with the degradation of the Mannich bridge and the loss of the aliphatic amine constituents; whereas the primary degradation step involves fragmentation and loss of aliphatic phenol by-products.

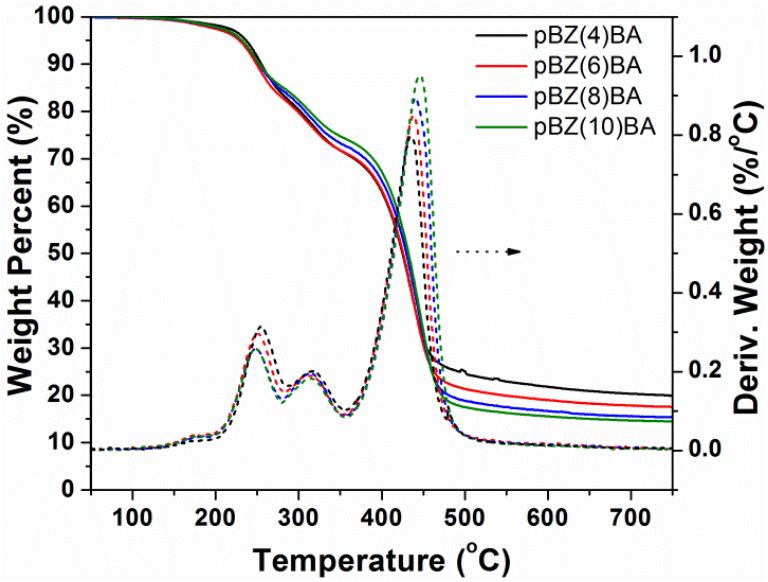


*Figure 7.* Degradation profiles and derivatives from TGA for the pBZ(n)BA series.

## Conclusions

The successfully synthesis of a series of novel aliphatic-bridged bisphenol-based benzoxazine monomers comprising four to ten methylene spacer units is reported. Thermally-accelerated cationic ring-opening polymerization of these bisbenzoxazine monomers provided flexible, uniform polybenzoxazine thermoset thin films under solvent-free conditions. FTIR and DSC analysis of the ring-opening polymerization show that the polymerizations proceed to high conversion, with minimal dependence on the length of the aliphatic-bridged bisphenol linker. However, thermomechanical properties of the pBZ(n)BA, such as rubbery storage modulus and glass transition temperature, show a strong dependence on the length of the aliphatic-bridged bisphenol linker where both properties decreased with increasing linker length. In particular, the glass transition temperature of the pBZ(n)BA series could be tailored over a 35 °C temperature range simply by changing the length of the aliphatic-bridged bisphenol linker. Tensile properties of the pBZ(n)BA series were shown to follow similar trends with Young's modulus decreasing and elongation at break increasing with increasing

aliphatic-bridged bisphenol linker length. It is important to note that the presence and conformational flexibility of the ether linkage in the aliphatic bisphenol structure plays an important role in lowering the $T_g$ and improving the flexibility and mechanical properties of the pBZ(n)BA materials. Regarding thermal stability, the pBZ(n)BA materials all show a similar three mode degradation process by TGA consistent with other bisphenol-based polybenzoxazines, and additionally exhibit a decrease in char yield with increasing aliphatic chain length owing to a decrease in aromatic content in the thermoset network. While it is not expected that the aliphatic-bridged bisphenol-based benzoxazines will replace bisphenol-A derivatives in high temperature, high modulus applications, the flexible derivatives may find use in membrane and coatings applications where improved flexibility and tuneable thermomechanical properties are beneficial.

## Acknowledgments

The author gratefully acknowledges financial support from the National Science Foundation (NSF CAREER DMR-1056817) and the Office of Naval Research (Award N00014-07-1-1057). ADB acknowledges support from a fellowship from the National Science Foundation GK-12 program “Molecules to Muscles” (Award #0947944) through The University of Southern Mississippi. GT was funded through an NSF-REU (DMR-1005127).

REFERENCES


1. Yagci, Y.; Kiskan, B.; Ghosh, N. N., *J. Polym. Sci. A: Polym. Chem.* **2009,** *47* (21), 5565-5576.
2. Ghosh, N.; Kiskan, B.; Yagci, Y. *Prog. Polym. Sci.* **2007,** *32* (11), 1344-1391.
3. Ishida, H.; Allen, D. J. *J. Polym. Sci. B Polym. Phys.* **1996,** *34* (6), 1019-1030.
4. Ishida, H.; Agag, T. *Handbook of Benzoxazine Resins*. Elsevier: Amsterdam, **2011**.
5. Ning, X.; Ishida, H., *J. Polym. Sci. A: Polym. Chem.* **1994,** *32* (6), 1121-1129.
6. Takeichi, T.; Agag, T. *High Perform. Polym.* **2006,** *18* (5), 777-797.
7. Kim, H. D.; Ishida, H. *J. Phys. Chem. A* **2002,** *106* (14), 3271-3280.
8. Kim, H.-D.; Ishida, H. *Macromol. Symp.* **2003,** *195* (1), 123-140.
9. Jang, J.; Seo, D. *J. Appl. Polym. Sci.* **1998,** *67* (1), 1-10.
10. Ishida, H.; Lee, Y. H. *Polym. Polym. Compos.* **2001,** *9* (2), 121-134.
11. Ishida, H.; Allen, D. J. *Polymer* **1996,** *37* (20), 4487-4495.
12. Yeganeh, H.; Razavi-Nouri, M.; Ghaffari, M. *Polym. Advan. Technol.* **2008,** *19* (8), 1024-1032.
13. Takeichi, T.; Guo, Y. *Polymer Journal* **2001,** *33* (5), 437-443.
14. Agag, T.; Tsuchiya, H.; Takeichi, T. *Polymer* **2004,** *45* (23), 7903-7910.
15. Liu, Y.; Zheng, S. *J. Polym. Sci. A: Polym. Chem.* **2006,** *44* (3), 1168-1181.
16. Wu, Y. C.; Kuo, S. W. *Polymer* **2010,** *51* (17), 3948-3955.
17. Huang, K. W.; Kuo, S. W. *Polym. Composite* **2011,** *32* (7), 1086-1094.
18. Ergin, M.; Kiskan, B.; Gacal, B.; Yagci, Y. *Macromolecules* **2007,** *40* (13), 4724-4727.

19. Oie, H.; Sudo, A.; Endo, T. *J. Polym. Sci. A: Polym. Chem.* **2011,** *49* (14), 3174-3183.

20. Agag, T.; Vietmeier, K.; Chernykh, A.; Ishida, H. *J. Appl. Polym. Sci.* **2012,** *125* (2), 1346-1351.

21. Kukut, M.; Kiskan, B.; Yagci, Y. *Des. Monomers Polym.* **2009,** *12* (2), 167-176.

22. Chernykh, A.; Liu, J.; Ishida, H. *Polymer* **2006,** *47* (22), 7664-7669.

23. Chou, C. I.; Liu, Y. L. *J. Polym. Sci. A: Polym. Chem.* **2008,** *46* (19), 6509-6517.

24. Kiskan, B.; Yagci, Y.; Ishida, H. *J. Polym. Sci. A: Polym. Chem.* **2008,** *46* (2), 414-420.

25. Nagai, A.; Kamei, Y.; Wang, X. S.; Omura, M.; Sudo, A.; Nishida, H.; Kawamoto, E.; Endo, T. *J. Polym. Sci. A: Polym. Chem.* **2008,** *46* (7), 2316-2325.

26. Velez-Herrera, P.; Doyama, K.; Abe, H.; Ishida, H. *Macromolecules* **2008,** *41* (24), 9704-9714.

27. Chernykh, A.; Agag, T.; Ishida, H. *Polymer* **2009,** *50* (2), 382-390.

28. Kiskan, B.; Aydogan, B.; Yagci, Y. *J. Polym. Sci. A: Polym. Chem.* **2009,** *47* (3), 804-811.

29. Agag, T.; Geiger, S.; Alhassan, S. M.; Qutubuddin, S.; Ishida, H. *Macromolecules* **2010,** *43* (17), 7122-7127.

30. Aydogan, B.; Sureka, D.; Kiskan, B.; Yagci, Y. *J. Polym. Sci. A: Polym. Chem.* **2010,** *48* (22), 5156-5162.

31. Liu, J.; Agag, T.; Ishida, H. *Polymer* **2010,** *51* (24), 5688-5694.

32. Agag, T.; Arza, C. R.; Maurer, F. H. J.; Ishida, H. *J. Polym. Sci. A: Polym. Chem.* **2011,** *49* (20), 4335-4342.

33. Dogan Demir, K.; Kiskan, B.; Yagci, Y. *Macromolecules* **2011,** *44* (7), 1801-1807.

34. Lin, C. H.; Chang, S. L.; Shen, T. Y.; Shih, Y. S.; Lin, H. T.; Wang, C. F. *Polym. Chem.* **2012,** *3* (4), 935-945.

35. Allen, D. J.; Ishida, H. *J. Appl. Polym. Sci.* **2006,** *101* (5), 2798-2809.

36. Allen, D. J.; Ishida, H. *Polymer* **2007,** *48* (23), 6763-6772.

37. Allen, D. J.; Ishida, H. *Polymer* **2009,** *50* (2), 613-626.

38. Agag, T.; Akelah, A.; Rehab, A.; Mostafa, S. *Polym. Int.* **2012,** *61* (1), 124-128.

39. Hamerton, I.; Howlin, B. J.; Klewpatinond, P.; Takeda, S. *Macromolecules* **2009,** *42* (20), 7718-7735.

40. Agag, T.; Jin, L.; Ishida, H. *Polymer* **2009,** *50* (25), 5940-5944.

41. Flory, P. J. *Polymer* **1979,** *20* (11), 1317-1320.

42. Li, X.; Xia, Y.; Xu, W.; Ran, Q.; Gu, Y. *Polym. Chem.* **2012,** *3* (6), 1629-1633.

43. Hsiao, S.-H.; Chang, H.-Y. *J. Polym. Sci. A: Polym. Chem.* **1996,** *34* (8), 1421-1431.

44. Ishida, H.; Allen, D. J. *Journal of Polymer Science Part B: Polymer Physics* **1996,** *34* (6), 1019-1030.

45. Ardhyananta, H.; Kawauchi, T.; Ismail, H.; Takeichi, T. *Polymer* **2009,** *50* (25), 5959-5969.

46. Low, H. Y.; Ishida, H. *J. Polym. Sci., Part B: Polym. Phys.* **1998,** *36* (11), 1935-1946.

# CHAPTER IV

# SOLVENT-FREE COPOLYMERIZATION OF RIGID AND FLEXIBLE BIS-1,3-BENZOXAZINES: FACILE TUNABILITY OF POLYBENZOXAZINE NETWORK PROPERTIES

## Introduction

Polybenzoxazines (pBZ) are a relatively new class of addition-cure, thermosetting phenolic resins that have recently attracted much attention as matrices for high performance applications, such as aerospace and marine composites. Polybenzoxazine thermosets are derived from heterocyclic bis-1,3-benzoxazine monomers that undergo cationic ring-opening polymerization (ROP) at elevated temperatures (>150°C) – in the absence of catalysts and without byproducts – producing a cross-linked polymer network comprised of a phenol and a tertiary amine bridge as the structural motif (Scheme 6). Intermolecular and intramolecular hydrogen bonding interactions between the phenol and tertiary amine give rise to many salient features observed in polybenzoxazines, including high glass transition temperature ($T_g$), high thermal stability, low surface energy, low water adsorption, excellent dimensional stability, flame resistance, and stable dielectric constants.[1-4] Advancing the utility of pBZ materials for a broad array of applications continues to focus on reducing the temperature required for cure, increasing processability, and improving the mechanical properties of the thermoset resins. Efforts focused on the latter include rubber toughening,[5, 6] blending with epoxies,[7, 8] polyurethanes,[9, 10] inorganics,[11-14] monomer design,[15-19] and synthesis of side[20-23] and main-chain benzoxazine polymer precursors.[24-36] Strategies that focus on design of new monomer structures to tailor network properties take advantage of the inherent simplicity of benzoxazine synthesis to achieve outstanding versatility in molecular design of

benzoxazine precursors.[16, 18, 37] Recently, the synthesis of a series of novel aliphatic-bridged bisphenol-based benzoxazines that exhibited tunable thermomechanical and mechanical properties by varying the length of the aliphatic bridged bisphenol used in the monomer synthesis have been reported.[37] Using four to ten methylene units in the bisphenol bridge, the $T_g$ of the resulting thermosets could be varied over a range of 35 °C (from 66 °C– 101 °C); however, the approach required the synthesis of four individual benzoxazine monomers to span the reported range of thermomechanical properties. Strategies that enable broader tunability of polybenzoxazine network properties with fewer synthetic steps are desirable.

Copolymerization is a valuable tool for tailoring the properties of polymeric materials for a broad range of applications, but surprisingly few examples of copolymerization of compatible benzoxazine monomers have been reported to date.[38-42] In one early example, Su and Chang copolymerized a series of fluorinated benzoxazine monomers to tailor the dielectric properties of the resulting thermosets and, in addition, showed that the $T_g$ could be varied with monomer composition.[40] The same authors also reported the effects of bulky substituents on the copolymerization of adamantine functionalized benzoxazine monomers.[43] In 2007, Liu and coworkers reported the copolymerization of a siloxane-containing benzoxazine monomer and illustrated the effects of the flexible siloxane spacer on the thermal and thermomechanical properties of the networks.[39] In each of the aforementioned examples, solvent was employed to form homogeneous monomer mixtures, and as a result, required a solvent removal step prior to copolymerization. In this section, the copolymerization of two high $T_g$ benzoxazine monomers – one derived from bisphenol A and aniline (Araldite 35600) and another derived from 4,4'-thiophenol and aniline (Araldite 35900) – with a low $T_g$ flexible

aliphatic-bridged bisphenol-based benzoxazine monomer comprising ten methylene units under solvent-free conditions is reported. Taking full advantage of the inherently low melt viscosity of these benzoxazine monomers, cationic ring-opening polymerization (ROP) of melt-mixed monomer mixtures provides pBZ copolymer networks with excellent homogeneity.

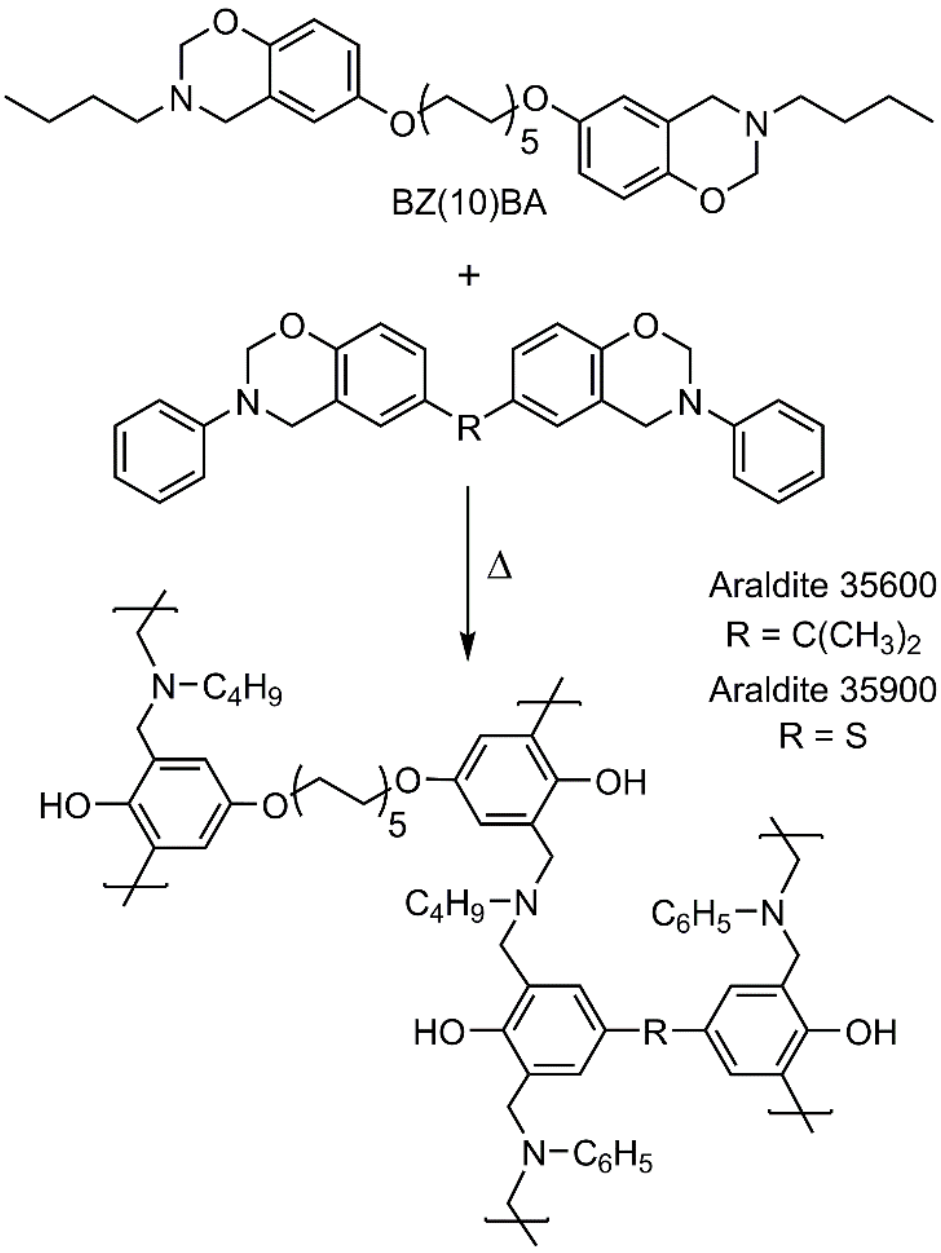


*Scheme 6.* Copolymerization of the flexible BZ(10)BA monomer with rigid Araldite monomers.

The copolymerization behavior as a function of comonomer feed is investigated using DSC. In addition, we show that simply by varying the composition of the monomer feed, the $T_g$ of the resulting pBZ networks can be tuned from 67 °C to 216 °C – a thermomechanical properties window of approximately 149 °C. The thermal stability of the pBZ networks as function of monomer feed composition is also discussed.

## Experimental

### *Materials*

All reagents and solvents were obtained at the highest purity available from Sigma Aldrich and used without further purification unless otherwise specified. Paraformaldehyde was purchased from Acros Organics. Anhydrous potassium carbonate, magnesium sulfate, and sodium hydroxide were purchased from Fisher Scientific. Araldite 35600 and Araldite 35900 were generously donated from Huntsman Advanced Materials. The synthesis of the aliphatic bridged benzoxazine monomer 1,10-bis((3-butyl-3,4-dihydro-2H-benzo[e][1,3]oxazin-6-yl)oxy) decane (BZ(10)BA) was prepared according to a previous publication.[37]

### *Synthesis of 4,4'-(Decane-1,10-diylbis(oxy))dibenzaldehyde*

Into a 250 mL round bottom flask fitted with a condenser, 8.612 g (0.0287 mol) of 1,10-dibromodecane, 7.007 g (0.0574 mol) of 4-hydroxybenzaldehyde and 15.8665 g (0.1148 mol) of anhydrous potassium carbonate were added to approximately 100 mL of dimethylformamide. The flask was set in an oil bath and refluxed at 110°C for 48 h. The solution was cooled to room temperature, diluted with dichloromethane, and washed with water. The organic layer was dried over $MgSO_4$ and evaporated under vacuum to an off white solid. (92.4% yield) $^1$H NMR ($CDCl_3$), ppm: $\delta$ = 1.29–1.81 (16H, m, $CH_2$), 3.98 (4H, t, $CH_2$–O), 6.94 (4H, s, CH, aromatic), 7.77 (4H, d, CH, aromatic), 9.82 (2H, s,

CH=O, aldehyde); $^{13}$C NMR ($CDCl_3$), ppm: δ = 25.91, 29.00, 29.27, 29.41 (8C, $CH_2$), 68.34 (2C, $CH_2$–O), 114.70 (4C, CH, aromatic), 129.68 (2C, C, aromatic), 131.91 (4C, CH, aromatic), 164.19 (2C, C, aromatic), 190.69 (2C, CH aldehyde).

*Synthesis of (Decane-1,10-diylbis(oxy))bis(4,1-phenylene) diformate*

Into a 500 mL round bottom flask, 8.415 g (0.022 mol) of 4,4'-(Decane-1,10-diylbis(oxy))dibenzaldehyde was dissolved in 150–200 mL of dichloromethane, and 14.68 g (0.0891 mol) of metachloroperoxybenzoic acid (MCPBA) was added in portions to the solution. The reaction was then capped and purged with nitrogen gas for 10 min, and then set to stir at room temperature for 3–4 h. 112 mL of a saturated sodium bicarbonate solution was added to the solution and stirred for an additional 2 h at room temperature. The solution was extracted with dichloromethane and washed with 10% sodium metabisulfite followed by washing with water. The organic layer was dried over $MgSO_4$ and evaporated under vacuum to give a light yellow solid. (93.3% yield) $^1$H NMR ($CDCl_3$), ppm: δ = 1.30–1.83 (16H, m, $CH_2$), 4.00 (4H, t, CH–O), 6.97 (4H, d, CH, aromatic), 7.10 (4H, d, CH, aromatic), 8.39 (2H, s, O–CH=O, formate); $^{13}$C NMR ($CDCl_3$), ppm: δ = 25.99, 29.00, 29.20, 29.33, 29.46 (8C, $CH_2$), 68.39 (2C, CH2–O), 115.21 (4C, CH, aromatic), 121.88 (4C, C, aromatic), 143.18 (2C, C, aromatic), 157.21 (2C, C, aromatic), 159.79 (2C, CH formate).

*Synthesis of 4,4'-(Decane-1,10-diylbis(oxy))diphenol*

Into a 500 mL round bottom flask fitted with a condenser, 3.002 g (0.0068 mol) of (Decane-1,10-diylbis(oxy))bis(4,1-phenylene) diformate was added to a solution of 1.082 g, (0.0271 mol) sodium hydroxide in 50 mL of ethanol and 20 mL of water. The solution was refluxed at 100°C for 24 h. The solution was cooled to room temperature and acidified with 3M HCl. The product precipitated and was extracted with ethyl acetate.

The organic layers were combined, washed with 3M HCl and water, and dried over $MgSO_4$. The solution was filtered, and solvent was removed by rotary evaporation to give a brown solid. (91.0% yield) $^1$H NMR(acetone-$d_6$), ppm: δ = 1.35–1.74 (16H, m, $CH_2$), 3.88 (4H, t, $CH_2$–O), 6.75 (8H, m, CH, aromatic), 7.81 (2H, s, OH); $^{13}$C NMR (acetone-$d_6$), ppm: δ = 25.92, 29.30, 29.39 (8C, $CH_2$), 68.12 (2C, $CH_2$–O), 115.33 (4C, CH, aromatic), 115.68 (4C, CH, aromatic), 151.13 (2C, C, phenol), 152.52 (2C, C, ether).

*Synthesis of 1,10-Bis((3-butyl-3,4-dihydro-2H-benzo[e][1,3]oxazin-6-yl)oxy) decane (BZ(10)BA)*

Into a 100 mL round bottom flask fitted with a condenser, 1.183 g (0.0033 mol) of 4,4'-(Decane-1,10-diylbis(oxy))diphenol, 0.4827 g (0.0066 mol) of butylamine and 0.3964 g (0.0132 mol) paraformaldehyde were suspended in 7.9 mL of xylene and placed in an oil bath heated to 120°C. Once at temperature, the reactants dissolved and aliquots were taken at 5 minute intervals and observed via $^1$H NMR to monitor the progress of the reaction. Upon completion of the reaction (~15 to 20 min), the reaction was cooled to room temperature, and the xylene was evaporated. The crude residue was then diluted with excess ethyl acetate and stirred with basic alumina for 10 min, filtered, and evaporated under vacuum to give an off white solid. The crude benzoxazine was then recrystallized in cold ethyl acetate to afford white crystals. (38.9% yield) $^1$H NMR ($CDCl_3$), ppm: δ = 0.91 (6H, t, $CH_3$), 1.27–1.80 (24H, m, $CH_2$), 2.73 (4H, t, ($CH_3$)–N), 3.87 (4H, t, $CH_2$–O), 3.95 (4H, s, $CH_2$, oxazine), 4.80 (4H, s, $CH_2$, oxazine), 6.50 (2H, s, CH, aromatic), 6.67 (4H, s, CH, aromatic); $^{13}$C NMR ($CDCl_3$), ppm: δ = 13.95 (2C, $CH_3$), 20.38, 26.04, 29.36, 29.38, 29.48, 30.26 (12C, CH2), 50.51 (2C, $CH_3$–N), 51.11 (2C, $CH_2$–N, oxazine), 68.51 (2C, CH2–O), 82.28 (2C, $CH_2$–O, oxazine), 112.92, 114.16, 116.85, 120.77, 147.98, 152.93 (12C, aromatic).

*Polybenzoxazine film preparation*

Due to the low melt viscosities of benzoxazine monomers, homogeneous mixtures of the monomer pairs at any ratio were easily achieved by heating the solid monomers in a test tube above their melting points (70 – 75 °C) followed by vortex mixing for less than 10 seconds. The benzoxazine monomer mixtures were then cured into films using previously reported methods.[37] Briefly, 150–200 mg of the monomer mixture was placed in the center of a RainX® coated 75×50 mm glass slide and heated gently with a heat gun until the monomer was molten and all air bubbles were removed. Teflon spacers (thickness ~130 μm) were inserted on the sides of a glass slide, and a second RainX® coated 75×50mm glass slide was gently placed on the top making sure bubbles were excluded when 'sandwiching' the monomer. The glass slides were clamped together, and the sandwiched monomer assembly was quickly placed in a preheated oven at 100 °C. The thermal step cure proceeded as follows: 100 °C for 1h, 140 °C for 1h, 160 °C for 2h, and180 °C for 4h. After the cure procedure, the film was removed from the glass slides and washed with methanol to remove any residual RainX® on the cured film.

*Characterization*

Using a Varian Mercury Plus 300 MHz NMR spectrometer operating at a frequency of 300 MHz with tetramethylsilane as an internal standard $^{1}$H-NMR and $^{13}$C-NMR measurements were performed in deuterated chloroform ($CDCl_3$) and deuterated acetone ($(CD_3)_2CO$) to determine purity of the synthesized molecules. The number of transients for $^{1}$H and $^{13}$C are 32 and 256, respectively, and a relaxation time of 5 s was used for the integrated intensity determination of $^{1}$H NMR spectra.

Differential scanning calorimetry (DSC) was performed to monitor the ring-opening polymerization using a TA instruments DSC Q200 differential scanning

calorimeter at a heating rate of 5 °C min $^{-1}$ and a nitrogen flow rate of 50 mL min $^{-1}$. Samples were crimped in hermetic aluminum pans with lids. Dynamic mechanical analysis(DMA) was performed on a TA Instruments Q800 DMA in tension film mode with a heating rate of 2 °C min $^{-1}$ from 30 °C to 300 °C at 1 Hz. Samples were prepared using the sandwich method previously described and cut into bars. The glass transition temperature, $T_g$, was taken as the peak of the tan δ curve.

Thermogravimetric analysis (TGA) was performed using a TA Instruments Q50 thermogravimetric analyzer with a platinum pan for samples containing Araldite 35600 and a ceramic pan for samples containing Araldite 35900. Samples were heated at 20 °C min $^{-1}$ from 40°C to 800°C under a nitrogen atmosphere to determine thermal stability.

Atomic force microscopy (AFM) images were collected with a Bruker Dimension Icon operating in tapping mode usingVISTAprobesT300R probes (silicon probe with aluminum reflective coating, spring constant: 40 N/m) to observe any phase separation that may occur.

## Results and discussion

### *Cationic ring-opening copolymerization (ROP)*

The bis-1,3-benzoxazine monomer comprising a ten methylene unit spacer, BZ(10)BA, was prepared in good yield and with high purity according to our previous publication.[37] According to Scheme 6, BZ(10)BA was copolymerized with two commercially available bisbenzoxazine monomers including Araldite 35600 and Araldite 35900. The monomer feed ratios were varied on a weight basis from 9:1 BZ(10)BA:Araldite to 1:9 BZ(10)BA:Araldite. Comonomer mixtures were prepared under solvent-free conditions by heating the solid monomers above the melting point followed by vortex mixing. The copolymerization behavior of the benzoxazine monomer

mixtures was monitored by DSC under nitrogen (50 mL min $^{-1}$) at heating rate of 5 °C min $^{-1}$ from room temperature to 300 °C. The DSC thermograms for the BZ(10)BA:Araldite 35600 and BZ(10)BA:Araldite 35900 are shown in Figures 8 and 9, respectively. It is well know that 1,3-benzoxazines exhibit exothermic transitions in the range of 200 – 250 °C – transitions that can be attributed to the cationic ring-opening polymerization process. Araldite 35600, the typical bisphenol A-aniline base benzoxazine monomer, shows a sharp exothermic transition with an onset around 207 °C and a peak maximum at 220 °C (Figure 8a). With the addition of BZ(10)BA into the monomer feed, the onsets and the peak maxima of the copolymerization exothermic transitions gradually shifted to higher temperatures where, for example, the 5:5 BZ(10)BA:Araldite 35600 feed ratio exhibited an onset of 213°C and a peak maximum at 231°C (Figure 8f).With further increases in the monomer feed ratio, the copolymerization cure behavior approaches that of pure BZ(10)BA which shows an onset of 231 °C and a peak maximum at 246 °C (Figure 8k). As shown in Figure 9a-k, the copolymerization behavior of BZ(10)BA:Araldite 35900 exhibited similar trends with exotherm peak maxima between that of neat Araldite 35900 (205 °C) and neat BZ(10)BA (246 °C). The exothermic enthalpies obtained from DSC for the homo- and copolymerizations of BZ(10)BA:Araldite 35600 and BZ(10)BA:Araldite 35900 are shown in Figure 10. In both comonomer systems, the exothermic enthalpies gradually decrease as the amount of BZ(10)BA in the feed is increased – from approximately 390 J/g for the neat Araldite monomers to 79 J/g for the neat BZ(10)BA monomer. The trends observed in the polymerization enthalpies and in the position of the exotherm peak maxima for both BZ(10)BA:Araldite 35600 and BZ(10)BA:Araldite 35900 comonomer systems can be explained in the context of several variables, including molecular structure and molecular

weight of the monomers. The increase in exotherm peak maxima and decrease in total exotherm at higher BZ(10)BA concentrations can be attributed to lower ring strain associated with the flexible, aliphatic substituted BZ(10)BA monomer.

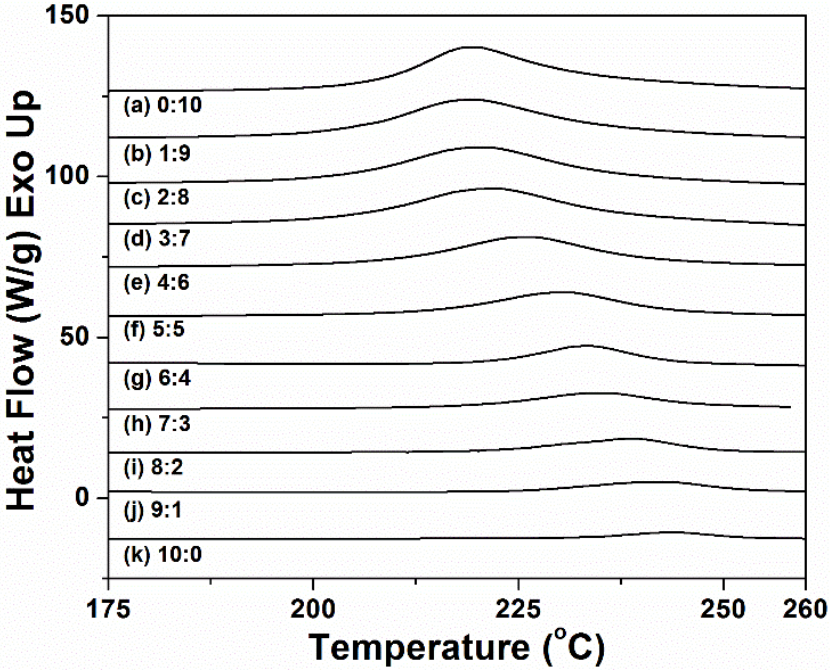


*Figure 8.* DSC thermograms of BZ(10)BA:Araldite 35600 comonomer feeds.

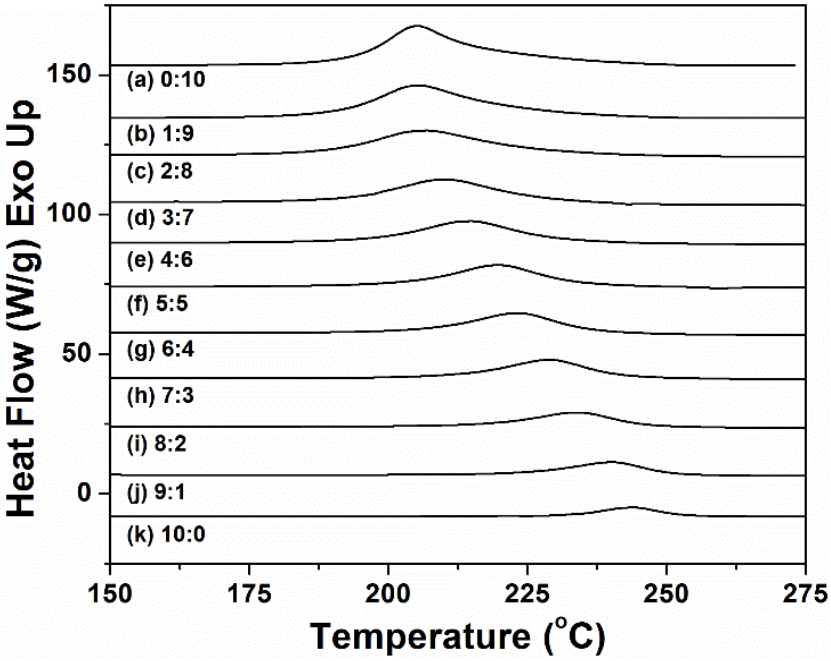


*Figure 9.* DSC thermograms of BZ(10)BA:Araldite 35900 comonomer feeds.

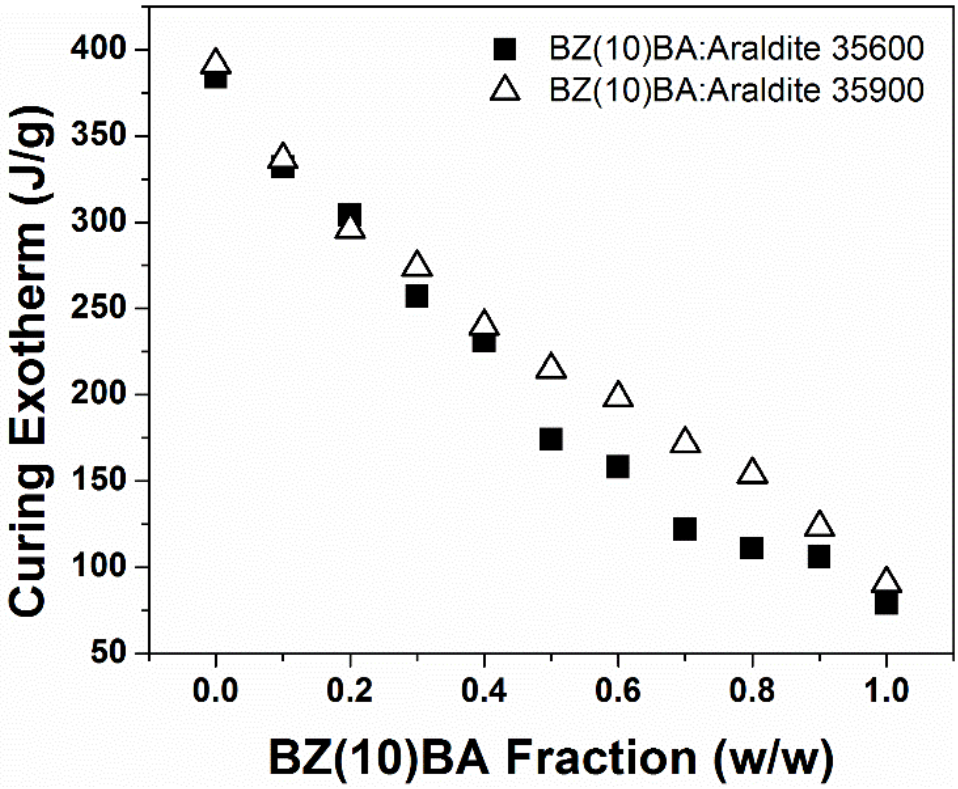


*Figure 10.* Exothermic enthalpies obtained from DSC for the homo- and copolymerizations of BZ(10)BA:Araldite 35600 (■) and BZ(10)BA:Araldite 35900 (△) as a function of monomer feed composition.

In contrast, the rigidity of the two aniline based Araldite monomers gives rise to higher ring strain, resulting in lower cure temperatures and higher polymerization enthalpies– an observation consistent with previous literature.[44] Activation energies ($E_a$) for the polymerizations, determined from the DSC data at various heating rates using the Ozawa method[45] (Figures B4-7) are also consistent with the observed trends. Namely, the $E_a$ values for Araldite 35600, Araldite 35900, and BZ(10)BA were 79.7 kJ/mol, 91.4 kJ/mol, and 119.2 kJ/mol, respectively, while the copolymerization $E_a$ values were intermediate to homopolymerizations. For example, the $E_a$ for copolymerization of 4:6 BZ(10)BA:Araldite 35600 monomer feed was 85.7 kJ/mol. It should be noted that the $E_a$ values for the Araldite monomers were obtained in the presence of ring-opened oligomer impurities that would effectively catalyze the ROP and lower the $E_a$. These impurities

were difficult to completely remove as shown in the GPC chromatograms (Figure B1). Additionally, the molecular weight of the benzoxazine monomers also played a role in the observed polymerization enthalpies, where the higher molecular weight of BZ(10)BA results in the dilution of the benzoxazine ring mass fraction and a decrease in the overall polymerization enthalpy. Monomer conversion of the ring-opening copolymerizations was measured using DSC by comparing the curing exotherm of the monomer in the first heating run with any residual exotherm observed in the oven cured polybenzoxazine samples. Figure 11a shows the exotherm for a 5:5 BZ(10)BA:Araldite 35600 monomer mixture, and the first and second DSC heating runs for a 5:5 BZ(10)BA:Araldite 35600 sample cured in the oven according to the previously described cure schedule. Figure 11b shows the conversion values calculated from DSC for the full range of comonomer feed compositions for both BZ(10)BA:Araldite 35600 and BZ(10)BA:Araldite 35900. For both comonomer systems, the results show an increase in conversion with increasing concentrations of BZ(10)BA, where samples containing greater than 30 wt% BZ(10)BA reach monomer conversions of approximately 98%. The lower conversion values for comonomer feeds rich in Araldite 35600 or 35900 can likely be attributed to an increased rigidity of the polymer network, resulting in vitrification and hindrance of the ring-opening polymerization under the current cure temperatures. Indeed, as discussed in the following DMA data, samples with high Araldite 35600 or 35900 content exhibit glass transition temperatures in the same range as the upper temperature employed in the cure schedule (i.e. 180 °C).

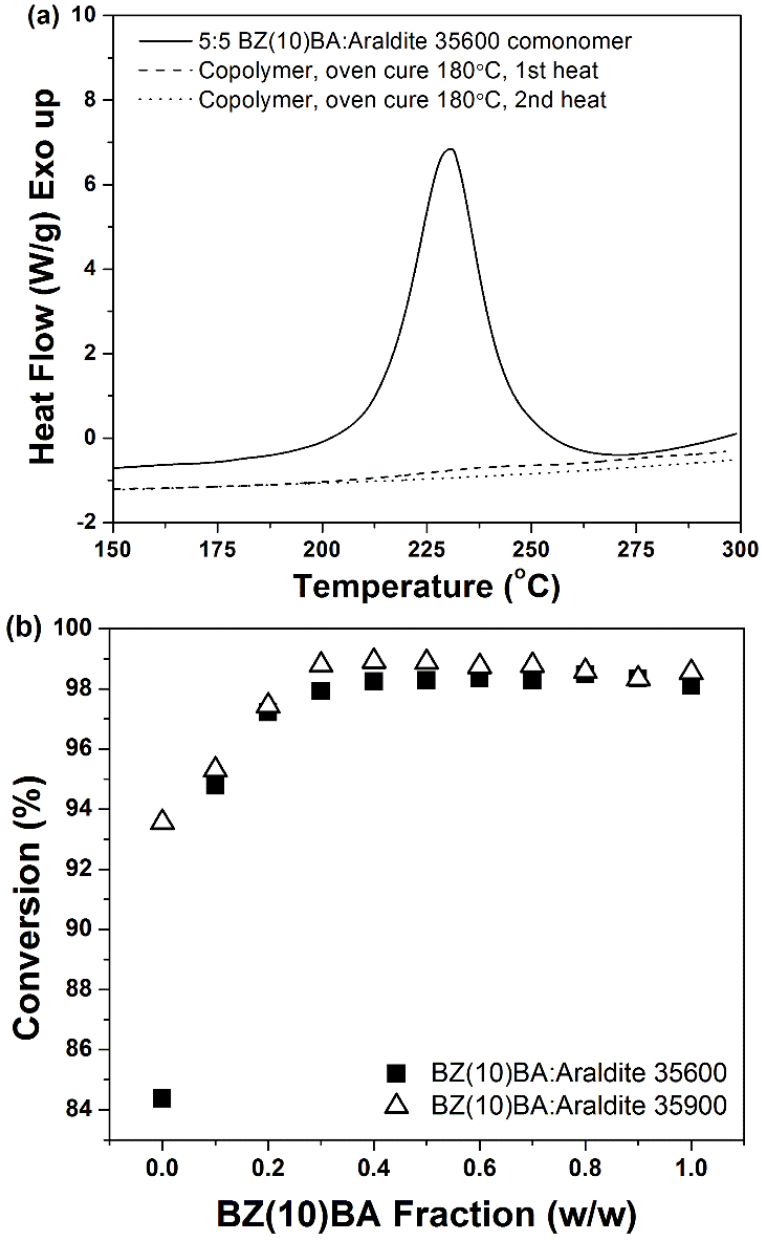


*Figure 11*. (a) DSC thermograms of 5:5 BZ(10)BA:Araldite 35600 monomer mixture and 1st and 2nd heating cycles for 5:5 BZ(10)BA:Araldite 35600 following oven cure. (b) Monomer conversion values as a function of monomer feed composition for BZ(10)BA:Araldite 35600 (■) and BZ(10)BA:Araldite 35900 (△).

*Thermomechanical Properties*

The thermomechanical properties of the cured polybenzoxazine films were investigated using dynamic mechanical analysis in tension mode. The ratio E''/E' of the loss and storage moduli gives tan δ, a damping term, which relates the energy dissipation

relative to the energy stored in the material upon periodic deformation. The glass transition temperature was determined from the peak maximum of the tan δ curve. Figure 12a and Figure 12b show the tan δ curves for the BZ(10)BA:Araldite 35600 and

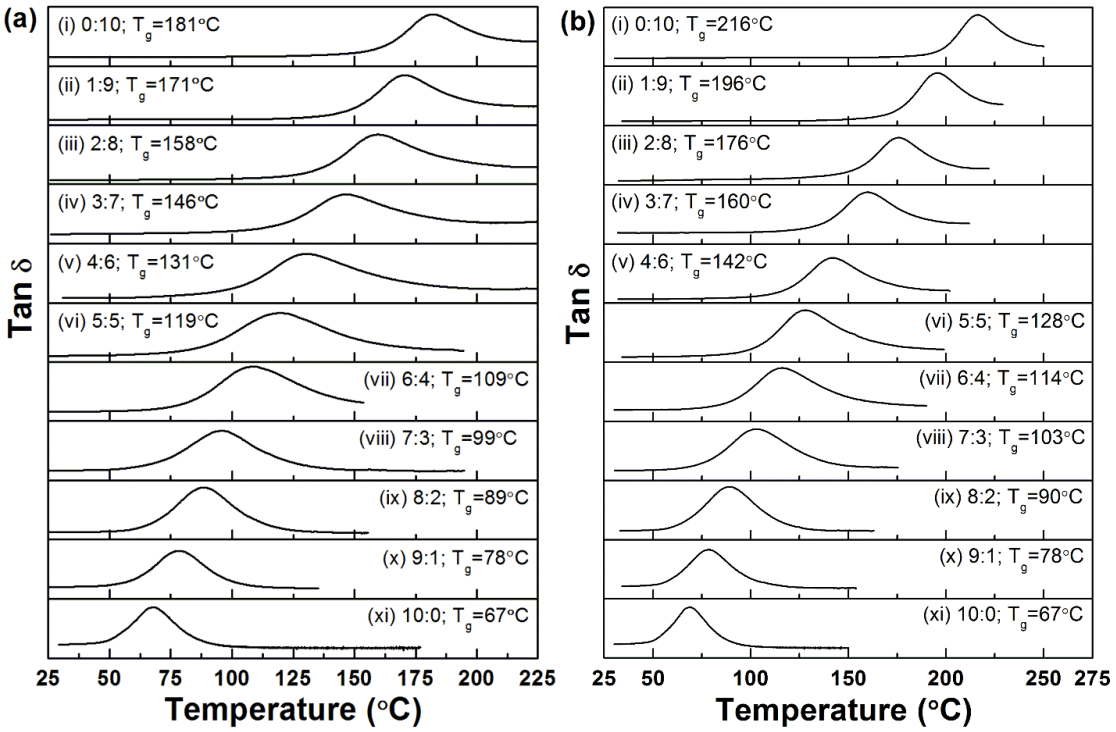


*Figure 12.* Tan δ vs. temperature plots for various monomer feed compositions for (a)BZ(10)BA:Araldite 35600 and (b) BZ(10)BA:Araldite 35900.

BZ(10)BA:Araldite 35900 copolymer series, respectively. Samples prepared from pure Araldite 35600 and 35900 showed $T_g$ values of 181 °C and 216 °C, respectively. As expected, the $T_g$ decreases rapidly for samples containing higher ratios of BZ(10)BA as indicated by a shift of the tan δ peak maxima to lower temperatures, with $T_g$ values approaching that of pure BZ(10)BA measured at 67 °C. Interestingly, samples prepared from all comonomer feed compositions exhibited a single symmetric tan δ transition providing insight into the miscibility of comonomers during copolymerization and into the homogeneity of the cured copolymer networks. Likewise, AFM analysis of the homopolymer and copolymer networks showed minimal evidence of phase separation

(Figures B2 and B3). In fact, if the cured copolymer benzoxazine networks are treated in the same manner as a statistical copolymer, then the trends observed in $T_g$ versus comonomer composition are well described by the Fox equation.[46, 47]

$$\frac{1}{T_g} = \frac{w_1}{T_{g,1}} + \frac{w_2}{T_{g,2}}$$

In the Fox Equation $T_g$, $T_{g,1}$and $T_{g,2}$ correspond to the glass transition of the statistical copolymer, component 1 and component 2, respectively, and $w_1$ and $w_2$ are the weight fractions of each component. While the Fox equation has traditionally been applied to miscible polymer blends and statistical copolymers, the copolymerization of two benzoxazine monomers with similar reactivities may result in statistically random copolymer network, and as such, can be treated similarly if the presence of cross-links are ignored. In this treatment, it is speculated that the length scale associated with the local composition that dictates $T_g$ is small (on the order of a few Kuhn lengths), or on the same order as the length between cross-links. Additionally, we assume there are no specific interactions between units. The idea of the local composition affecting $T_g$ is well-established in the miscible blend literature.[48, 49] Figure 13 shows the $T_g$ data obtained from the previously described DMA experiments fit to the Fox equation for both BZ(10)BA:Araldite 35600 and BZ(10)BA:Araldite 35900 copolymer networks. As shown, there is excellent agreement between the experimental $T_g$ data and that predicted by the Fox equation across the full range of comonomer feed compositions. Similar agreement between experimental $T_g$ data and the Fox equation was recently reported by Savin and coworkers for ternary thiol-ene polymer networks[50] and by others for various types of polymer networks.[51] The obvious utility in the observed agreement between the experimental $T_g$ data and the Fox equation is that it enables a straightforward empirical

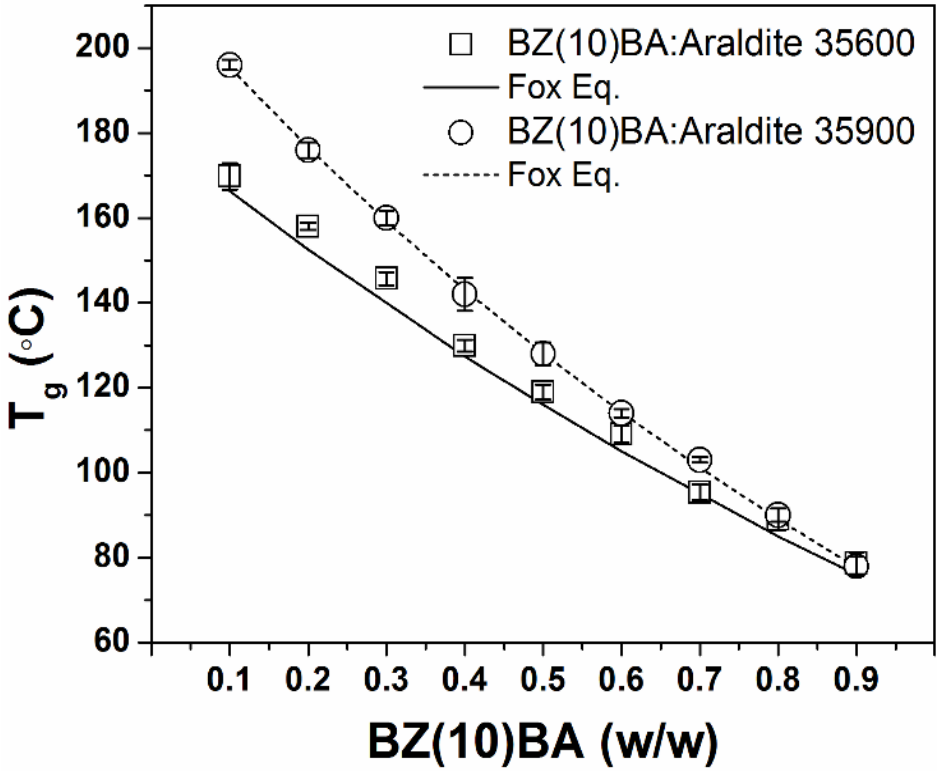


*Figure 13.* Glass transition temperature obtained from DMA for BZ(10)BA:Araldite 35600 (■) and BZ(10)BA:Araldite 35900 versus monomer feed composition. Lines represent predicted behavior based on the Fox equation.

tool to tune the $T_g$ of polybenzoxazine networks with a high degree of predictability, simply by varying the composition of comonomer feed. For additional comparison of the thermomechanical properties of the benzoxazine copolymer networks, the crosslink density ($\rho_x$) of the BZ(10)BA:Araldite networks was estimated from the rubbery plateau storage modulus at $T_g$ + 40 °C according to the theory of rubber elasticity,[52] where E´ is the rubbery storage modulus at temperature T, R is the

$$p_x = E'/2(1+\gamma)RT$$

gas constant, and γ is Poisson's ratio which is assumed to be 0.5 for incompressible networks. It should be mentioned that the above equation typically applies only to lightly cross-linked networks, thus the values should be taken as qualitative comparisons. The calculated $\rho_x$ values for the BZ(10)BA:Araldite networks show the expected trend of

increasing $\rho_x$ with increasing Araldite content. For example, the calculated $\rho_x$ values increase from $0.77\times10^{-3}$mol cm$^{-3}$ for pBZ(10)BA[37] to $1.64\times10^{-3}$mol cm$^{-3}$ for Araldite 35900, whereas the 5:5 BZ(10)BA:Araldite 35900 network exhibits an intermediate $\rho_x$ value of $1.29\times10^{-3}$ mol cm$^{-3}$. Similar trends were observed in the BZ(10)BA:Araldite 35600 networks. The increase in the cross-link density as a function of increasing Araldite, as expected, is consistent with increasing the rigidity and decreasing the distance between the reactive functional groups as the longer BZ(10)BA is replaced with Araldite. The crosslink densities and trends for the BZ(10)BA:Araldite networks also compare favorably with the crosslink density values previously published for bisphenol-A based benzoxazines ($1.1\times10^{-3}$mol cm$^{-3}$ to $1.7\times10^{-3}$mol cm$^{-3}$).[8, 15]

*Thermal Stability*

The thermal stability of the benzoxazine copolymer networks was investigated using thermal gravimetric analysis (TGA). Figures 14a and 14b show the weight loss and derivative weight loss thermograms, respectively, for the BZ(10)BA:Araldite 35600 copolymer networks. As illustrated by the 10% weight loss values ($T_d10\%$), the onset of thermal degradation depends on the ratio of the two monomers. BZ(10)BA:Araldite 35600 networks show an increase in the $T_d10\%$ temperature as the amount of Araldite 35600 in the copolymer network is increased. Such a trend is expected as the neat Araldite 35600 network shows higher thermal stability than the neat aliphatic bridged BZ(10)BA network. Similar trends in thermal degradation as a function of monomer composition are observed for BZ(10)BA:Araldite 35900 networks, as shown in Figure 15a. The thermal degradation data are summarized in Table 1. In both monomer systems, the char yield (CY) increases as the Araldite content increases – a trend that can be attributed to an increase in the aromatic content in the thermoset. For example, the

Table 1

*Summary of polymerization and thermal degradation parameters for the BZ(10)BA:Araldite copolymer networks.*

| BZ(10)BA:Araldite 35600 | $T_{d10}$ (°C) | CY (%) | $T_{onset}$ (°C) | $T_{peak}$ (°C) | Exotherm (J/g) |
|---|---|---|---|---|---|
| 10:0 | 252 | 14.4 | 232 | 244 | 79 |
| 9:1 | 258 | 17.1 | 229 | 242 | 106 |
| 8:2 | 258 | 19.6 | 225 | 239 | 111 |
| 7:3 | 260 | 21 | 222 | 235 | 122 |
| 6:4 | 263 | 22.8 | 218 | 233 | 158 |
| 5:5 | 264 | 23.6 | 213 | 231 | 174 |
| 4:6 | 275 | 24.1 | 208 | 226 | 231 |
| 3:7 | 285 | 24.6 | 204 | 222 | 257 |
| 2:8 | 298 | 25.1 | 202 | 221 | 304 |
| 1:9 | 311 | 25.9 | 202 | 220 | 332 |
| 0:10 | 328 | 26.5 | 201 | 220 | 384 |
| BZ(10)BA:Araldite 35900 | | | | | |
| 10:0 | 252 | 14.4 | 232 | 244 | 79 |
| 9:1 | 263 | 20.3 | 223 | 240 | 123 |
| 8:2 | 263 | 25.2 | 217 | 234 | 153 |
| 7:3 | 273 | 30.9 | 213 | 229 | 171 |
| 6:4 | 282 | 33 | 206 | 224 | 198 |
| 5:5 | 304 | 36.6 | 202 | 220 | 214 |
| 4:6 | 310 | 39.6 | 198 | 214 | 239 |
| 3:7 | 321 | 42.8 | 195 | 210 | 282 |
| 2:8 | 328 | 46.9 | 193 | 206 | 296 |
| 1:9 | 333 | 49.8 | 193 | 205 | 337 |
| 0:10 | 342 | 55.2 | 195 | 207 | 391 |

highest CY of 26.6% and 55.2% were observed for the neat Araldite 35600 and 35900 networks, respectively, while the CY decreased to 14.4% for the neat pBZ(10)BA network. Notably, networks comprising Araldite 35900 show the highest CY as a result of the sulfur core acting as a char promoter when compared to the aliphatic isopropyl core of the Araldite 35600.[53, 54] From the derivative weight loss curves, both the pBZ(10)BA and Araldite materials degrade in a three step process.

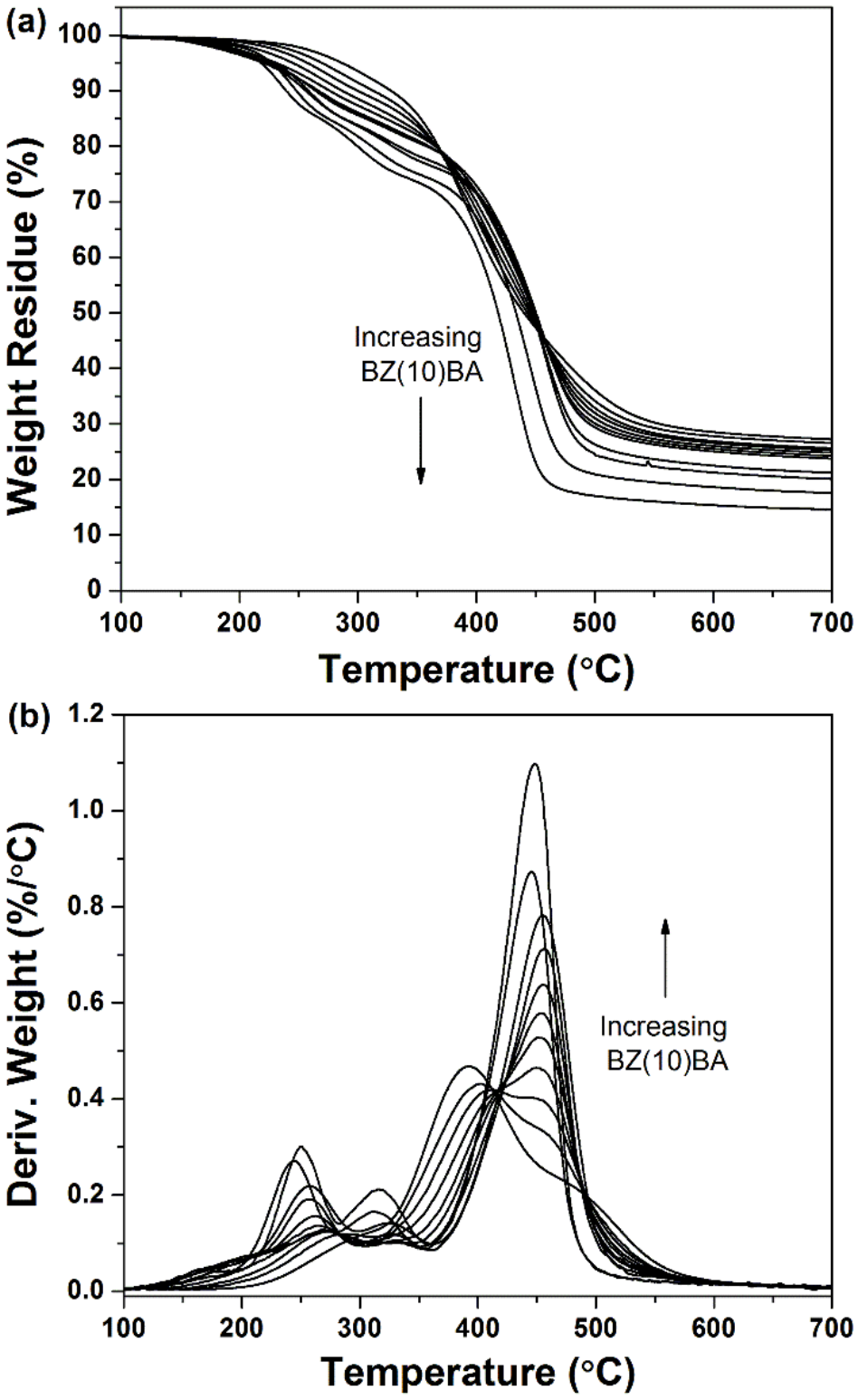


*Figure 14.* (a) Degradation profiles and (b) derivatives from TGA for the BZ(10)BA:Araldite 35600 series.

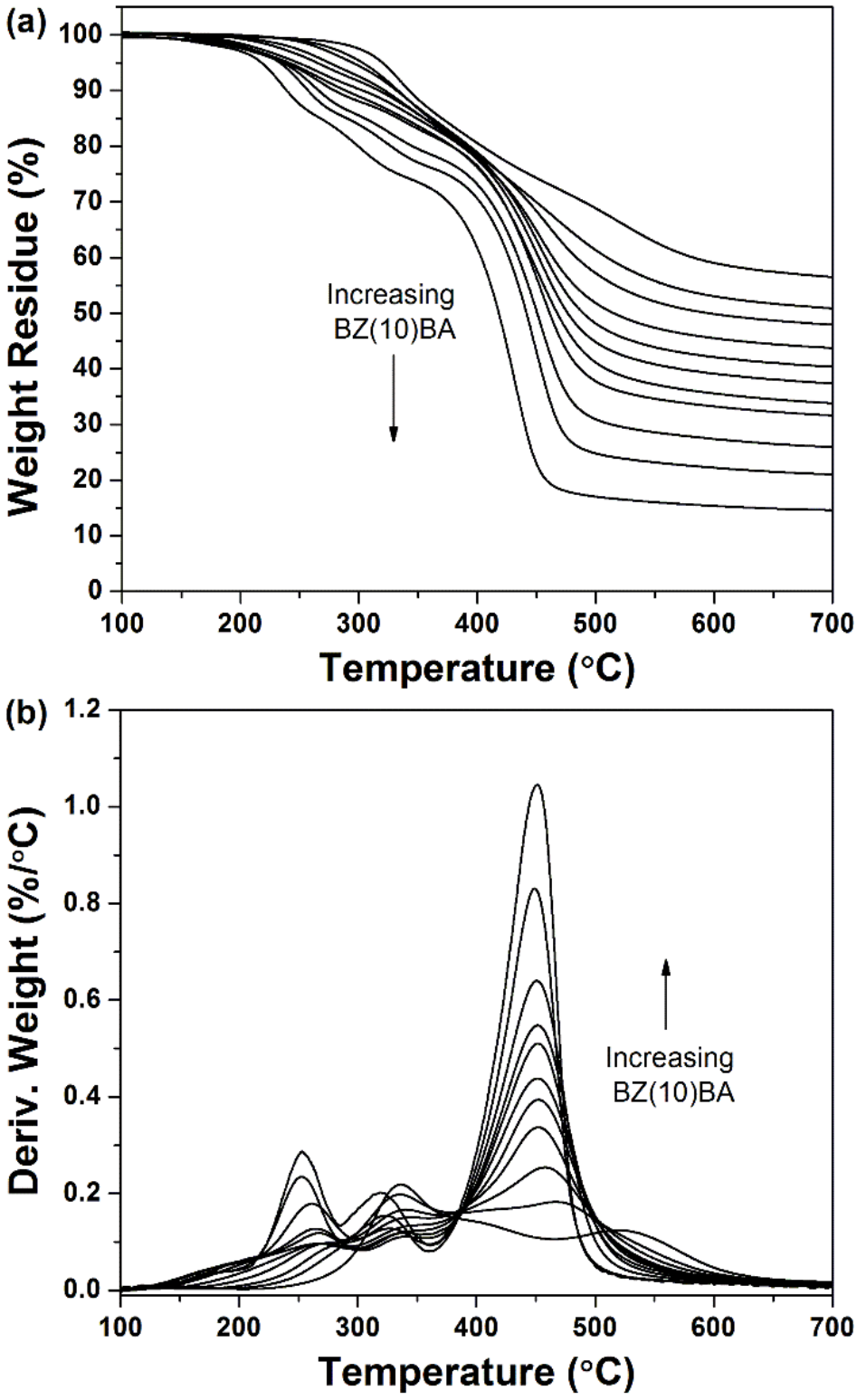


*Figure 15.* (a) Degradation profiles and (b) derivatives from TGA for the BZ(10)BA:Araldite 35900 series.

Without further analysis of the gaseous by-products by spectroscopic analysis, it is speculated that, based on previous observations of aliphatic amine derived benzoxazines,[55] that the lowest temperature degradation is associated with the degradation of the Mannich bridge and loss of the aliphatic amine constituents; whereas the higher temperature degradation step involves fragmentation and loss of aliphatic phenol byproducts.

## Conclusions

The successfully synthesized a series of polybenzoxazine copolymer networks comprised of high $T_{g,}$ commercially available benzoxazine monomers, Araldite 35600 and 35900) and BZ(10)BA, a low $T_g$, flexible aliphatic-bridged bisphenol-based benzoxazine monomer containing ten methylene units in the bridge are reported. Thermally accelerated cationic ring-opening polymerization provided homogeneous copolybenzoxazine thermosets under solvent-free conditions. DSC analysis of the ring-opening copolymerizations showed that the copolymerization behavior – in terms of polymerization onset temperature and total exothermic transition – depend greatly on the composition of the monomer feed. Samples containing larger concentrations of BZ(10)BA exhibited higher onset temperatures with lower polymerization enthalpies – a consequence of differences in molecular structure and molecular weight. Likewise, the addition of the flexible BZ(10)BA gave higher monomer conversions likely resulting from the added mobility of the less rigid monomer. The thermomechanical properties of the copolybenzoxazine networks, as assessed by DMA, show a strong dependence on the monomer feed ratio. Simply, the higher Araldite content resulted in a higher $T_g$ of the network. The most salient feature of benzoxazine copolymerization was revealed in the tailorability in thermomechanical properties. For example, the $T_g$ could be varied over a

114°C span for the BZ(10)BA:Araldite 35600 networks and over a 149 °C span for the BZ(10)BA:Araldite 35900, simply by changing the monomer ratio. Additionally, we found excellent agreement between the experimental $T_g$ data and that predicted by the Fox equation across the full range of comonomer feed compositions for both comonomer systems. The obvious utility in the observed agreement between the experimental $T_g$ data and the Fox equation is that it enables a straightforward empirical tool to tune the $T_g$ of polybenzoxazine networks with a high degree of predictability, simply by varying the composition of comonomer feed.

## Acknowledgments

The author gratefully acknowledges financial support from the National Science Foundation (NSF CAREER DMR-1056817) and the Office of Naval Research (Award N00014-07-1-1057). ADB acknowledges support from a fellowship from the National Science Foundation GK-12 program “Molecules to Muscles” (Award #0947944) through The University of Southern Mississippi. GT was funded through an NSF-REU (DMR-1005127).

# REFERENCES


1. Ishida, H.; Agag, T. *Handbook of Benzoxazine Resins*. Elsevier: Amsterdam, **2011**.
2. Kim, H. D.; Ishida, H. *J. Phys. Chem. A* **2002,** *106*, 3271-3280.
3. Kim, H.-D.; Ishida, H. *Macromol. Symp.* **2003,** *195*, 123-140.
4. Yang, P.; Wang, X.; Fan, H.; Gu, Y. *Phys. Chem. Chem. Phys.* **2013,** *DOI: 10.1039/C3CP51001H* Advance Article.
5. Ishida, H.; Lee, Y. H. *Polym. Polym. Compos.* **2001,** *9*, 121-134.
6. Jang, J.; Seo, D. *J. Appl. Polym. Sci.* **1998,** *67*, 1-10.
7. Ishida, H.; Allen, D. J. *Polymer* **1996,** *37*, 4487-4495.
8. Li, X.; Xia, Y.; Xu, W.; Ran, Q.; Gu, Y. *Polym. Chem.* **2012,** *3*, 1629-1633.
9. Takeichi, T.; Guo, Y. *Polymer Journal* **2001,** *33*, 437-443.
10. Yeganeh, H.; Razavi-Nouri, M.; Ghaffari, M. *Polym. Advan. Technol.* **2008,** *19*, 1024-1032.
11. Agag, T.; Tsuchiya, H.; Takeichi, T. *Polymer* **2004,** *45*, 7903-7910.
12. Huang, K. W.; Kuo, S. W. *Polym. Composite* **2011,** *32*, 1086-1094.
13. Liu, Y.; Zheng, S. *J. Polym. Sci. A: Polym. Chem.* **2006,** *44*, 1168-1181.
14. Wu, Y. C.; Kuo, S. W. *Polymer* **2010,** *51*, 3948-3955.
15. Allen, D. J.; Ishida, H. *J. Appl. Polym. Sci.* **2006,** *101*, 2798-2809.
16. Allen, D. J.; Ishida, H. *Polymer* **2007,** *48*, 6763-6772.
17. Allen, D. J.; Ishida, H. *Polymer* **2009,** *50*, 613-626.
18. Agag, T.; Akelah, A.; Rehab, A.; Mostafa, S. *Polym. Int.* **2012,** *61*, 124-128.
19. Liu, Y.; Li, Z.; Zhang, J.; Zhang, H.; Fan, H.; Run, M. *J. Therm. Anal. Calorim.* **2013,** *111*, 1523-1530.

20. Agag, T.; Vietmeier, K.; Chernykh, A.; Ishida, H. *J. Appl. Polym. Sci.* **2012,** *125,* 1346-1351.

21. Ergin, M.; Kiskan, B.; Gacal, B.; Yagci, Y. *Macromolecules* **2007,** *40,* 4724-4727.

22. Kukut, M.; Kiskan, B.; Yagci, Y. *Des. Monomers Polym.* **2009,** *12,* 167-176.

23. Oie, H.; Sudo, A.; Endo, T. *J. Polym. Sci. A: Polym. Chem.* **2011,** *49,* 3174-3183.

24. Chernykh, A.; Agag, T.; Ishida, H. *Polymer* **2009,** *50,* 382-390.

25. Chernykh, A.; Liu, J.; Ishida, H. *Polymer* **2006,** *47,* 7664-7669.

26. Chou, C. I.; Liu, Y. L. *J. Polym. Sci. A: Polym. Chem.* **2008,** *46,* 6509-6517.

27. Kiskan, B.; Aydogan, B.; Yagci, Y. *J. Polym. Sci. A: Polym. Chem.* **2009,** *47,* 804-811.

28. Kiskan, B.; Yagci, Y.; Ishida, H. *J. Polym. Sci. A: Polym. Chem.* **2008,** *46,* 414-420.

29. Nagai, A.; Kamei, Y.; Wang, X. S.; Omura, M.; Sudo, A.; Nishida, H.; Kawamoto, E.; Endo, T. *J. Polym. Sci. A: Polym. Chem.* **2008,** *46,* 2316-2325.

30. Velez-Herrera, P.; Doyama, K.; Abe, H.; Ishida, H. *Macromolecules* **2008,** *41,* 9704-9714.

31. Agag, T.; Arza, C. R.; Maurer, F. H. J.; Ishida, H. *J. Polym. Sci. A: Polym. Chem.* **2011,** *49,* 4335-4342.

32. Agag, T.; Geiger, S.; Alhassan, S. M.; Qutubuddin, S.; Ishida, H. *Macromolecules* **2010,** *43,* 7122-7127.

33. Aydogan, B.; Sureka, D.; Kiskan, B.; Yagci, Y. *J. Polym. Sci. A: Polym. Chem.* **2010,** *48,* 5156-5162.

34. Dogan Demir, K.; Kiskan, B.; Yagci, Y. *Macromolecules* **2011,** *44,* 1801-1807.

35. Lin, C. H.; Chang, S. L.; Shen, T. Y.; Shih, Y. S.; Lin, H. T.; Wang, C. F. *Polym. Chem.* **2012,** *3*, 935-945.

36. Liu, J.; Agag, T.; Ishida, H. *Polymer* **2010,** *51*, 5688-5694.

37. Baranek, A. D.; Kendrick, L. L.; Narayanan, J.; Tyson, G. E.; Wand, S.; Patton, D. L. *Polym. Chem.* **2012,** *3*, 2892-2900.

38. Huang, M. T.; Ishida, H. *Polym. and Polym. Compos.* **1999,** *7*, 233-247.

39. Liu, Y.-L.; Hsu, C.-W.; Chou, C.-I. *J. Polym. Sci., A: Polym. Phys.* **2007,** *45*, 1007-1015.

40. Su, Y.-C.; Chang, F.-C. *Polymer* **2003,** *44*, 7989-7996.

41. Zhang, K.; Zhuang, Q.; Liu, X.; Cai, R.; Yang, G.; Han, Z. *RSC Adv.* **2013,** *3*, 5261-5270.

42. Wang, C.; Sun, J.; Liu, X.; Sudo, A.; Endo, T. *Green Chem.* **2012,** *14*, 2799-2806.

43. Su, Y. C.; Chen, W. C.; Chang, F. C. *J. Appl. Polym. Sci.* **2004,** *94*, 932-940.

44. Wang, J.; Wu, M.; Liu, W.; Yang, S.; Bai, J.; Ding, Q.; Li, Y. *European Polym. J.* **2010,** *46*, 1024-1031.

45. Ozawa, T. *J. Therm. Anal.* **1970,** *2*, 301-324.

46. Fox, T. G. *Bull. Ame. Phys. Soc.* **1956,** *1*, 123.

47. Heimenz, P. C., Lodge, Timothy P. *Polymer Chemistry*. 2nd ed.; CRC Press: Boca Raton, 2007.

48. Lodge, T. P.; McLeish, T. C. B. *Macromolecules* **2000,** *33*, 5278-5284.

49. Savin, D. A.; Larson, A. M.; Lodge, T. P., *J. Polym. Sci. B: Polym. Phys.* **2004,***42*, 1155-1163.

50. McNair, O.; Sparks, B.; Janisse, A.; Brent, D.; Patton, D.; Savin, D. *Macromolecules* **2013**, Accepted.

51. Stanzione, J. F.; Jensen, R. E.; Costanzo, P. J.; Palmese, G. R. *ACS Appl. Mater. Interfaces* **2012,** *4*, 6142-6150.

52. Flory, P. J. *Polymer* **1979,** *20*, 1317-1320.

53. Borah, J.; Lin, G.; Wang, C. *Adv. Mat. Res.* **2010,** *87-88*, 271-275.

54. Deng, Y.; Wang, Y.-Z.; Ban, D.-M.; Liu, X.-H.; Zhou, Q. *J. Anal. Appl. Pyrol.* **2006,** *76*, 198-202.

55. Low, H. Y.; Ishida, H. *J. Polym. Sci., Part B: Polym. Phys.* **1998,** *36*, 1935-1946.

# CHAPTER V

# QUATERNARY AMMONIUM FUNCTIONAL POLYBENZOXAZINES FOR AEM APPLICATIONS

## Introduction

Anion exchange membranes (AEM) have gained a lot of interest over the past decade because of their versatility in a variety of applications requiring transport and/or removal of ions (Figure 16). Some common backbones used in AEMs include: radiation grafted fluorinated ethylene propylene (FEP) and ethylene tetrafluoroethylene (ETFE);[1-3] poly(sulfone);[4-6] poly(etherimide);[7] poly(phenylene);[8] PVA;[9] and chitosan.[10] However, there is much less diversity in the types of cations studied. Quaternary ammonium derivatives[11] (---$N^{(+)}R_{i3}$) are the most common with most of the variation being in the aliphatic or aromatic groups ($R_i$) attached to the central N atom. Amongst these R groups, trimethyl amine-based AEMs remain among the most stable ammonium-based derivatives for AEM applications.[11] Phosphonium, proazaphosphatranium, and phosphatranium cations have only recently been reported.[12, 13] Phosphazenium based anion conductive polymers have also been recently reported in patent literature.[14]

One major drawback for AEMs compared to other ion-exchange membrane types is the low mobility of anions. This necessitates a high concentration of tethered cationic charge carriers or a high ion-exchange capacity (IEC) to achieve reasonable ionic conductivity.[4] Additionally, the incorporation of a high concentration of ionic groups has a detrimental effect on the mechanical stability. Strategies such as blending,[15-17] (semi)interpenetrating networks[18, 19] and addition of inorganic additives[20-23] have been used to counteract this. A more attractive approach to improve dimensional stability and solvent resistance includes cross-linking. Multi (di-, tri-, or tetra)-functional groups,

containing cross-linkers have been widely adopted, and some examples include di-amines (react with halogenoalkyl groups),[5, 24-27] di-thiol (with allyl groups),[28] di-aldehyde (with hydroxyl-alkyl groups),[9, 29-32] tri/tetra-alkoxysilanes (with hydroxyl-alkyl or alkoxysilanyl groups),[33, 34] and tetraepoxy (with phenol groups).[35-37] Additionally, a bi-cycloalkene ring-opening with simultaneous polymerization-cross-linking technique was recently reported to prepare high-performance AEMs.[36, 37] However, the cross-linking techniques mentioned above require the introduction of a separate cross-linker molecule or specific polymer structures which usually takes at least two reaction-steps, increasing the process complexity as well as lowering the IEC. In addition, problems exist when the cross-linker has a distinctive molecular structure that is not compatible with the polymer chain, which can lead to poor membrane quality or make cross-linking impossible.

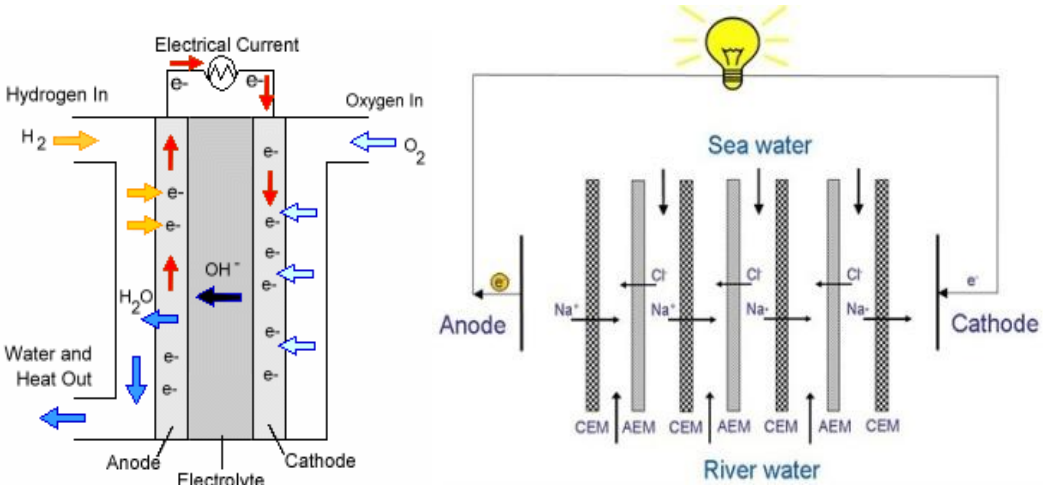


*Figure 16.* AEM devises used in energy generation including alkaline fuel cell (left); reverse electrodialysis (right).

One way to allow for a highly cross-linked network with no additional chemistry is through the use of polybenzoxazines (pBZ). Polybenzoxazines are a class of thermoset resins that show a variety of high performance properties suitable for AEM materials, including high thermal and chemical resistance. Benzoxazine monomers are synthesized via the Mannich reaction from phenolic and primary amine derivatives and formaldehyde

(Scheme 1). The simplistic nature of benzoxazine synthesis and the broad availability of starting materials offer unprecedented flexibility in the molecular design of monomers. To date, numerous BZ monomer derivatives (allyl, acetylene, propargyl ether, nitrile, maleimide, and methacrylate) have been reported. Benzoxazines undergo thermally activated cationic ring-opening polymerization (ROP) and yield a polymer backbone, consisting of a phenol and a tertiary amine bridge as the repeating motif, and it is through the versatile monomer synthesis and ease of polymerization/cross-linking that polybenzoxazines are being explored as an AEM material. The closest example of this type of work was done by Sawaryn et. al. who designed linear polyelectrolytes based on a monofunctional benzoxazine monomer with a pendant ionizable group (methyl imidazole).[38] Through their experiments, high concentrations of cationic moieties were incorporated into the linear polybenzoxazine as there were two ionizable groups per repeat unit; however, characterization of these materials was limited to structural and thermal techniques with no membrane applications or properties were reported.

The overarching goal of this research is the rationale design of a series of inexpensive, flexible, cross-linked anion-conducting materials based on polybenzoxazine thin films. The defining characteristic of these systems is the ability to bestow polybenzoxazine thin films with a high ion exchange capacity (IEC) – wherein the entire film is comprised of a continuous, cross-linked ionic network – while achieving optimal chemical stability, water uptake, flexural strength and modulus, and thermomechanical properties for membrane applications. In this study flexible 4, 6, 8, and 10 carbon as well as a short chain polyethylene glycol core bisbenzoxazines are synthesized with pendent quaternizable amines which are converted following polymerization to cationic moieties through simple alkylation chemistry.

# Experimental

## *Materials*

All reagents and solvents were obtained at the highest purity available from Aldrich Chemical Company and used without further purification unless otherwise specified. Paraformaldehyde was purchased from Acros Organics. Anhydrous potassium carbonate, magnesium sulfate, and sodium hydroxide were purchased from Fisher Scientific. The synthesis of compounds 3–5 starting with 1,4-dibromobutane, 1,6-dibromohexane, 1,8-dibromooctane, 1,10-dibromodecane, and 1,2-bis(2-chloroethoxy ethane) were adapted from literature.[39, 40]

## *Synthesis of aliphatic-bridged dibenzaldehyde compounds (3)*

Into a 250mL round bottom flask fitted with a condenser, 0.0287 mol of the dihalogenated species (1,4-dibromobutane, 1,6-dibromohexane, 1,8-dibromooctane, 1,10-dibromodecane or 1,2-bis(2-chloroethoxy)ethane), 7.007 g (0.0574 mol) of 4-hydroxybenzaldehyde and 15.8665 g (0.1148mol) of anhydrous potassium carbonate were added to approximately 100 mL of dimethylformamide. The flask was set in an oil bath and refluxed at 110 °C for 48 h. The solution was cooled to room temperature, diluted with dichloromethane, and washed with water. The organic layer was dried over $MgSO_4$ and evaporated under vacuum to an off white solid. *4,4'-(butane-1,4-diylbis(oxy))dibenzaldehyde* **(3a).** (83.9% yield) $^1$H NMR ($CDCl_3$), ppm: δ=1.99 (4H, m, $CH_2$), 4.09 (4H, t, $CH_2$-O), 6.95 (4H, d, CH, aromatic) 7.78 (4H, d, CH, aromatic), 9.83 (2H, s, CH=O, aldehyde); $^{13}$C NMR ($CDCl_3$), ppm: δ=25.90 (2C, $CH_2$), 67.86 (2C, $CH_2$-O), 114.83 (4C, CH, aromatic) 130.06 (2C, C, aromatic) 132.10 (4C, CH, aromatic), 164.05 (2C, C, aromatic) 190.85 (2C, CH aldehyde). *4,4'-(hexane-1,6-diylbis(oxy))dibenzaldehyde* **(3b).** (94.5% yield) $^1$H NMR ($CDCl_3$), ppm: δ=1.52-1.92

(8H, m, $CH_2$), 4.07 (4H, t, $CH_2$-O), 6.98 (4H, d, CH, aromatic) 7.83 (4H, d, CH, aromatic), 9.88 (2H, s, CH=O, aldehyde); $^{13}$C NMR ($CDCl_3$), ppm: δ=25.76, 28.97 (4C, $CH_2$), 68.15 (2C, $CH_2$-O), 114.71 (4C, CH, aromatic) 129.81 (2C, C, aromatic) 131.96 (4C, CH, aromatic), 164.11 (2C, C, aromatic) 190.74 (2C, CH aldehyde). *4'-(octane-1,8-diylbis(oxy))dibenzaldehyde* **(3c).** (94.9% yield) $^1$H NMR ($CDCl_3$), ppm: δ=1.39-1.89 (12H, m, $CH_2$), 4.13 (4H, t, $CH_2$-O), 7.11 (4H, d, CH, aromatic) 7.87 (4H, d, CH, aromatic), 9.89 (2H, s, CH=O, Aldehyde); $^{13}$C NMR ($CDCl_3$), ppm: δ=25.88, 29.01, 29.20 (6C, $CH_2$), 68.31 (2C, $CH_2$-O), 114.71 (4C, CH, aromatic) 129.74 (2C, C, aromatic) 131.95 (4C, CH, aromatic), 164.18 (2C, C, aromatic) 190.75 (2C, CH aldehyde). *4,4'-(decane-1,10-diylbis(oxy))dibenzaldehyde* **(3d).** (92.4% yield) $^1$H NMR ($CDCl_3$), ppm: δ=1.29-1.81 (16H, m, $CH_2$), 3.98 (4H, t, $CH_2$-O), 6.94 (4H, s, CH, aromatic) 7.77 (4H, d, CH, aromatic), 9.82 (2H, s, CH=O, Aldehyde); $^{13}$C NMR ($CDCl_3$), ppm: δ=25.91, 29.00 29.27, 29.41 (8C, $CH_2$), 68.34 (2C, $CH_2$-O), 114.70 (4C, CH, aromatic) 129.68 (2C, C, aromatic) 131.91 (4C, CH, aromatic), 164.19 (2C, C, aromatic) 190.69 (2C, CH aldehyde). *4,4'-(((ethane-1,2-diylbis(oxy))bis(ethane-2,1-diyl))bis(oxy))dibenzaldehyde* **(3e).** (78.4% yield) $^1$H NMR ($CDCl_3$), ppm: δ= 3.75 (4H, s, $CH_2$-O), 3.88 (4H, t, $CH_2$-O), 4.19 (4H, t, $CH_2$-O), 7.00 (4H, d, CH, aromatic), 7.80 (4H, d, CH, aromatic), 9.85 (2H, s, CH, Aldehyde); $^{13}$C NMR ($CDCl_3$), ppm: δ=67.68, 69.48, 70.87 (6C, $CH_2$-O), 114.81 (4C, CH, aromatic) 129.96 (2C, C, aromatic) 131.91 (4C, CH, aromatic), 163.75 (2C, C, aromatic) 190.78 (2C, CH aldehyde).

*Synthesis of aliphatic-bridged diformate compounds (4)*

Into a 500 mL round bottom flask, 0.022 mol of dibenzaldehyde (3) was dissolved in 150-200 mL of dichloromethane, and metachloroperoxybenzoic acid (MCPBA) (14.68 g, 0.0891 mol) was added in portions to the solution. The reaction was then capped and

purged with nitrogen gas for 10 min, and then set to stir at room temperature for 3-4 h. 112 mL of a saturated sodium bicarbonate solution was added to the solution and stirred for another 2 h at room temperature. The solution was extracted with dichloromethane and washed with 10% sodium metabisulfite followed by washing with water. The organic layer was dried over $MgSO_4$ and evaporated under vacuum to give a light yellow solid. *(Butane-1,4-diylbis(oxy))bis(4,1-phenylene) diformate* **(4a).** (97.3% yield) $^1$H NMR ($CDCl_3$), ppm: δ=1.97 (4H, m, $CH_2$), 4.02 (4H, t, $CH_2$-O), 6.88 (4H, d, CH, aromatic) 7.04 (4H, d, CH, aromatic), 8.28 (2H, s, O-CH=O, formate); $^{13}$C NMR ($CDCl_3$), ppm: δ=25.93 (2C, $CH_2$), 67.84 (2C, $CH_2$-O), 115.22 (4C, CH, aromatic) 121.94 (4C, C, aromatic) 143.31 (2C, C, aromatic), 157.03 (2C, C, aromatic) 159.70 (2C, CH formate). *(Hexane-1,6-diylbis(oxy))bis(4,1-phenylene) diformate* **(4b).** (84.3% yield) $^1$H NMR ($CDCl_3$), ppm: δ=1.49-1.88 (8H, m, $CH_2$), 3.96 (4H, t, $CH_2$-O), 6.89 (4H, d, CH, aromatic) 7.03 (4H, d, CH, aromatic), 8.28 (2H, s, O-CH=O, formate); $^{13}$C NMR ($CDCl_3$), ppm: δ=25.79, 29.15 (4C, $CH_2$), 68.22 (2C, $CH_2$-O), 115.22 (4C, CH, aromatic) 121.89 (4C, C, aromatic) 143.23 (2C, C, aromatic), 157.16 (2C, C, aromatic) 159.74 (2C, CH formate). *(Octane-1,8-diylbis(oxy))bis(4,1-phenylene) diformate* **(4c).** (94.4% yield) $^1$H NMR ($CDCl_3$), ppm: δ=1.37-1.84 (12H, m, $CH_2$), 4.13 (4H, t, $CH_2$-O), 6.97 (4H, d, CH, aromatic) 7.10 (4H, d, CH, aromatic), 8.39 (2H, s, O-CH=O, formate); $^{13}$C NMR ($CDCl_3$), ppm: δ=25.93, 29.00 29.16, 29.24 (6C, $CH_2$), 68.35 (2C, $CH_2$-O), 115.21 (4C, CH, aromatic) 121.87 (4C, C, aromatic) 143.19 (2C, C, aromatic), 157.20 (2C, C, aromatic) 159.73 (2C, CH formate). *(Decane-1,10-diylbis(oxy))bis(4,1-phenylene) diformate* **(4d).** (93.3% yield) $^1$H NMR ($CDCl_3$), ppm: δ=1.30-1.83 (16H, m, $CH_2$), 4.00 (4H, t, $CH_2$-O), 6.97 (4H, d, CH, aromatic) 7.10 (4H, d, CH, aromatic), 8.39 (2H, s, O-CH=O, formate); $^{13}$C NMR ($CDCl_3$), ppm: δ=25.99, 29.00 29.20, 29.33, 29.46 (8C, $CH_2$),

68.39 (2C, $CH_2$-O), 115.21 (4C, CH, aromatic) 121.88 (4C, C, aromatic) 143.18 (2C, C, aromatic), 157.21 (2C, C, aromatic) 159.79 (2C, CH formate). *(((ethane-1,2-diylbis(oxy))bis(ethane-2,1-diyl))bis(oxy))bis(4,1-phenylene)diformate*: **(4e).** (84.5% yield) $^1$H NMR ($CDCl_3$), ppm: δ= 3.74 (4H, s, $CH_2$-O), 3.85 (4H, t, $CH_2$-O), 4.09 (4H, t, $CH_2$-O), 6.90 (4H, d, CH, aromatic), 7.01 (4H, d, CH, aromatic), 8.26 (2H, s, CH, Formate); $^{13}$C NMR ($CDCl_3$), ppm: δ=67.79, 69.69, 70.82 (6C, $CH_2$-O), 115.37 (4C, CH, aromatic) 121.37 (2C, CH, aromatic), 143.43 (4C, C, aromatic), 156.80 (2C, C, aromatic) 159.81 (2C, CH formate).

*Synthesis of aliphatic-bridged diphenol compounds (5).*

Into a 500mL round bottom flask fitted with a condenser, 0.0068mol of diformate (4) was added to sodium hydroxide (1.082 g, 0.0271mol) in 50 mL of ethanol and 20 mL of water, and the solution was then refluxed at 100°C for 24 h. The solution was cooled to room temperature and acidified using 3M HCl. The product precipitated and was extracted using ethyl acetate. The organic layers were combined, washed with 3M HCl, water, and dried over $MgSO_4$. The solution was filtered, and the solvent was removed by rotary evaporation to give a brown solid. *4,4'-(butane-1,4-diylbis(oxy))diphenol* **(5a).** (94.9% yield) $^1$H NMR (acetone-$d_6$), ppm: δ=1.90 (4H, m, $CH_2$), 3.97 (4H, t, $CH_2$-O), 6.76 (8H, m, CH, aromatic) 7.82 (2H, s, OH); $^{13}$C NMR (acetone-$d_6$), ppm: δ=26.05 (2C, $CH_2$), 68.04 (2C, $CH_2$-O), 115.82 (4C, CH, aromatic) 116.12 (4C, CH, aromatic), 151.53 (2C, C, phenol) 151.86 (2C, C, ether). *4,4'-(hexane-1,6-diylbis(oxy))diphenol* **(5b).** (89.6% yield) $^1$H NMR (acetone-$d_6$), ppm: δ=1.48-1.82 (8H, m, $CH_2$), 3.91 (4H, t, $CH_2$-O), 6.75 (8H, m, CH, aromatic) 7.81 (2H, s, OH); $^{13}$C NMR (acetone-$d_6$), ppm: δ=25.81, 29.27 (4C, $CH_2$), 68.24 (2C, $CH_2$-O), 115.78 (4C, CH, aromatic) 116.12 (4C, CH, aromatic), 151.48 (2C, C, phenol) 151.92 (2C, C, ether). *4,4'-(octane-1,8-*

*diylbis(oxy))diphenol* **(5c).** (92.5% yield) $^{1}$H NMR (acetone-$d_6$), ppm: δ=1.34-1.79 (12H, m, $CH_2$), 3.89 (4H, t, $CH_2$-O), 6.75 (8H, m, CH, aromatic) 7.81 (2H, s, OH); $^{13}$C NMR (acetone-$d_6$), ppm: δ=25.87, 29.27, (6C, $CH_2$), 68.28 (2C, $CH_2$-O), 115.75 (4C, CH, aromatic) 116.10 (4C, CH, aromatic), 151.48 (2C, C, phenol) 151.93 (2C, C, ether). *4,4'-(decane-1,10-diylbis(oxy))diphenol* **(5d).** (91.0% yield) $^{1}$H NMR (acetone-$d_6$), ppm: δ=1.35-1.74 (16H, m, $CH_2$), 3.88 (4H, t, $CH_2$-O), 6.75 (8H, m, CH, aromatic) 7.81 (2H, s, OH); $^{13}$C NMR (acetone-$d_6$), ppm: δ=25.92, 29.30 29.39 (8C, $CH_2$), 68.12 (2C, $CH_2$-O), 115.33 (4C, CH, aromatic) 115.68 (4C, CH, aromatic), 151.13 (2C, C, phenol) 152.52 (2C, C, ether). *4,4'-(((ethane-1,2-diylbis(oxy))bis(ethane-2,1-diyl))bis(oxy))diphenol* **(5e).** (88.6% yield) $^{1}$H NMR (acetone-$d_6$), ppm: δ= 3.66 (4H, s, $CH_2$-O), 3.76 (4H, t, $CH_2$-O), 4.02 (4H, t, $CH_2$-O), 6.77 (8H, m, CH, aromatic), 7.90 (2H, s, phenol); $^{13}$C NMR (acetone-$d_6$), ppm: δ=67.91, 69.61, 70.49 (6C, $CH_2$-O), 115.47 (4C, CH, aromatic) 115.73 (2C, CH, aromatic), 151.26 (4C, C, phenol), 152.26 (2C, C, aromatic).

*Synthesis of aliphatic-bridged bisbenzoxazine monomers (6).*

Into a 100mL round bottom flask fitted with a condenser, 0.0033 mol of the phenol (5a-e), dimethylethylene diamine (0.5818 g, 0.0066 mol) and paraformaldehyde (0.3964 g, 0.0132 mol) were suspended in 7.9 mL of xylene and placed in an oil bath heated to 120°C. Once at temperature, the reactants dissolved, and aliquots were taken at 5 minute intervals and observed via $^{1}$H-NMR to monitor the progress of the reaction. Upon completion of the reaction (~15 – 20min), the reaction was cooled to room temperature, and the xylene was evaporated. The crude residue was then diluted with excess ethyl acetate and stirred with basic alumina for 10 min, filtered, and evaporated under vacuum to give an off white solid. The crude benzoxazine was then recrystallized in cold ethyl acetate to afford white crystals. *2,2'-(6,6'-(butane-1,4-diylbis(oxy))bis(2H-*

*benzo[e][1,3]oxazine-6,3(4H)-diyl))bis(N,N-dimethylethanamine) [BZ(4)DMEDA]* **(6a)**. (54.3% yield) $^{1}$H NMR ($CDCl_3$), ppm: δ=1.25-1.47 (12H, m, $CH_2$), 1.72 (4H, m, $CH_2$), 2.24 (12H, s, N-$CH_3$), 2.45 (4H, t, $CH_2$-amine), 2.85 (4H, t, $CH_2$-oxazine), 3.84 (4H, t, $CH_2$-O), 3.98 (4H, s, oxazine), 4.82 (4H, s, oxazine), 6.48 (2H, s, aromatic) 6.67 (4H, s, aromatic); $^{13}$C NMR ($CDCl_3$), ppm: δ=26.04, 29.37, 29.49, (8C, $CH_2$), 45.70 (4C, $CH_3$-N), 49.03 (4C, N-$CH_3$), 50.57 (2C, oxazine), 57.75 (2C, $CH_2$-N), 68.46 (2C, $CH_2$-O), 82.61 (2C, oxazine), 112.87, 114.24, 116.90 (6C, CH, aromatic), 147.87 (2C, C, aromatic),152.92 (2C, C, aromatic). *2,2'-(6,6'-(hexane-1,6-diylbis(oxy))bis(2H-benzo[e][1,3]oxazine-6,3(4H)-diyl))bis(N,N-dimethylethanamine) [BZ(6)DMEDA* **(6b)**. (66.3% yield) $^{1}$H NMR ($CDCl_3$), ppm: δ=2.23 (12H, s, N-$CH_3$), 2.44 (4H, t, $CH_2$-amine), 2.83 (4H, t, $CH_2$-oxazine), 3.71 (4H, s, $CH_2$-O), 3.80 (4H, t, $CH_2$-O), 3.96 (4H, s, oxazine), 4.02 (4H, t, $CH_2$-O), 4.80 (4H, s, oxazine), 6.50 (2H, s, aromatic), 6.67 (4H, s, aromatic); $^{13}$C NMR ($CDCl_3$), ppm: δ=26.04, 29.37, 29.49, (8C, $CH_2$), 45.70 (4C, $CH_3$-N), 49.03 (4C, N-$CH_3$), 50.57 (2C, oxazine), 57.75 (2C, $CH_2$-N), 68.46 (2C, $CH_2$-O), 82.61 (2C, oxazine), 112.87, 114.24, 116.90 (6C, CH, aromatic), 147.87 (2C, C, aromatic),152.92 (2C, C, aromatic). *2,2'-(6,6'-(octane-1,8-diylbis(oxy))bis(2H-benzo[e][1,3]oxazine-6,3(4H)-diyl))bis(N,N-dimethylethanamine) [BZ(8)DMEDA]* **(6c)**. (64.2% yield) $^{1}$H NMR ($CDCl_3$), ppm: δ=1.25-1.47 (12H, m, $CH_2$), 1.72 (4H, m, $CH_2$), 2.24 (12H, s, N-$CH_3$), 2.45 (4H, t, $CH_2$-amine), 2.85 (4H, t, $CH_2$-oxazine), 3.84 (4H, t, $CH_2$-O), 3.98 (4H, s, oxazine), 4.82 (4H, s, oxazine), 6.48 (2H, s, aromatic) 6.67 (4H, s, aromatic); $^{13}$C NMR ($CDCl_3$), ppm: δ=26.04, 29.37, 29.49, (8C, $CH_2$), 45.70 (4C, $CH_3$-N), 49.03 (4C, N-$CH_3$), 50.57 (2C, oxazine), 57.75 (2C, $CH_2$-N), 68.46 (2C, $CH_2$-O), 82.61 (2C, oxazine), 112.87, 114.24, 116.90 (6C, CH, aromatic), 147.87 (2C, C, aromatic),152.92 (2C, C, aromatic). *2,2'-(6,6'-(decane-1,10-diylbis(oxy))bis(2H-*

*benzo[e][1,3]oxazine-6,3(4H)-diyl))bis(N,N-dimethylethanamine) [BZ(10)DMEDA]* **(6d)**. (72.4% yield) $^{1}$H NMR ($CDCl_3$), ppm: δ=1.25-1.47 (12H, m, $CH_2$), 1.72 (4H, m, $CH_2$), 2.24 (12H, s, N-$CH_3$), 2.45 (4H, t, $CH_2$-amine), 2.85 (4H, t, $CH_2$-oxazine), 3.84 (4H, t, $CH_2$-O), 3.98 (4H, s, oxazine), 4.82 (4H, s, oxazine), 6.48 (2H, s, aromatic) 6.67 (4H, s, aromatic); $^{13}$C NMR ($CDCl_3$), ppm: δ=26.04, 29.37, 29.49, (8C, $CH_2$), 45.70 (4C, $CH_3$-N), 49.03 (4C, N-$CH_3$), 50.57 (2C, oxazine), 57.75 (2C, $CH_2$-N), 68.46 (2C, $CH_2$-O), 82.61 (2C, oxazine), 112.87, 114.24, 116.90 (6C, CH, aromatic), 147.87 (2C, C, aromatic), 152.92 (2C, C, aromatic). *2,2'-(6,6'-(((ethane-1,2-diylbis(oxy))bis(ethane-2,1-diyl))bis(oxy))bis(2H-benzo[e][1,3]oxazine-6,3(4H)-diyl))bis(N,N-dimethylethanamine) [BZ(EO)$_3$DMEDA]* **(6e)**. (59.8% yield) $^{1}$H NMR ($CDCl_3$), ppm: δ=1.25-1.47 (12H, m, $CH_2$), 1.72 (4H, m, $CH_2$), 2.24 (12H, s, N-$CH_3$), 2.45 (4H, t, $CH_2$-amine), 2.85 (4H, t, $CH_2$-oxazine), 3.84 (4H, t, $CH_2$-O), 3.98 (4H, s, oxazine), 4.82 (4H, s, oxazine), 6.48 (2H, s, aromatic) 6.67 (4H, s, aromatic); $^{13}$C NMR ($CDCl_3$), ppm: δ=45.66 (4C, N-$CH_3$), 49.00 (4C, $CH_2$-N), 50.53 (2C, oxazine), 57.70 (2C, $CH_2$-N), 67.95, 69.85, 70.79 (6C, $CH_2$-O), 82.61 (2C, oxazine), 113.17, 114.43, 116.91, 120.58 (6C, CH, aromatic), 148.15 (2C, C, aromatic),152.53 (2C, C, aromatic).

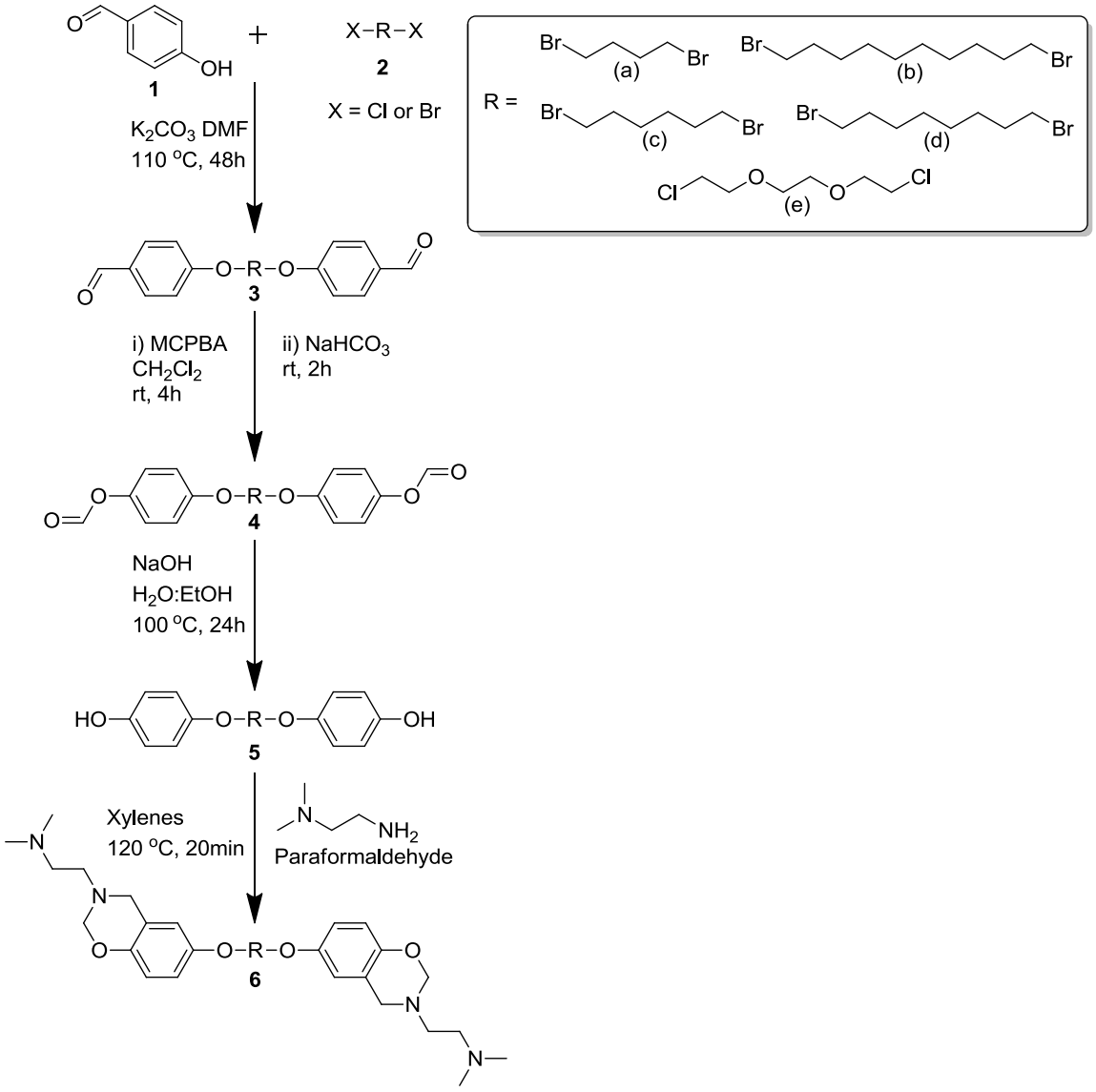


*Scheme 9.* Synthetic route for the alkyl-bridged bisbenzoxazine monomer series BZ(R)DMEDA and the core structures.

*Polybenzoxazine Film Preparation*

The benzoxazines were cured into films using previously reported methods.[40] Briefly, ~100 mg of the monomer was placed in the center of a RainX® coated 75×50 mm glass slide and heated gently with a heat gun until all air bubbles were removed. Teflon spacers (thickness ~55 µm) were inserted on the sides of a glass slide and a second RainX® coated 75×50mm glass slide was gently placed on the top making sure bubbles were excluded when 'sandwiching' the monomer. The glass slides were clamped

together, and the sandwiched monomer assembly was quickly placed in a preheated oven at 100°C. The thermal step cure proceeded as follows: 100°C for 1 h, 140°C for 1 h, 160°C for 2 h, and 180°C for 4 h. After the cure, the film was removed from the glass slides and washed with methanol to remove any residual RainX® on the cured film.

*Quaternization & Ion-Exchange*

Quaternization of the pendent tertiary amines and Mannich Bridge was accomplished through an alkylation process using methyl iodide ($CH_3I$). Films were submerged in neat methyl iodide for 24h at room temperature under mild agitation. A rinse with methanol followed to remove any excess methyl iodide. The quaternized films were then ion exchanged in appropriate aqueous potassium salt solutions to obtain various counter-ions (0.1 M KX; X = $Cl^-$, $Br^-$, $OH^-$), followed by rinsing with excess deionized (DI) water to remove the excess ions.

*Characterization and Measurements*

$^1$H-NMR and $^{13}$C-NMR were performed in deuterated chloroform ($CDCl_3$) and deuterated acetone ($(CD_3)_2CO$) to determine the purity of the synthesized molecules, using a Varian Mercury Plus 300 MHz NMR spectrometer operating at a frequency of 300 MHz with tetramethylsilane as an internal standard. The number of transients for $^1$H and $^{13}$C are 32 and 256, respectively, and a relaxation time of 5 s was used for the

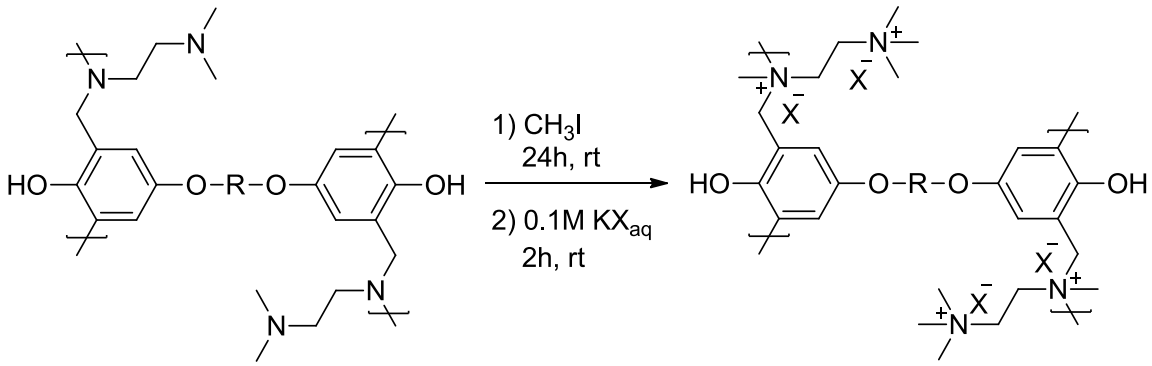


*Scheme 10*. Quaternization and ion exchange of pBZ(R)DMEDA.

integrated intensity determination of $^{1}H$ NMR spectra. The ROP conversion and quaternization process were analyzed using Fourier transform infrared spectroscopy in a grazing-angle attenuated total reflectance mode (gATR-FTIR), using a ThermoScientific FTIR instrument (Nicolet 8700) equipped with a VariGATR$^{TM}$ accessory (grazing angle 65°, germanium crystal; Harrick Scientific). Spectra were collected with a resolution of 4 $cm^{-1}$ by accumulating a minimum of 128 scans per sample. All spectra were collected while purging the VariGATR$^{TM}$ attachment and FTIR instrument with $N_2$ gas along the infrared beam path to minimize the peaks corresponding to atmospheric moisture and $CO_2$. Spectra were analyzed and processed using Omnic software. Differential scanning calorimetry was also performed to monitor conversion of the ROP on a TA instruments DSC Q200 differential scanning calorimeter at a heating rate of 5°C $min^{-1}$ and a nitrogen flow rate of 50 mL $min^{-1}$. Samples were crimped in hermetic aluminum pans with lids.

Equilibrium water uptake was measured using a TA Q5000SA Moisture Analyzer Water Uptake. The films were subject to 80°C and 90% RH for 4h to equilibrate followed by a desorption to 0% RH at 80°C for 4h. Water uptake was measured using the equation below.

$$\frac{Sample\ Mass\ @\ 90\%\ RH - Sample\ Mass\ @\ 0\%\ RH}{Sample\ mass\ @\ 0\%\ RH} * 100$$

Ion Exchange Capacity (IEC) was determined by using standard back titration methods. The quaternized films were washed in a 0.1M KOH solution 4 times for 30 minutes each to exchange all of the anions for $OH^-$, followed by rinsing with water and then immersing in 10 mL of a standardized 0.05M $HCl_{(aq)}$ solution overnight with mild agitation. The $HCl_{(aq)}$ solution was then back titrated to its equivalence point with standardized 0.05M $NaOH_{(aq)}$. The sample was then washed with HCl 4 times for 30

minutes each to all counter-ions are all $Cl^-$, washed with water and dried under vacuum for at least 12 hours to obtain the mass of the dried film in which $Cl^-$ is the counter-ion. The IEC was then measured based on (equation 1)

$$\frac{OH^- \, neutarlized \, (mmol)}{Mass \, of \, sample \, (g)} = IEC \, (mmol/g)$$

In plane conductivities were measured at 80°C in DI water using a BekkTech 4 point-probe sample analyzer. The samples were allowed to equilibrate for 20 min in 80°C in DI water prior to taking a conductivity reading using a Keithley 2400 Source Meter. Conductivity through the basal plane was determined in triplicate and reported as an average. The average conductivity of the DI water alone was also measured and subtracted from the reported values.

## Results and Discussion

*Monomer Synthesis:*

The diphenol synthesis was adopted from previous work[40] (Scheme 9). The bisbenzoxazines were synthesized similar to previous publications by the Mannich condensation of the diphenols, DMEDA, and paraformaldehyde in xylenes at 120°C.[40] Additional purification via recrystallization afforded white crystals with high purity as shown by the representative $^1$H NMR of BZ(10)DMEDA in Figure 17.

*Ring Opening Polymerization (ROP)*

Cationic ring-opening polymerization was carried out according to a stepwise heating protocol of 100°C (1 h), 140°C (1 h), 160°C (2 h), and 180°C (4 h). The curing protocol was developed by considering the onset of thermal degradation obtained from previous TGA experiments.[40] The polymerization process of the BZ(R)DMEDA monomers was followed by gATR-FTIR. For example, the characteristic benzoxazine

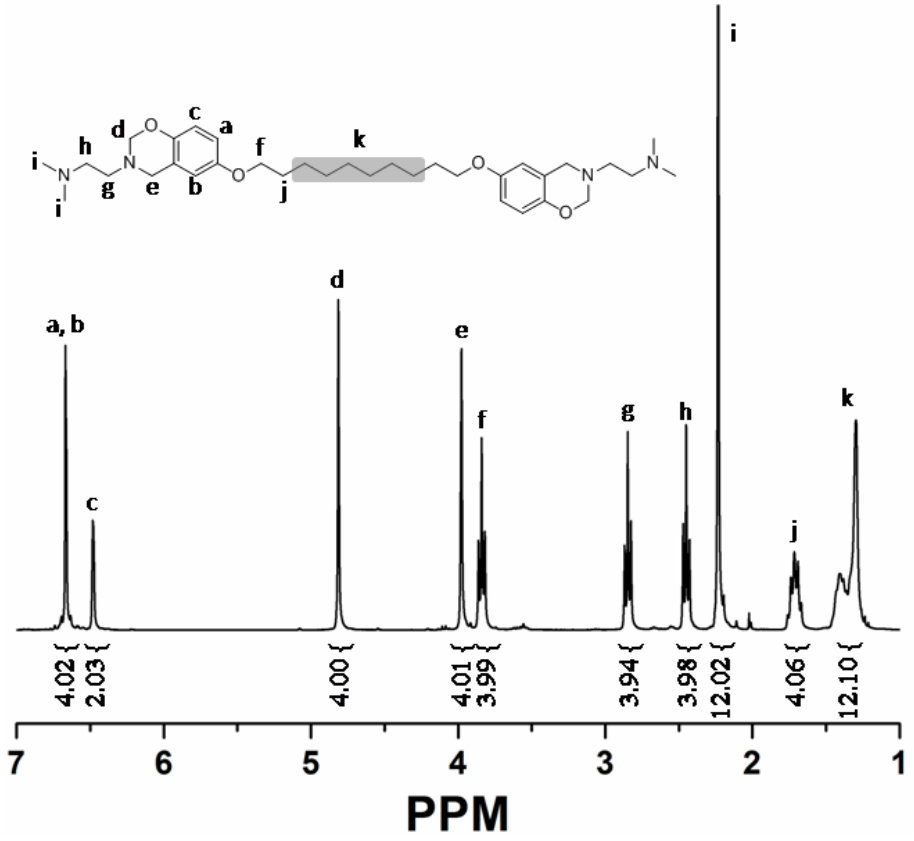


*Figure 17*. $^{1}$H NMR of bisbenzoxazine monomer BZ(10)DMEDA (6d).

peaks observed for BZ(10)DMEDA appear at 928 $cm^{-1}$ assigned to the out of plane C–H vibration of the benzene ring attached to the oxazine ring and another at 1222 $cm^{-1}$ due to C–O–C asymmetric stretch of the oxazine ring, and two peaks at 1498 $cm^{-1}$ and 803 $cm^{-1}$ assigned to the vibration of the tri-substituted benzene ring. These peaks are no longer present following the thermal cure at 180°C. The diminished intensities of these peaks indicate high conversion is achieved for the ROP. Additionally, a new peak appears at 1480 $cm^{-1}$, corresponding to the tetra-substituted benzene ring that results from ring-opening polymerization of the benzoxazine. Similar results are observed for all monomers and polymers alike shown in Table C1of Appendix C.

Following gATR-FTIR experiments, DSC was used to further probe the thermal curing behavior of the benzoxazine monomers. The DSC thermograms for the monomer

series are shown in Figure 19. Monomer melting points – reported as the peak of the endothermic transition – range between 70.0-78.5°C but with no observable trend. The PEG based BZ monomer, however, shows no melting point as a result of the additional ether groups which makes crystallization more difficult in this case. Polymerization exotherms also seem independent to the monomer core showing peak temperatures ranging from 183-192°C with no obvious trend. The exotherm magnitude is highest for BZ(4)DMEDA, at 137.4 $Jg^{-1}$, and continuously decreases with longer aliphatic chain lengths to 84.3 $Jg^{-1}$ for BZ(10)DMEDA – an expected result attributed to dilution of the benzoxazine ring mass fraction which is consistent with previous reports for other flexible benzoxazines.[40-42]

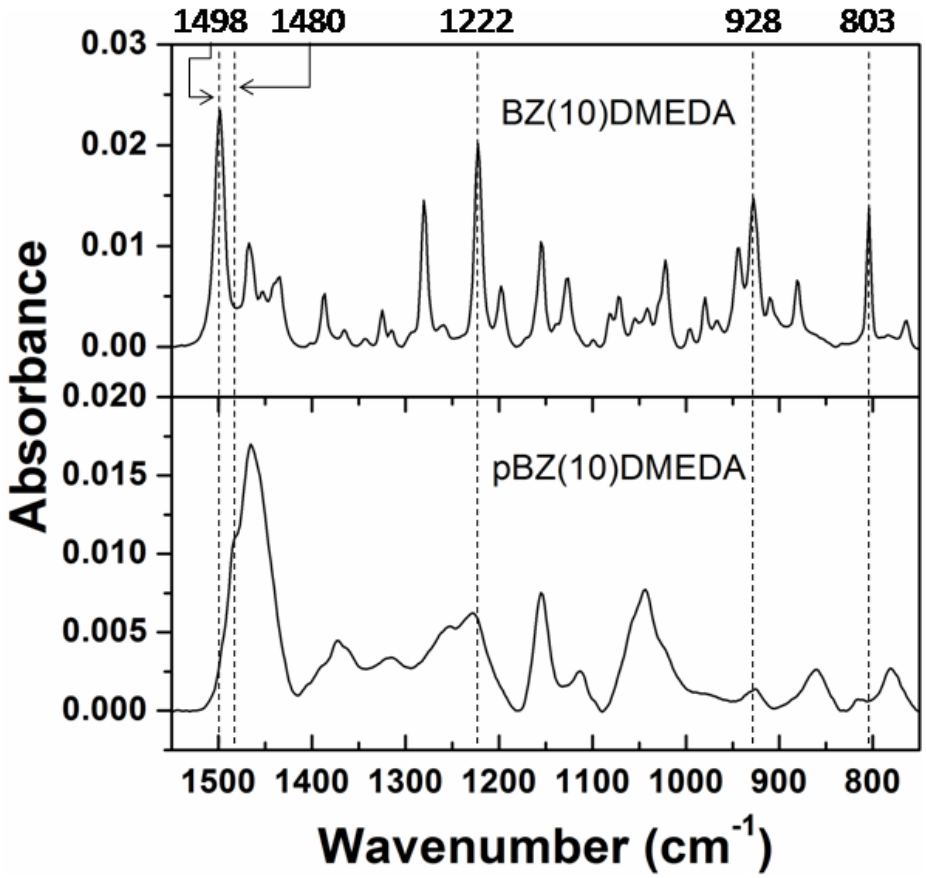


*Figure 18*. FTIR spectra of (top) BZ(10)DMEDA monomer and (bottom) pBZ(10)DMEDA polymer following cationic ring-opening polymerization at 180 °C. The results shown are representative for the monomer series.

Consistent with our FTIR data previously discussed, the second heating cycle (Figure 19, dashed lines) for each monomer exhibits little residual exotherm, indicating the ring-opening polymerization proceeds to near quantitative conversion under the DSC ramp conditions (i.e. $T_{max}$ 300°C). A summary of the DSC data can be found in Table C2. As a side note, one sees a significant reduction of the peak exotherm temperature with the incorporation of the pendant tertiary amine. Comparing previous experiments of *n*-butyl pendent benzoxazines[40] with the current materials, one sees comparable melting points differing by an average of 4°C; however, the peak exotherm temperature significantly decreases by an average of 66.5°C. A representative DSC is shown in Figure C1. Additionally, isothermal (180°C) rheological experiments show a sharp increase in viscosity after an hour for the *n*-butyl pendent benzoxazine compared to only about 2 minutes for the tertiary amine pendent benzoxazine (Figure C2).

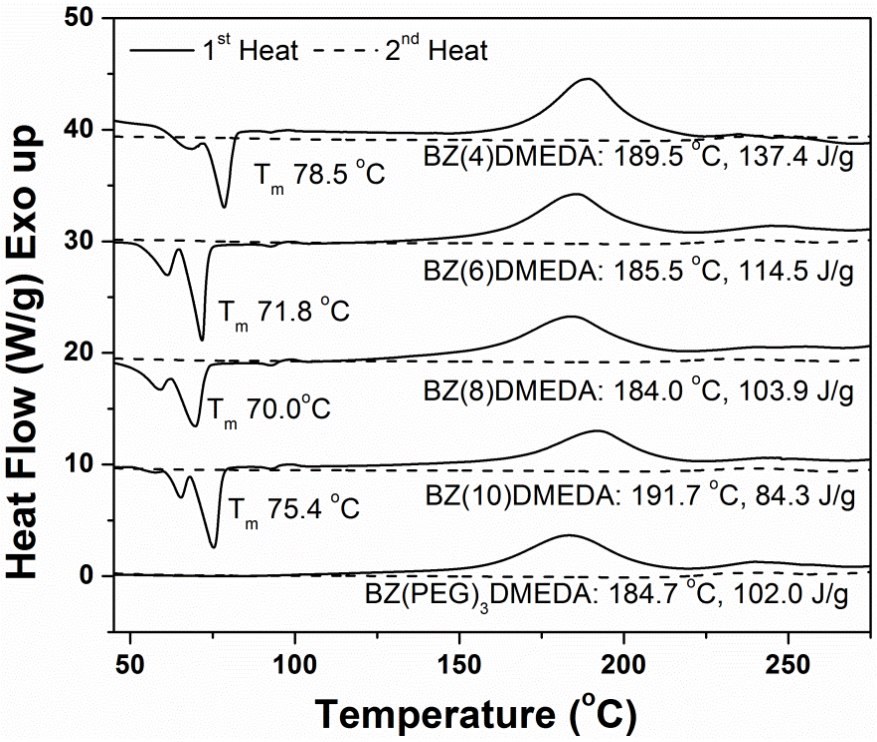


*Figure 19*. DSC thermograms for the BZ(R)DMEDA monomer series. First (solid line) and second (dashed line) heating cycles are shown.

It has been previously reported that once polymerization begins, the tertiary amine formed (Mannich bridge) will catalyze further ring opening processes to occur.[43] The results shown seem to confirm this hypothesis.

*Quaternization:*

Submersing the polybenzoxazine films in methyl iodide allows swelling of the network followed by quaternization of the tertiary amines, affording a simple post-polymerization alkylation process of the amines in the material. Using gATR-FTIR, a broad absorbance peak at 3430 $cm^{-1}$ for both the quaternized monomer and polymer was observed indicating the present of quaternary amines (Figure 20). This peak was confirmed to be associated with a quaternary amine by comparing the quaternized and unquaternized monomers with $^{1}H$ NMR experiments (Figures C3-C4). Note: pre-quaternized monomers were polymerized; however, during the curing process, the films foamed creating numerous voids making an unusable membrane material. Moreover, the degree of quaternization, or ion-exchange capacity (IEC), was investigated using standard back titration methods. The theoretical and measured IEC values are shown in Figure 21. The IEC as expected increases as the molecular weight of the monomers decreases; however, deviations from the theoretical values are inconsistent. The more flexible pBZ(10)DMEDA only reached 49% of its theoretical IEC compared to 86% for pBZ(4)DMEDA. The Hofmann elimination appears to be the most obvious explanation for the decrease in IEC as β-hydrogens present in the membrane will degrade the pendant quaternary amine into an olefin and release a tertiary amine that reduces the measured IEC. The longer cores are more susceptible to this degradation process possibly due to the added flexibility which increases the availability of the β-hydrogens to free hydroxide ions. Additionally, as shown in Figure 21, the longer the films stayed in the KOH

solution the lower the IEC dropped, further pointing toward the possibility that the membranes are unstable under alkaline conditions. Additional analysis is required; however, it is clear that using the hydroxide counter-ion will be problematic.

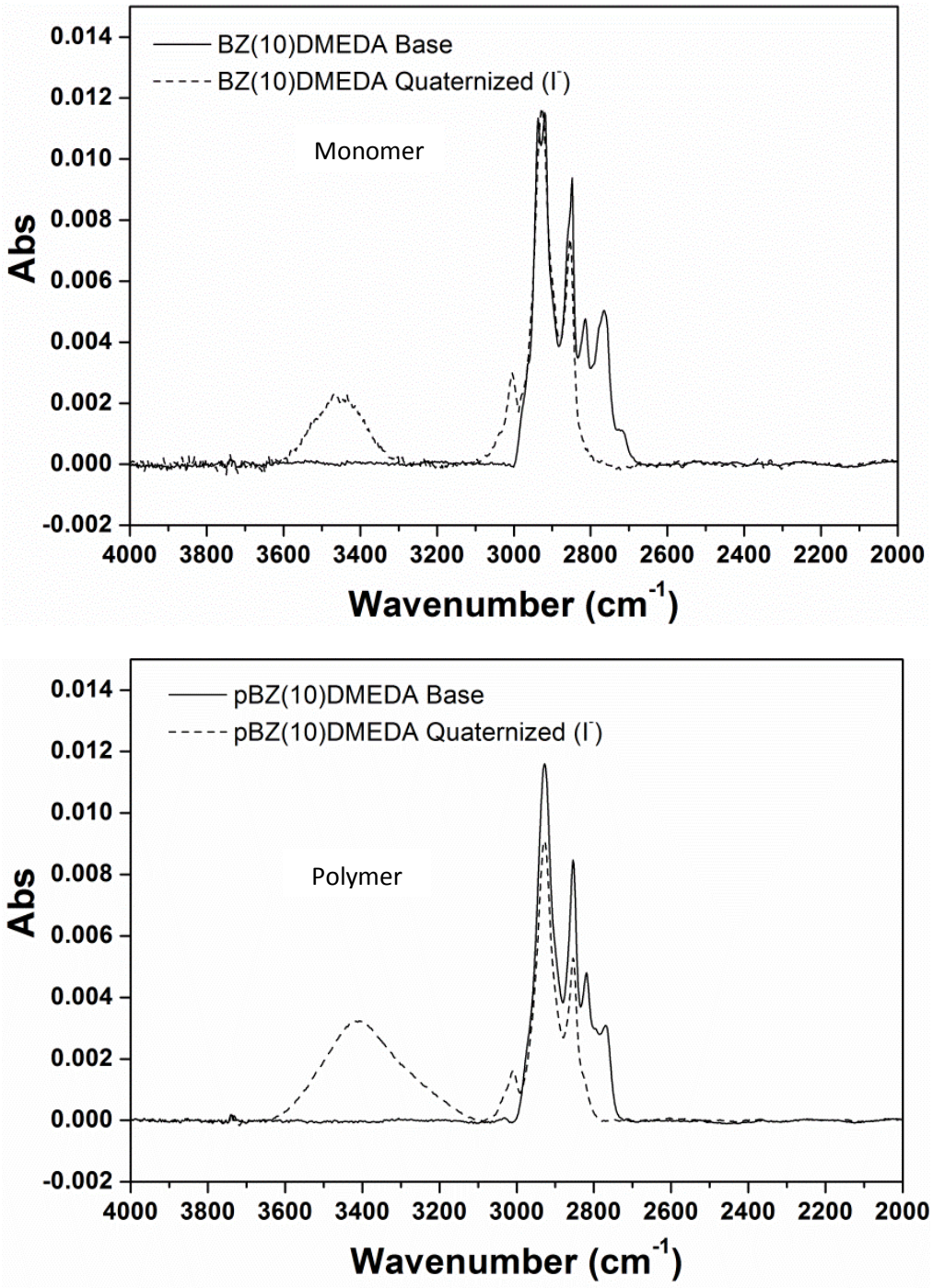


*Figure 20*. IR spectra of the BZ(10)DMEDA monomer pre and post quaternization with methyl iodide (top); and IR spectra of the cured pBZ(10)DMEDA film pre and post quaternization with methyl iodide (bottom).

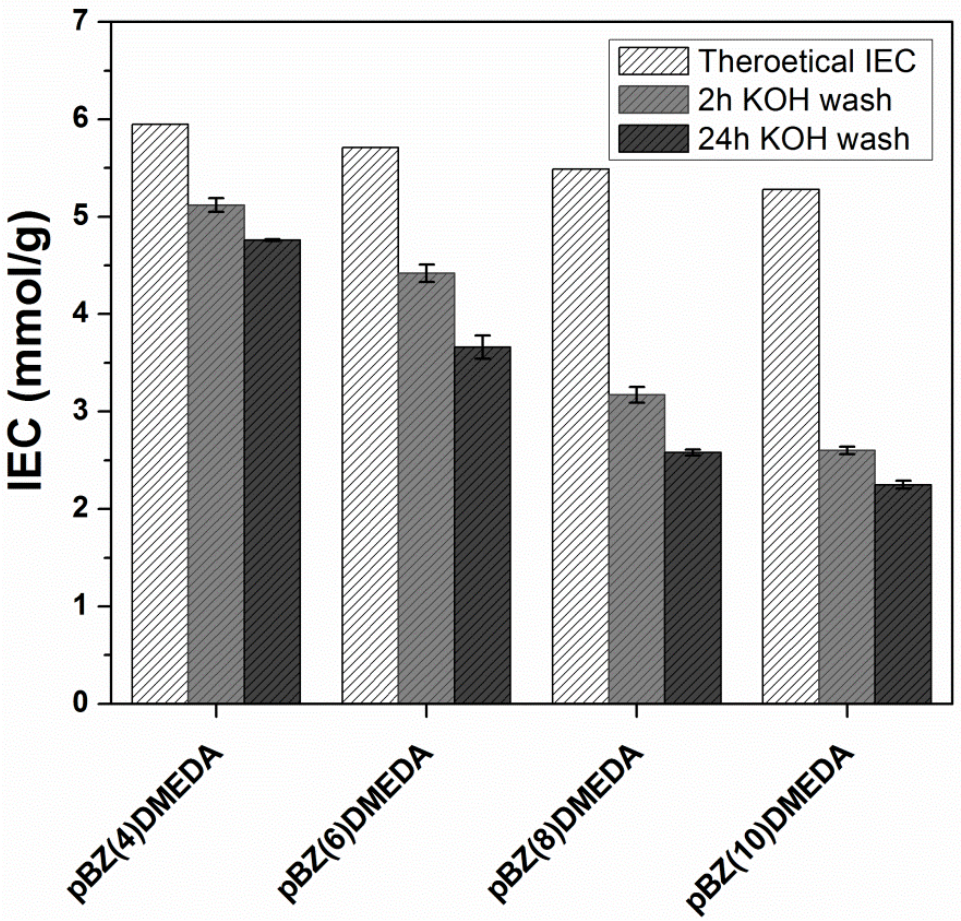


*Figure 21*. IEC results for the BZ(R)DMEDA monomer series at 2h and 24h KOH washes.

*Conductivity measurements*

The efficiency of AEM materials is most commonly related to the ionic conductivity and can be done using a variety of methods and under different conditions. For this work conductivity was measured in DI water at 80°C and analyzed against a variety of parameters including the counter-ion and core length.

*Counter-ion*

Different counter ions were analyzed by soaking the films in a 0.1 M solution of KX (X = $Cl^-$, $Br^-$, $OH^-$) four times for 30 minutes, each to exchange the $I^-$ for other anions. This process was followed by a 30 minutes wash with DI water. As shown in Figure 22 the counter-ion has a significant effect on the ion conductivity. The results

from the ion conductivity of the halogens ($I^-$, $Cl^-$, $Br^-$) can possibly be explained in terms of their size, where the smaller ions have higher mobility through the highly cross-linked network that resulted in an increased conductivity. However, the same cannot be explained for the $OH^-$. The films appeared to degrade, as discussed in the previous section, and turned an irreversible dark brown, but the most convincing sign that it was degrading was the strong amine odor that the films gave off. If the Hofmann elimination were taking place, the tertiary amine given off would be trimethyl amine which is a colorless gas with a fishy or ammoniacal aroma.

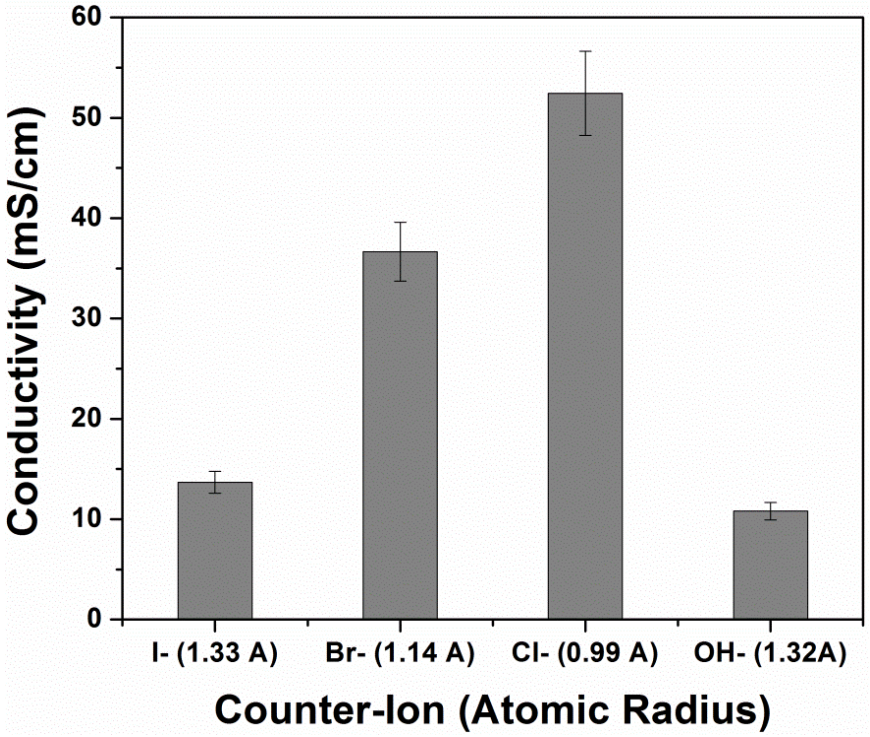


*Figure 22*. Dependence of the counter-ion ($I^-$, $Br^-$, $Cl^-$, OH) vs. conductivity for a single membrane material (quaternized pBZ(10)DMEDA).

To probe this further, films exchanged with $I^-$, $Br^-$, $Cl^-$, and $OH^-$ and were left in DI water for an additional 24 hours prior to testing the conductivity. The $OH^-$ containing counter-ion dropped to 3.2 mS/cm, whereas all the halogen counter-ions showed stable conductivities over the 24 hours. The results support the idea that the materials are

unstable under alkaline (basic) conditions, and because of this, the remainder of the conductivity measurements utilizes $Cl^-$ as the counter-ion due to its high conductivity and high stability.

*Core length*:

By changing the core length of the network, a variety of concerted AEM properties change. IEC, being one of them, decreases with increasing core length as discussed earlier. One would expect a higher IEC to produce the highest conductivity as a larger concentration of cationic charge carriers could facilitate better mobility of the anions; however, as shown in Figure 22, this is not occurring for the benzoxazine based AEMs. The highest IEC correlates to the lowest conductivity (pBZ(4)DMEDA) which contradicts the preconceived notion that IEC and conductivity are directly related. One notable aspect for these materials is that they all contain very high IEC values (up to 5.12 mmol/g). These results are associated with the design of the monomers which contain two pendant amines along with two additional amines that become available post polymerization via the Mannich bridge. The IEC values reported in this project are of the highest reported, and it is speculated that the limiting factor for these materials is not the concentration of charge carriers (Table 2).

Water uptake, also being an important property in AEMs, was analyzed and showed an increase with increasing core length - most notably going from pBZ(4)DMEDA (~6%) to pBZ(6)DMEA (~21%) followed by a leveling off for longer cores. The rational for this sudden increase requires further investigation; however, a possible explanation could be found in the thermal properties of the networks. The short cored pBZ(4)DMEDA shows the highest $T_g$ (Figure C5) of all the samples which suggests that the material could have been glassy under the testing conditions (80°C)

limiting chain mobility, reducing swelling, and reducing water uptake. This increased water uptake for the longer core also correlates to an increase in ion conductivity (Table 2). This seems logical when comparing to other AEM materials as conductivity is maximized at higher water uptake (>50%).

Table 2

*Summary of membrane properties (IEC, water uptake, and conductivity).*

| Sample | Measured IEC (mmol/g) | Water Uptake (%) | Conductivity (mS/cm) |
|---|---|---|---|
| pBZ(4)DMEDA | 5.12 ± 0.07 | 6.3 ± 0.315 | 4.3 ± 0.344 |
| pBZ(6)DMEDA | 4.42 ± 0.09 | 20.2 ± 1.01 | 49.25 ± 3.94 |
| pBZ(8)DMEDA | 3.17 ± 0.08 | 20.8 ± 1.04 | 51.3 ± 4.104 |
| pBZ(10)DMEDA | 2.6. ± 0.04 | 20.3 ± 1.06 | 52.45 ± 4.196 |

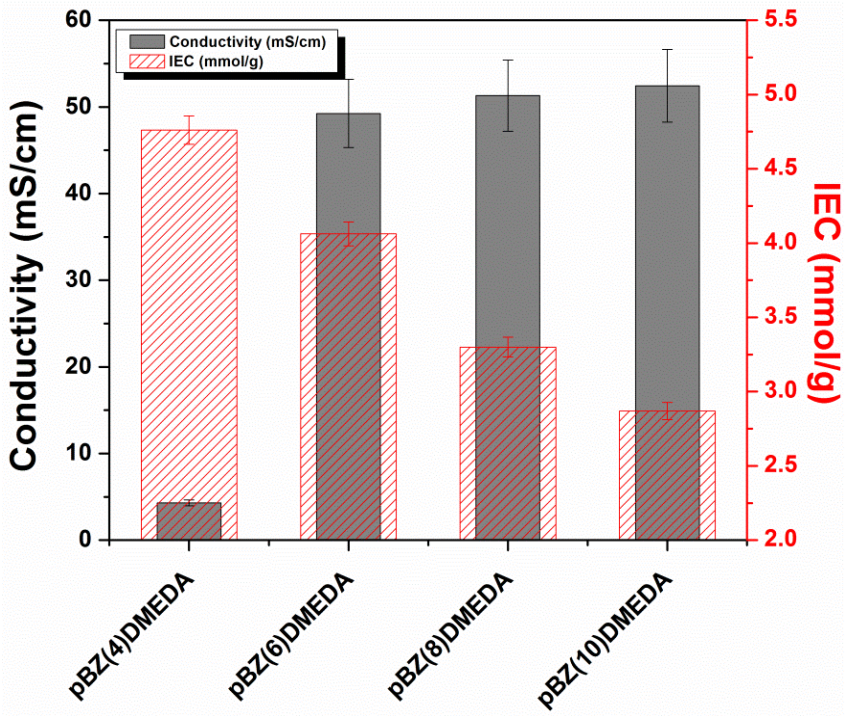


*Figure 23*. Dependence of the IEC vs. conductivity for the benzoxazine series pBZ(R)DMEDA.

To further expand the relationship between water uptake and conductivity, a hydrophilic monomer containing an ethylene glycol based core [BZ(PEG)$_3$DMEDA] was

synthesized. After polymerization and quaternization, moisture analysis results show a twofold increase in water uptake for the more hydrophilic network; however, the increase in water uptake diminished the mechanical stability beyond a testable material. On the other hand, by combining an aliphatic monomer [BZ(10)DMEDA] and the hydrophilic monomer [BZ(PEG)$_3$DMEDA], copolymer networks can be made to both increase water uptake from the hydrophilic monomer while retaining substantial mechanical stability from the aliphatic monomer. Compared to BZ(10)DMEDA, a copolymerization containing 75:25 BZ(10)DMEDA:BZ(PEG)$_3$DMEDA (w/w), showed an increase in water uptake to 25.7% and revealed a significant increase in conductivity to 67.4 mS/cm. This observation reinforces the idea that water uptake plays a significant role in the efficiency of highly cross-linked benzoxazine networks as an AEM material.

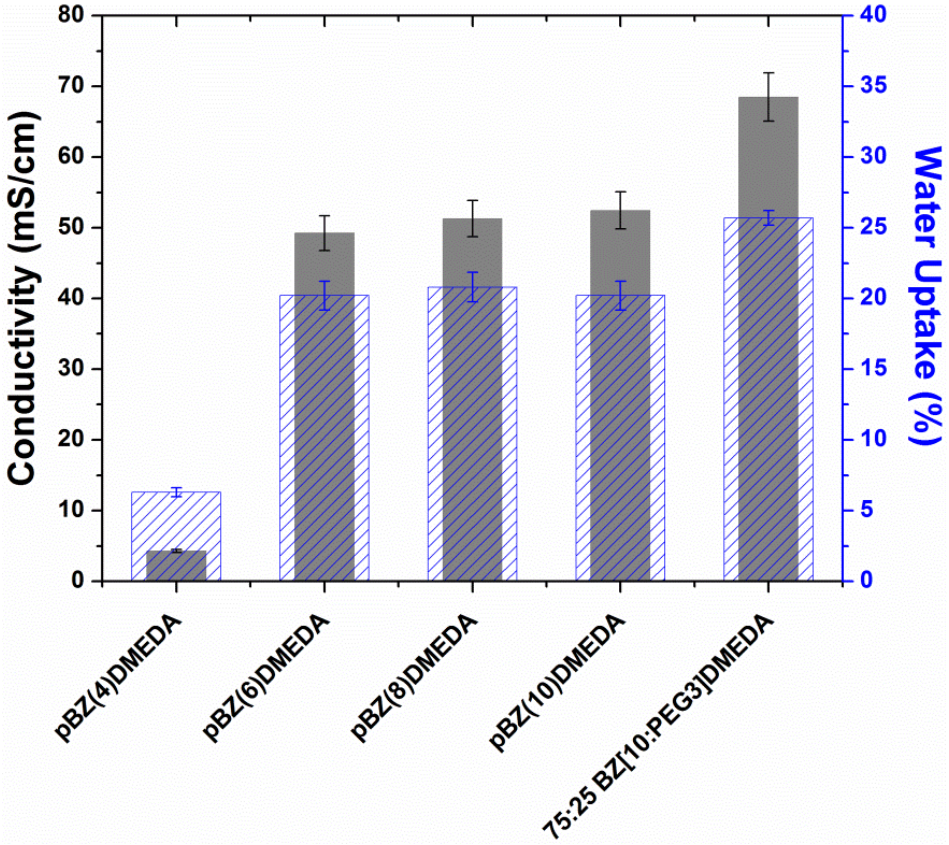


*Figure 24*. Dependence of water uptake vs. conductivity for benzoxazine series pBZ(R)DMEDA.

# Conclusions

The successful synthesis of a series of flexible benzoxazine monomers containing pendant tertiary amines with ease and to high purity has been reported. Thermally accelerated cationic ring-opening polymerization of these bisbenzoxazine monomers provided flexible, uniform polybenzoxazine thermoset thin films under solvent-free conditions. FTIR and DSC analysis of the ring-opening polymerization show that the polymerizations proceed to high conversion, with minimal dependence on the length of the aliphatic-bridged bisphenol linker. Additionally, the tertiary amines appeared to have a catalytic effect on the polymerization as the peak curing exotherms decreased to sub-200°C temperatures; however, further investigation is required. Post polymerization functionalization using methyl iodide showed to be a facile approach to quaternize the tertiary amines, creating a high concentration of cationic charge carriers within the material. To observe this gATR-FTIR was used showing a broad absorbance peak at 3430 $cm^{-1}$ for both the quaternized monomer and polymer, indicating the present of quaternary amines. To determine the concentration of quaternary amines (IEC), back titrations were used; however, instabilities of the amines under alkaline conditions were observed. β-hydrogens present in the material can be abstracted by a hydroxide anion and degrade the pendant quaternary amine into an olefin, releasing a tertiary amine and reducing the measured IEC. Additionally, when comparing conductivities the instabilities of the hydroxide counter-ion are also seen as the highest conductivity reaches only 10.8 mS/cm and consistently drops at longer exposure times. As a result of the instabilities of the hydroxide the counter-ion, $Cl^-$ was utilized as the counter-ion for further analysis due to its high conductivity and high stability. When comparing the conductivities of the different cores, the IEC appeared to have a minimal effect on the

overall conductivity as the design of the monomers incorporates a possible four quaternary amines per repeat unit, affording extremely high IEC values. Additionally, the hydroxide counter-ion showed instabilities in both the IEC and conductivity measurements in which $Cl^-$ was the primary counter-ion utilized.

Water uptake, however, proved to be a more accurate representation of how the core affects conductivity. The short cored [pBZ(4)DMEDA] network only showed a ~6% water uptake which correlates to a 4.3 mS/cm ($Cl^-$) conductivity, whereas the long cored [pBZ(6, 8, and10)DMEDA] networks show water uptake around 21% and a conductivity ranging between 49-53 mS/cm. The rationale for this could be found in the thermal properties of the networks as the $T_g$ of pBZ(4)DMEDA may exceed the measurement conditions of 80°C. Further investigation revealed that a copolymer containing 25% of a hydrophilic PEG cored monomer and 75% of pBZ(10)DMEDA showed both a higher water uptake and conductivity than any of the aliphatic cored networks. Under solvent free conditions, the monomers were melted, mixed, and cured to form homogeneous networks with a modest increase in water uptake of 5%, which correlated to an increase in conductivity of 16 mS/cm further defining these materials as being water uptake dependent.

## Acknowledgments

The author gratefully acknowledges financial support from the National Science Foundation (NSF CAREER DMR-1056817) and the Office of Naval Research (Award N00014-07-1-1057). ADB acknowledges support from a fellowship from the National Science Foundation GK-12 program “Molecules to Muscles” (Award #0947944) through The University of Southern Mississippi. GT was funded through an NSF-REU (DMR-1005127).

# REFERENCES


1. Herman, H.; Slade, R. C. T.; Varcoe, J. R. *Journal of Membrane Science* **2003,** *218* (1-2), 147-163.
2. Slade, R. C. T.; Varcoe, J. R. *Solid State Ionics* **2005,** *176* (5-6), 585-597.
3. Varcoe, J. R.; Slade, R. C. T. *Electrochemistry Communications* **2006,** *8* (5), 839-843.
4. Hibbs, M. R.; Hickner, M. A.; Alam, T. M.; McIntyre, S. K.; Fujimoto, C. H.; Cornelius, C. J. *Chemistry of Materials* **2008,** *20* (7), 2566-2573.
5. Wang, G.; Weng, Y.; Chu, D.; Chen, R.; Xie, D. *Journal of Membrane Science* **2009,** *332* (1-2), 63-68.
6. Zhou, J.; Unlu, M.; Vega, J. A.; Kohl, P. A. *Journal of Power Sources* **2009,** *190* (2), 285-292.
7. Wang, G.; Weng, Y.; Chu, D.; Xie, D.; Chen, R. *Journal of Membrane Science* **2009,** *326* (1), 4-8.
8. Hibbs, M. R.; Fujimoto, C. H.; Cornelius, C. J. *Macromolecules* **2009,** *42* (21), 8316-8321.
9. Xiong, Y.; Fang, J.; Zeng, Q. H.; Liu, Q. L. *Journal of Membrane Science* **2008,** *311* (1-2), 319-325.
10. Wan, Y.; Peppley, B.; Creber, K. A. M.; Bui, V. T.; Halliop, E. *Journal of Power Sources* **2006,** *162* (1), 105-113.
11. Sata, T.; Tsujimoto, M.; Yamaguchi, T.; Matsusaki, K. *Journal of Membrane Science* **1996,** *112* (2), 161-170.
12. Gu, S.; Cai, R.; Luo, T.; Chen, Z.; Sun, M.; Liu, Y.; He, G.; Yan, Y. *Angewandte Chemie International Edition* **2009,** *48* (35), 6499-6502.

13. Kong, X.; Wadhwa, K.; Verkade, J. G.; Schmidt-Rohr, K. *Macromolecules* **2009,** *42* (5), 1659-1664.

14. Pivovar, B.; Thorn, D. Anion-conducting polymer, composition, and membrane. 7,439,275 B2, **2008**.

15. Swier, S.; Ramani, V.; Fenton, J. M.; Kunz, H. R.; Shaw, M. T.; Weiss, R. A. *Journal of Membrane Science* **2005,** *256* (1-2), 122-133.

16. Hou, H.; Sun, G.; He, R.; Sun, B.; Jin, W.; Liu, H.; Xin, Q. *International Journal of Hydrogen Energy* **2008,** *33* (23), 7172-7176.

17. Hou, H.; Sun, G.; He, R.; Wu, Z.; Sun, B. *Journal of Power Sources* **2008,** *182* (1), 95-99.

18. Fu, J.; Qiao, J.; Lv, H.; Ma, J.; Yuan, X.-Z.; Wang, H. *ECS Trans* **2010,** *25* (13), 15-23.

19. Sata, T.; Kawamura, K.; Matsusaki, K. *Journal of Membrane Science* **2001,** *181* (2), 167-178.

20. Tripathi, B. P.; Kumar, M.; Shahi, V. K. *Journal of Membrane Science* **2010,** *360* (1-2), 90-101.

21. Wu, Y.; Wu, C.; Xu, T.; Fu, Y. *Journal of Membrane Science* **2009,** *329* (1-2), 236-245.

22. Zhang, S.; Wu, C.; Xu, T.; Gong, M.; Xu, X. *Journal of Solid State Chemistry* **2005,** *178* (7), 2292-2300.

23. Zhang, S.; Xu, T.; Wu, C. *Journal of Membrane Science* **2006,** *269* (1-2), 142-151.

24. Agel, E.; Bouet, J.; Fauvarque, J. F. *Journal of Power Sources* **2001,** *101* (2), 267-274.

25. Park, J.-S.; Park, S.-H.; Yim, S.-D.; Yoon, Y.-G.; Lee, W.-Y.; Kim, C.-S. *Journal of Power Sources* **2008,** *178* (2), 620-626.

26. Hong, J.-H.; Hong, S.-K. *Journal of Applied Polymer Science* **2010,** *115* (4), 2296-2301.

27. Hong, J.-H.; Li, D.; Wang, H. *Journal of Membrane Science* **2008,** *318* (1-2), 441-444.

28. Stoica, D.; Ogier, L.; Akrour, L.; Alloin, F.; Fauvarque, J. F. *Electrochimica Acta* **2007,** *53* (4), 1596-1603.

29. Wan, Y.; Peppley, B.; Creber, K. A. M.; Bui, V. T.; Halliop, E. *Journal of Power Sources* **2008,** *185* (1), 183-187.

30. Wang, E. D.; Zhao, T. S.; Yang, W. W. *International Journal of Hydrogen Energy* **2010,** *35* (5), 2183-2189.

31. Xiong, Y.; Liu, Q. L.; Zhang, Q. G.; Zhu, A. M. *Journal of Power Sources* **2008,** *183* (2), 447-453.

32. Yang, C.-C.; Chiu, S.-J.; Chien, W.-C.; Chiu, S.-S. *Journal of Power Sources* **2010,** *195* (8), 2212-2219.

33. Wu, Y.; Wu, C.; Xu, T.; Lin, X.; Fu, Y. *Journal of Membrane Science* **2009,** *338* (1-2), 51-60.

34. Wu, Y.; Wu, C.; Xu, T.; Yu, F.; Fu, Y. *Journal of Membrane Science* **2008,** *321* (2), 299-308.

35. Wu, Y.; Wu, C.; Varcoe, J. R.; Poynton, S. D.; Xu, T.; Fu, Y. *Journal of Power Sources* **2010,** *195* (10), 3069-3076.

36. Clark, T. J.; Robertson, N. J.; Kostalik Iv, H. A.; Lobkovsky, E. B.; Mutolo, P. F.; Abruna, H. c. D.; Coates, G. W. *Journal of the American Chemical Society* **2009,**

*131* (36), 12888-12889.

37. Robertson, N. J.; Kostalik, H. A.; Clark, T. J.; Mutolo, P. F.; Abruna, H. c. D.; Coates, G. W. *Journal of the American Chemical Society* **2010,** *132* (10), 3400-3404.

38. Sawaryn, C.; Landfester, K.; Taden, A. *Macromolecules* **2011,** *44* (19), 7668-7674.

39. Hamerton, I.; Howlin, B. J.; Klewpatinond, P.; Takeda, S. *Macromolecules* **2009,** *42* (20), 7718-7735.

40. Baranek, A. D.; Kendrick, L. L.; Narayanan, J.; Tyson, G. E.; Wand, S.; Patton, D. L. *Polymer Chemistry* **2012,** *3* (10), 2892-2900.

41. Allen, D. J.; Ishida, H. *Polymer* **2007,** *48* (23), 6763-6772.

42. Agag, T.; Takeichi, T. *Macromolecules* **2001,** *34* (21), 7257-7263.

43. Xu, L.; Situ, Y.; Hu, J.-f.; Zeng, H.-w.; Chen, H.q. *J. Cent. South Univ. Technol.* **2009,** *16* (3), 0392-0398.

# CHAPTER VI

# CONCLUSIONS AND FUTURE WORK

With the array of tangible properties available to polybenzoxazines, an almost limitless potential of applications are available. This dissertation highlights the versatile monomer and polymer synthesis in an effort to expand the knowledge and understanding of what polybenzoxazines are capable of achieving. Through this work, both flexible and functional polybenzoxazine networks directed toward thin film applications have been achieved.

In the first study, a series of novel aliphatic-bridged bisphenol-based benzoxazine monomers comprising four to ten methylene spacer units (pBZ(n)BA) was synthesized. The four step synthesis of each monomer proceeded in high-to-moderate yields and was attainable in high purity. Thermally-accelerated cationic ring-opening polymerization of these bisbenzoxazine monomers provided flexible, uniform polybenzoxazine thermoset thin films under solvent-free conditions. The curing process proceeded to high conversion (>95%) as the flexible cores allowed higher mobility of the benzoxazines groups, and suppressed vitrification of the network at the curing profile was used. The thermomechanical properties of the pBZ(n)BA, such as rubbery storage modulus and glass transition temperature, show a strong dependence on the length of the aliphatic-bridged bisphenol linker where both properties decreased with increasing linker length. In particular, changing the length of the aliphatic-bridged bisphenol linker enables tailoring the $T_g$ of the pBZ(n)BA series from 67°C to 101°C. Tensile properties of the pBZ(n)BA series were shown to follow similar trends with Young's modulus decreasing and elongation at break increasing, with increasing aliphatic-bridged bisphenol linker length. Regarding thermal stability, the pBZ(n)BA materials all show a similar three mode

degradation process consistent with other bisphenol-based polybenzoxazines and exhibit a decrease in char yield with increasing aliphatic chain length, which is owed to a decrease in aromatic content in the thermoset network.

In the second project, the copolymerization of a flexible aliphatic-bridged bisphenol-based benzoxazine monomer comprising ten methylene units (BZ(10)BA) with two rigid benzoxazine monomers (commercially available Araldite 35600 and 35900) via a solvent free cationic ring opening polymerization process was reported. The effects of monomer feed composition on polymerization behavior, thermomechanical transitions, and thermal degradation properties were reported. The ring-opening copolymerizations showed that – in terms of polymerization onset temperature and total exothermic transition – they depend greatly on the composition of the monomer feed. Samples containing larger concentrations of BZ(10)BA exhibited higher onset temperatures with lower polymerization enthalpies. The thermomechanical properties of the copolybenzoxazine networks showed a strong dependence on the monomer feed ratio, where higher Araldite content resulted in a both a higher storage modulus and $T_g$ of the network. The most salient feature of benzoxazine copolymerization was revealed in the tailorability in thermomechanical properties, which were varied by 149 °C simply by changing the monomer feed ratio to which the $T_g$ was observed to be accurately predicted using the Fox equation.

In the third and final project the synthesis of tertiary amine functional benzoxazine monomers that represent the vast tailorability of polybenzoxazines was reported. The tertiary amines appeared to have a catalytic affect on the polymerization as the peak curing exotherms showed sub-200°C temperatures. Post polymerization functionalization using methyl iodide showed to be a facile approach to quaternize the

tertiary amines, creating a high concentration of cationic charge carriers within the material. However, β-hydrogens in the material proved to be susceptible to the hydroxide counter-ion as they can be abstracted and consequently, degrade the pendant quaternary amine into an olefin that release a tertiary amine and reduces the measured IEC. As a result of the instabilities of the hydroxide counter-ion, $Cl^-$ was utilized as the counter-ion for further analysis due to its high conductivity and high stability. When comparing the conductivities of the different cores the IEC appeared to have a minimal effect on the overall conductivity; however, water uptake proved to be a more accurate representation of how the core affects the conductivity. The shortest core [pBZ(4)DMEDA] showed the lowest water uptake and conductivity, and the longer (6, 8 and 10) cores showed the higher water uptake around 21% and a higher conductivity ranging between 49-53 mS/cm. The rationale for this could be found in the thermal properties of the networks as the $T_g$ of pBZ(4)DMEDA may exceed the measurement conditions of 80°C. Additionally, the water uptake can be increased by combining a hydrophilic PEG cored monomer with an aliphatic monomer. Under solvent free conditions, the monomers were melted, mixed, and cured to form homogeneous networks with both the hydrophilic monomer and an aliphatic monomer. The copolymer showed an increase in both the water uptake and conductivity when compared to the neat aliphatic cored network, providing further evidence that the ion conductivity is limited by water uptake.

# APPENDIX A

## FLEXIBLE ALIPHATIC-BRIDGED BISPHENOL-BASED POLYBENZOXAZINES

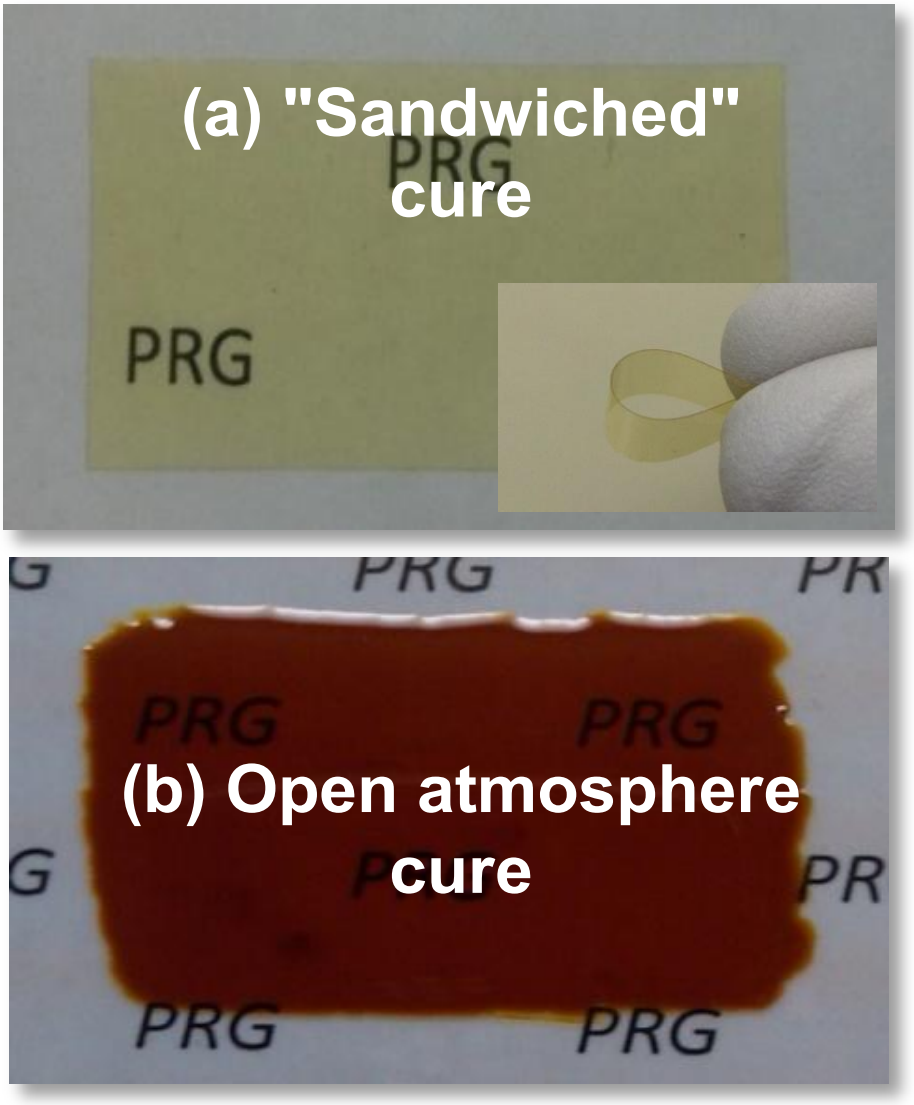


*Figure A1*. Photos of pBZ(10)BA thermally cured at 180 °C in (a) sandwich configuration and (b) open configuration. Using the sandwich method, highly uniform films with dimensions up to 15 cm × 15 cm were easily prepared with thickness controlled by a PTFE spacer.

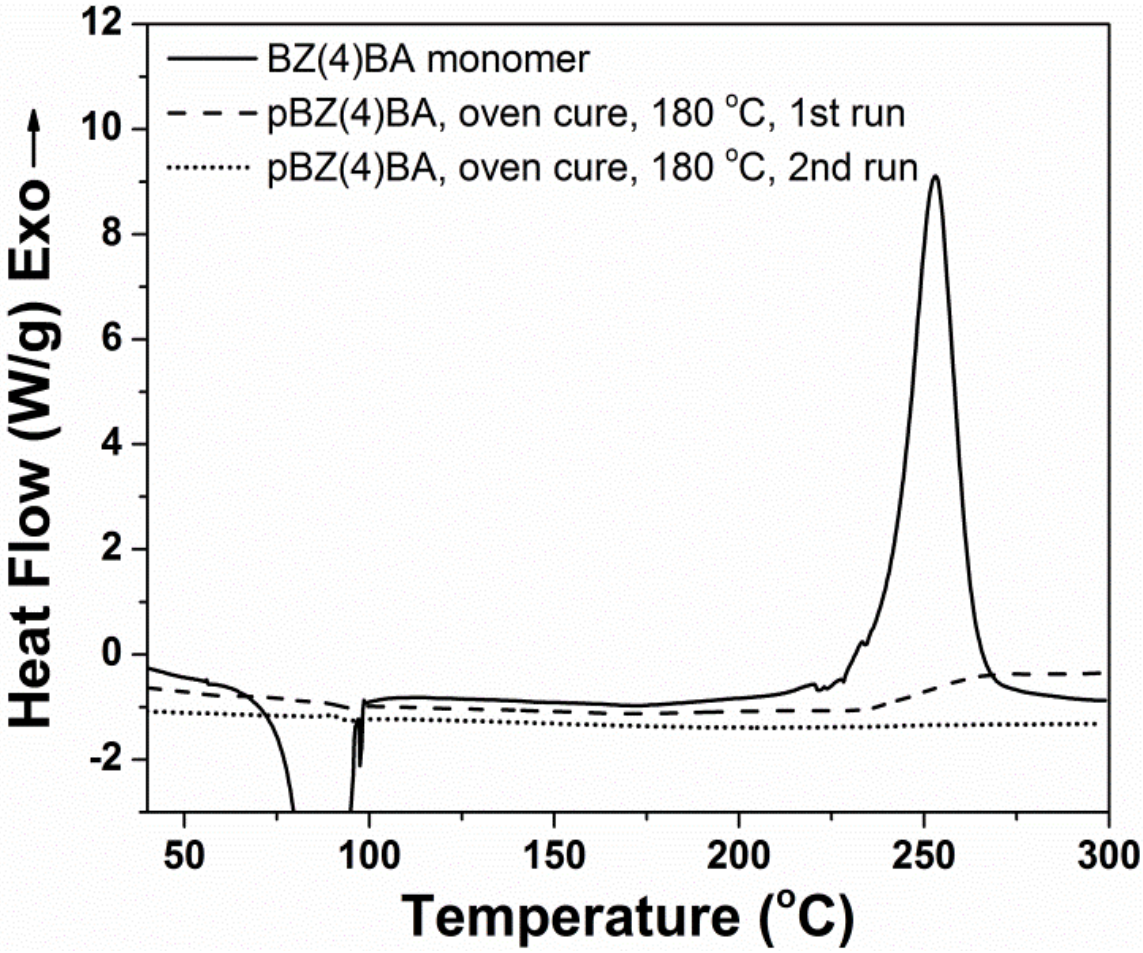


*Figure A2.*DSC thermograms of pBZ(4)BA oven cured according to the cure schedule of 100 °C (1h), 140 °C (1h), 160 °C (2h), and 180 °C (8h). First and second heating cycles for pBZ(4)BA are shown compared with the monomer polymerization.

Table A1

*Thermomechanical, tensile and thermal degradation properties for the pBZ(n)BA series.*

| | pBZ(4)BA | pBZ(6)BA | pBZ(8)BA | pBZ(10)BA |
|---|---|---|---|---|
| MW Monomer (g/mol) | 468.63 | 496.68 | 524.73 | 552.79 |
| $T_g$ (°C) | 100.9 | 81.9 | 76.1 | 66.5 |
| E′ 30 °C (MPa) | 796 | 722 | 728 | 602 |
| E′ $T_g$+40 °C (MPa) | 12.7 | 9.03 | 8.55 | 7.35 |
| ρ (g/cm$^3$) | 1.1 | 1.12 | 1.1 | 1.11 |
| $p_x$(×10$^{-3}$mol cm$^{-3}$) | 1.23 | 0.915 | 0.88 | 0.771 |
| $M_c$ (g/mol) | 949 | 1259 | 1231 | 1418 |
| Young's Modulus (MPa) | 19.5 | 16.6 | 14.1 | 13 |
| Elongation at Break (%) | 6.47 | 6.94 | 8.43 | 9.71 |
| $T_d$2% (°C) | 206 | 186 | 193 | 195 |
| $T_d$5% (°C) | 236 | 228 | 231 | 231 |
| $T_d$10% (°C) | 255 | 249 | 252 | 252 |
| Char Yield (%) | 19.7 | 17.4 | 15.3 | 14.4 |

[a] $p_x$ is crosslink density; $M_c$ is molecular weight between cross-links
$T_d$ is the degradation temperature at the indicated weight loss

# APPENDIX B

# SOLVENT-FREE COPOLYMERIZATION OF RIGID AND FLEXIBLE BIS-1,3-BENZOXAZINES: FACILE TUNABILITY OF POLYBENZOXAZINE NETWORK PROPERTIES

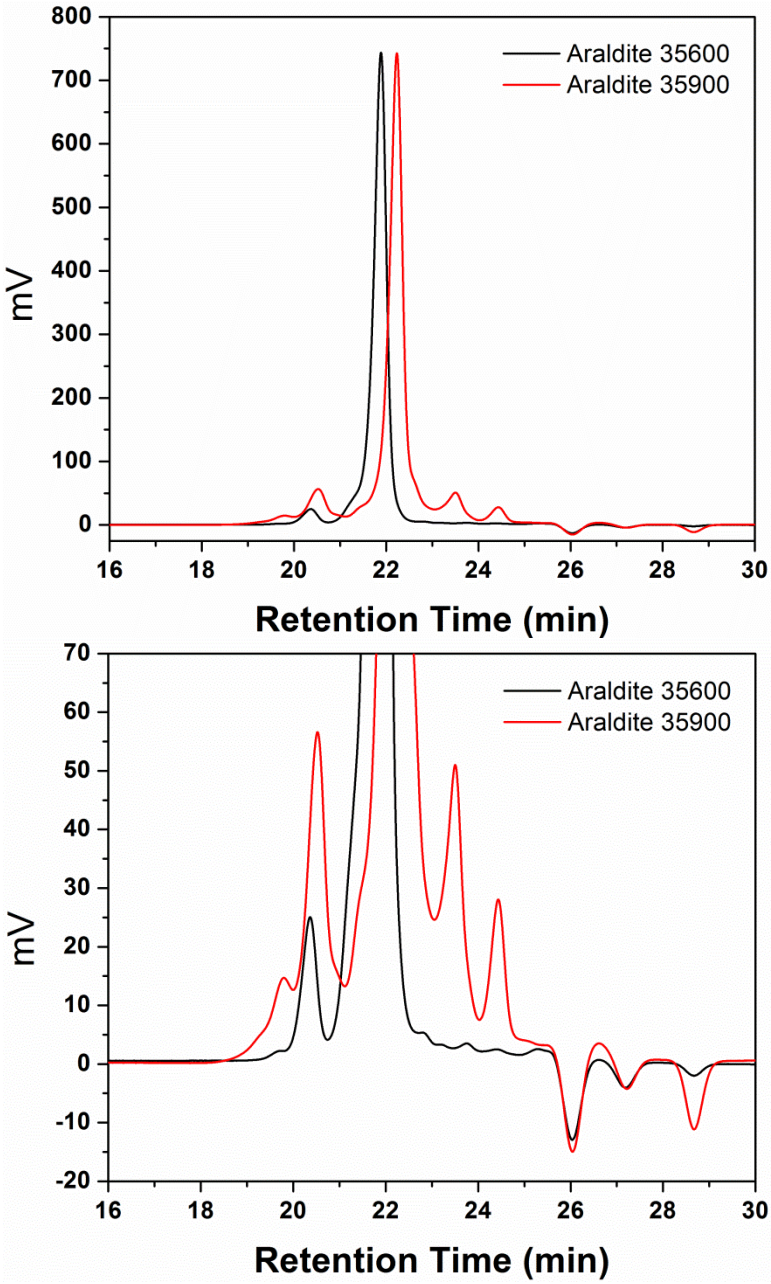


*Figure B1*. GPC traces for Araldite 35600 and Araldite 35900 monomers.

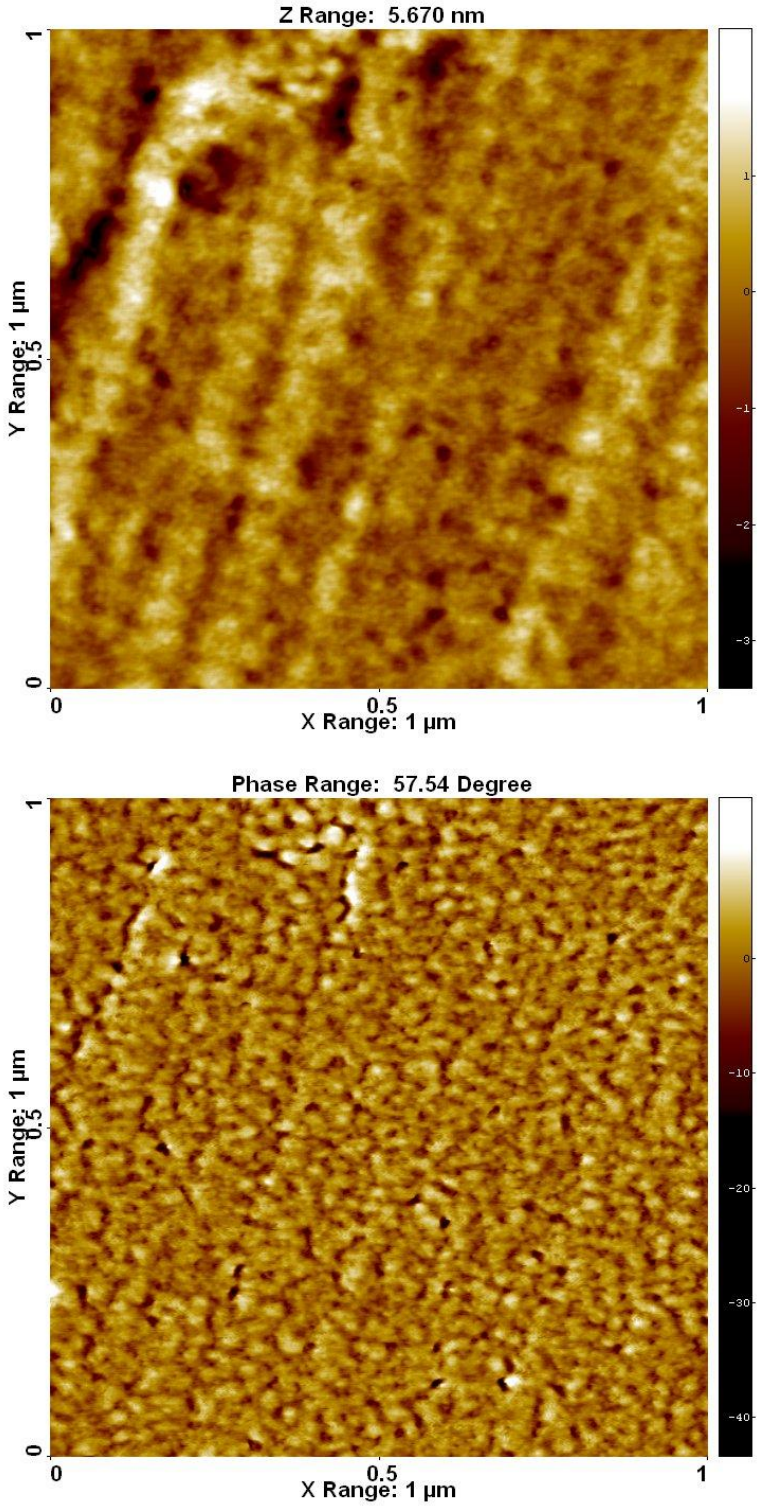


*Figure B2*. Atomic force microscopy images for a polybenzoxazine network derived from Araldite 35600; (top) height image, (bottom) phase image.

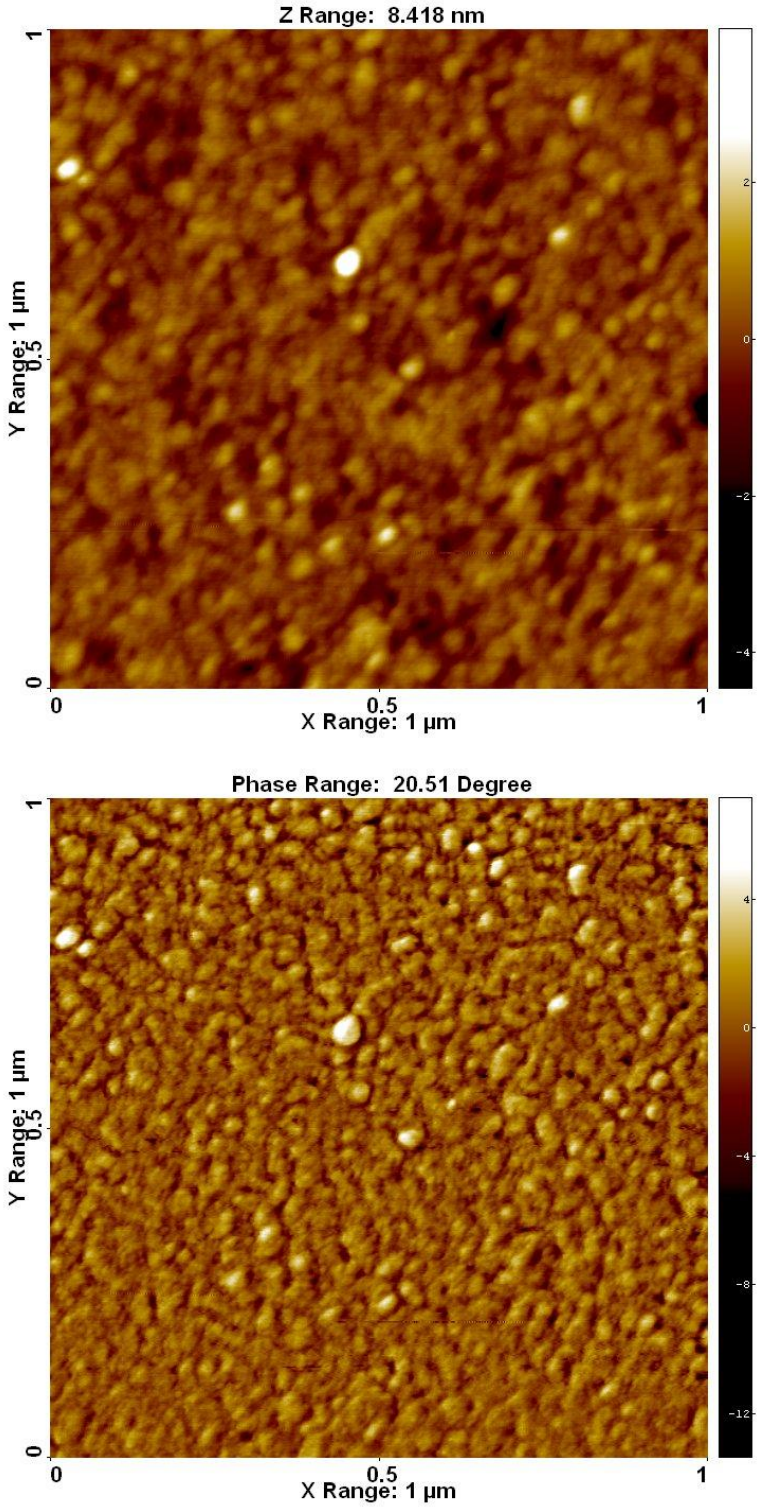


*Figure B3*. Atomic force microscopy images for a polybenzoxazine network derived from 5:5 Araldite 35600:BZ(10)BA; (top) height image, (bottom) phase image.

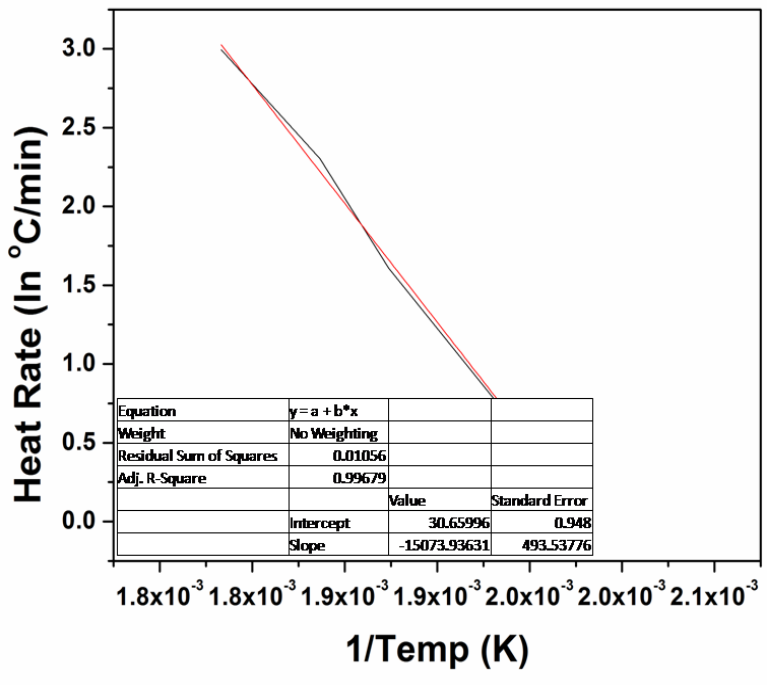


*Figure B4*. Plot of the heating rate Vs the peak exotherm temperature for BZ(10)BA to determine activation energy from the slope of the best fit line.

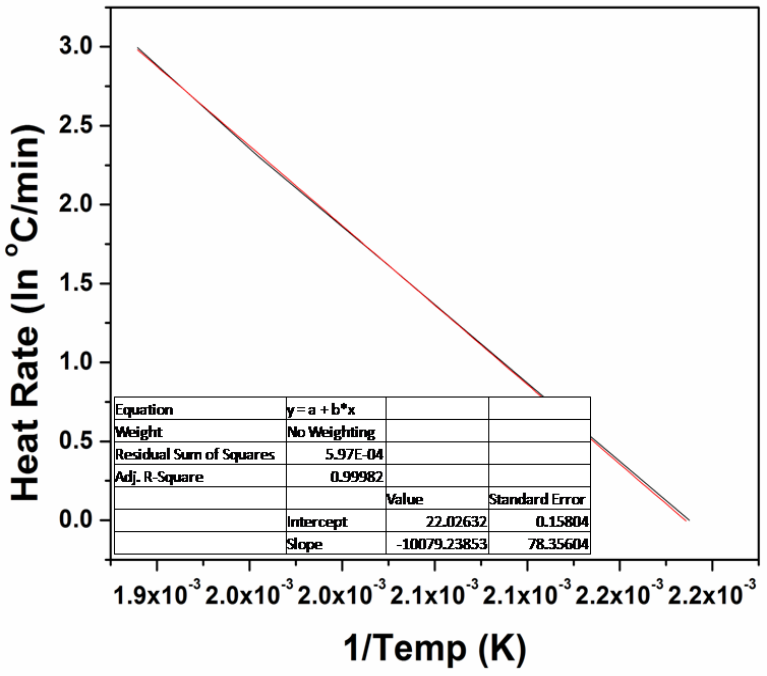


*Figure B5*. Plot of the heating rate Vs the peak exotherm temperature for Araldite 35600 to determine activation energy from the slope of the best fit line.

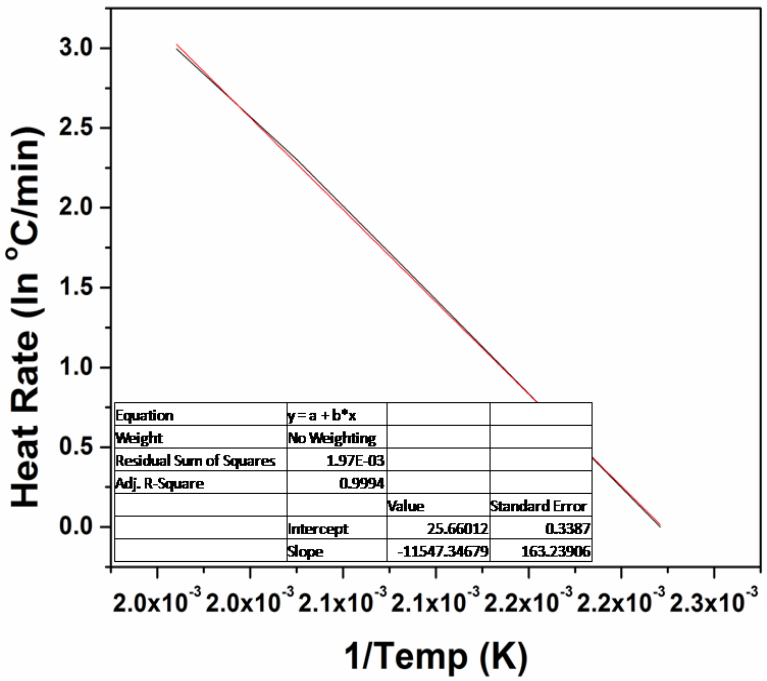


*Figure B6*. Plot of the heating rate Vs the peak exotherm temperature for Araldite 35900 to determine activation energy from the slope of the best fit line.

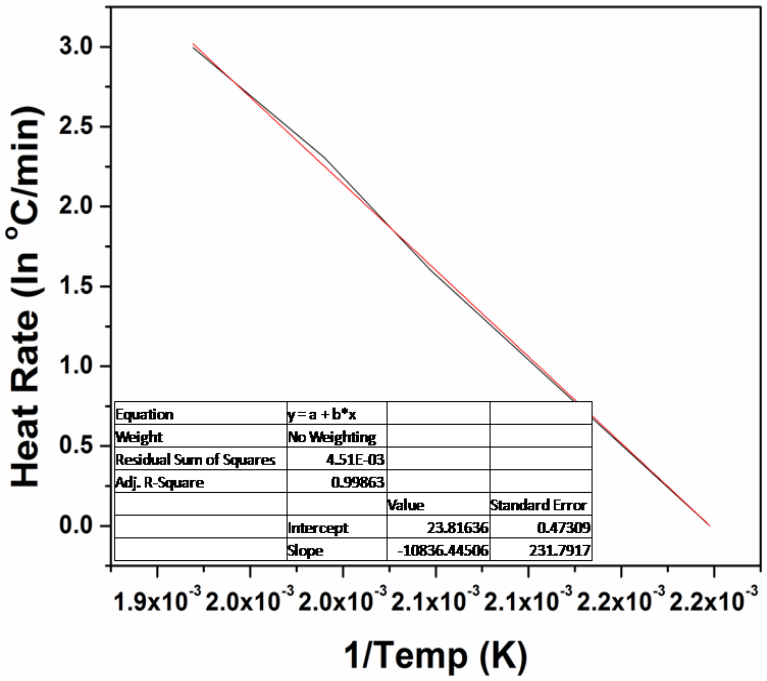


*Figure B7*. Plot of the heating rate Vs the peak exotherm temperature for a 4:6 copolymer of BZ(10)BA and Araldite 35600 to determine activation energy from the slope of the best fit line.

# APPENDIX C

# QUATERNARY AMMONIUM FUNCTIONAL POLYBENZOXAZINES FOR AEM APPLICATIONS

Table C1

*gATR-FTIR peak placements for the characteristic monomer and polymer functional groups.*

| Sample | C-H Benzoxazine Vib. ($cm^{-1}$) | C–O–C oxazine stretch ($cm^{-1}$) | tri-sub. Benzene ring ($cm^{-1}$) | tetra-sub. Benzene ring ($cm^{-1}$) |
|---|---|---|---|---|
| BZ(4)DMEDA | 928 | 1220 | 1498, 806 | 1480 |
| BZ(6)DMEDA | 923 | 1222 | 1498, 804 | 1480 |
| BZ(8)DMEDA | 912 | 1222 | 1497, 820 | 1480 |
| BZ(10)DMEDA | 928 | 1222 | 1498, 803 | 1480 |
| $BZ(PEG)_3DMEDA$ | 936 | 1225 | 1495, 814 | 1478 |

Table C2

*Ring opening exotherms for the neat monomer and oven cured polymer and the subsequent conversion.*

| Sample | Monomer exotherm (J/g) | Post cure exotherm (J/g) | Conversion (%) |
|---|---|---|---|
| BZ(4)DMEDA | 137.4 | 2.2 | 98.4 |
| BZ(6)DMEDA | 114.5 | 4.6 | 96 |
| BZ(8)DMEDA | 103.9 | 3.6 | 96.5 |
| BZ(10)DMEDA | 84.3 | 4.1 | 95.1 |
| $BZ(PEG)_3DMEDA$ | 102 | 2.9 | 97.2 |

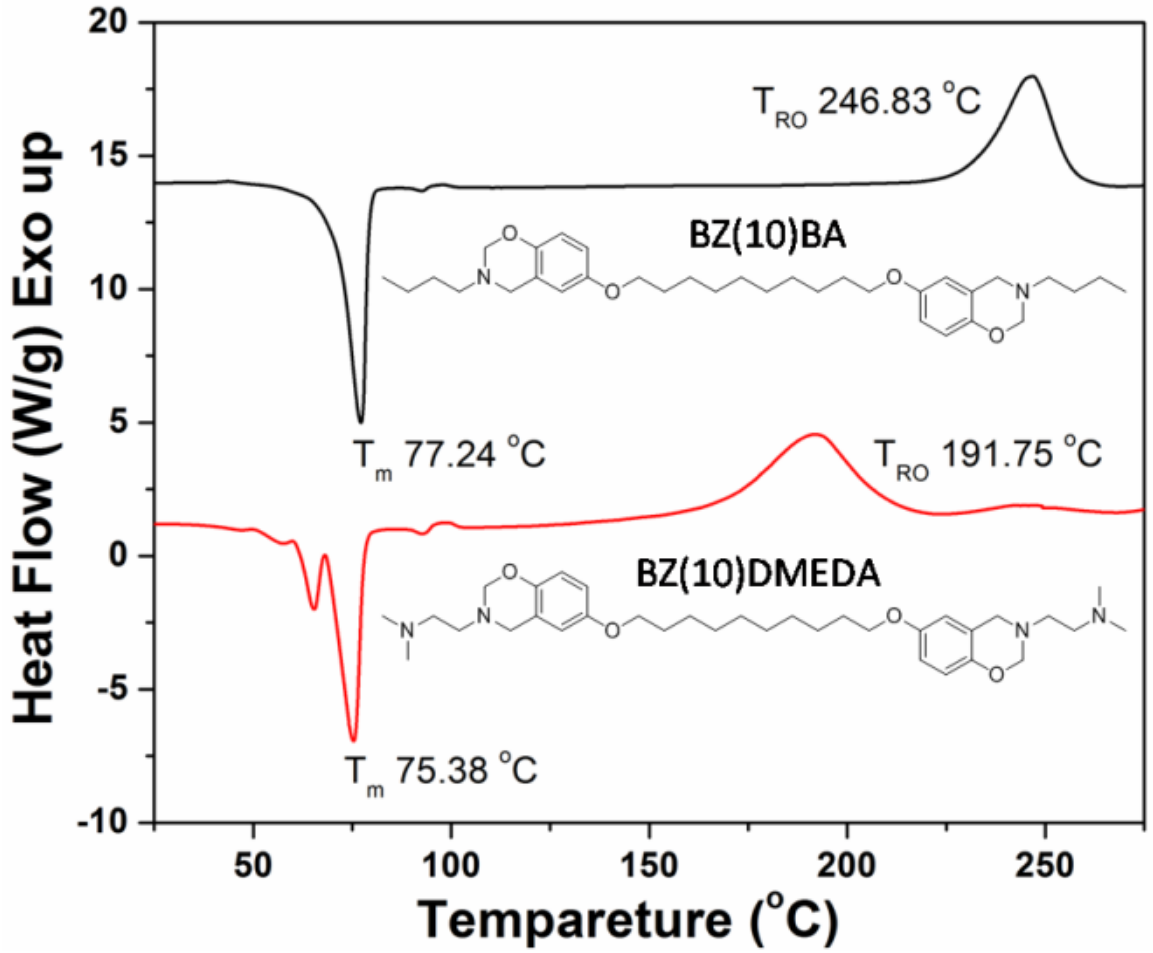


*Figure C1*. DSC Thermograms of BZ(10)BA and BZ(10)DMEDA at 5C/min.

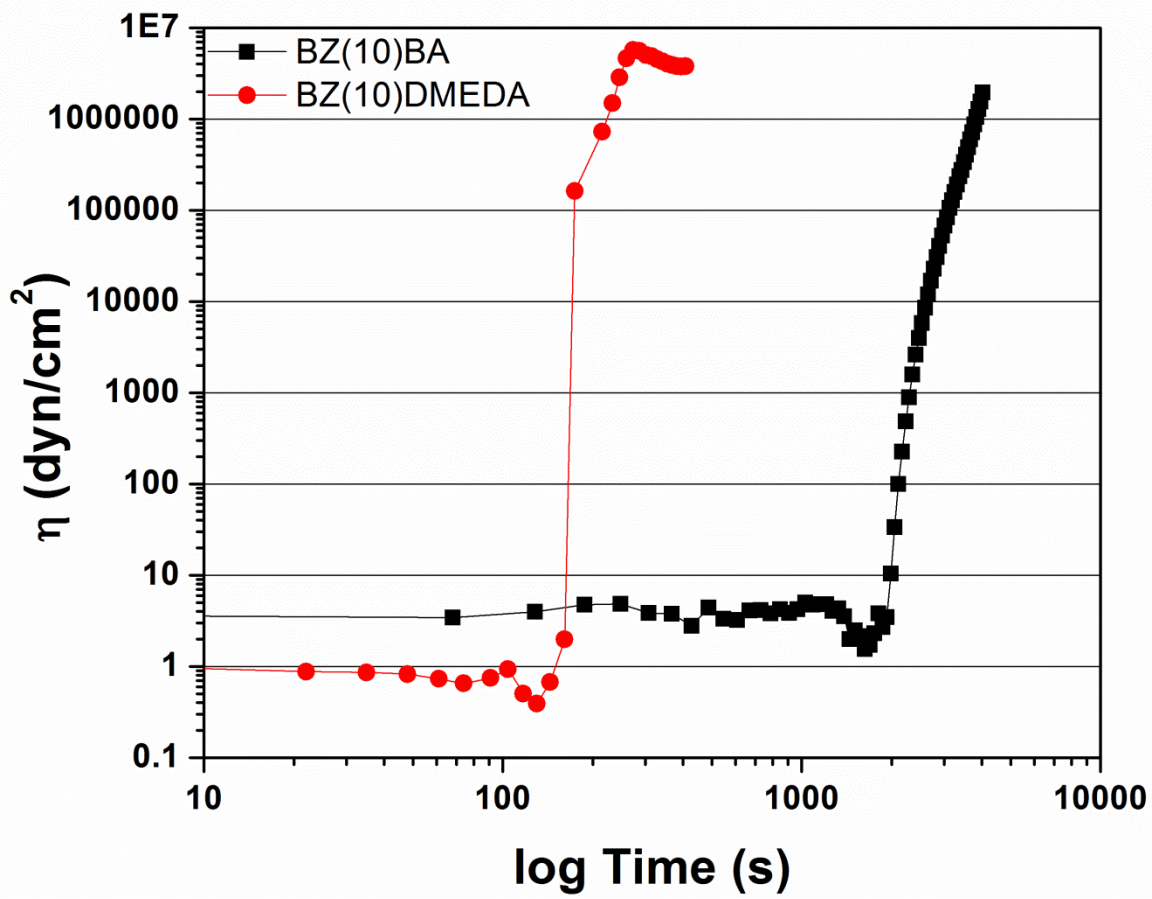


*Figure C2*. Viscosity Vs Time for monomers BZ(10)BA (black) and BZ(10)DMEDA (red) at an isothermal curing temperature of 180°C.

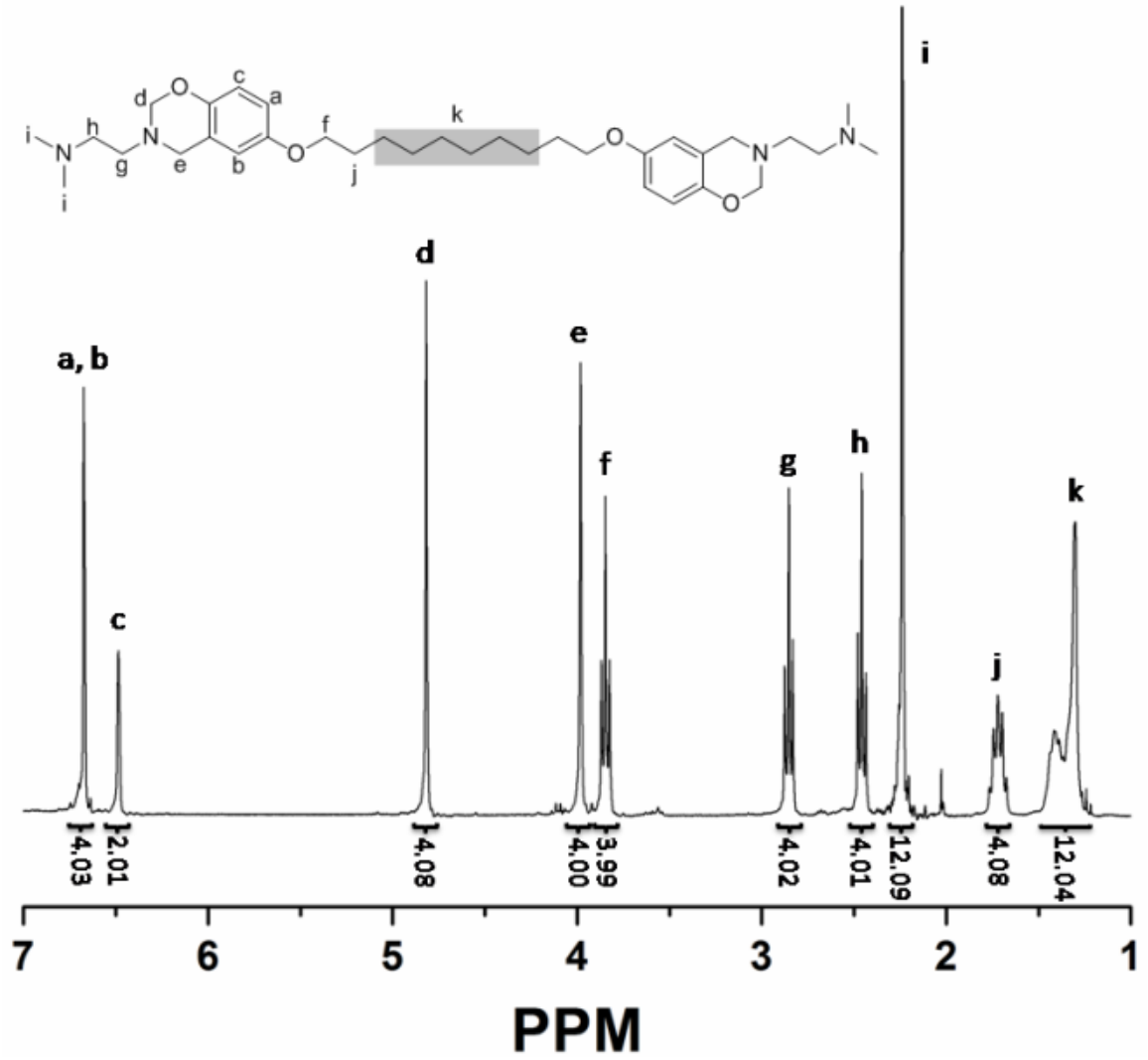


*Figure C3*. $^{1}$H NMR of BZ(10)DMEDA.

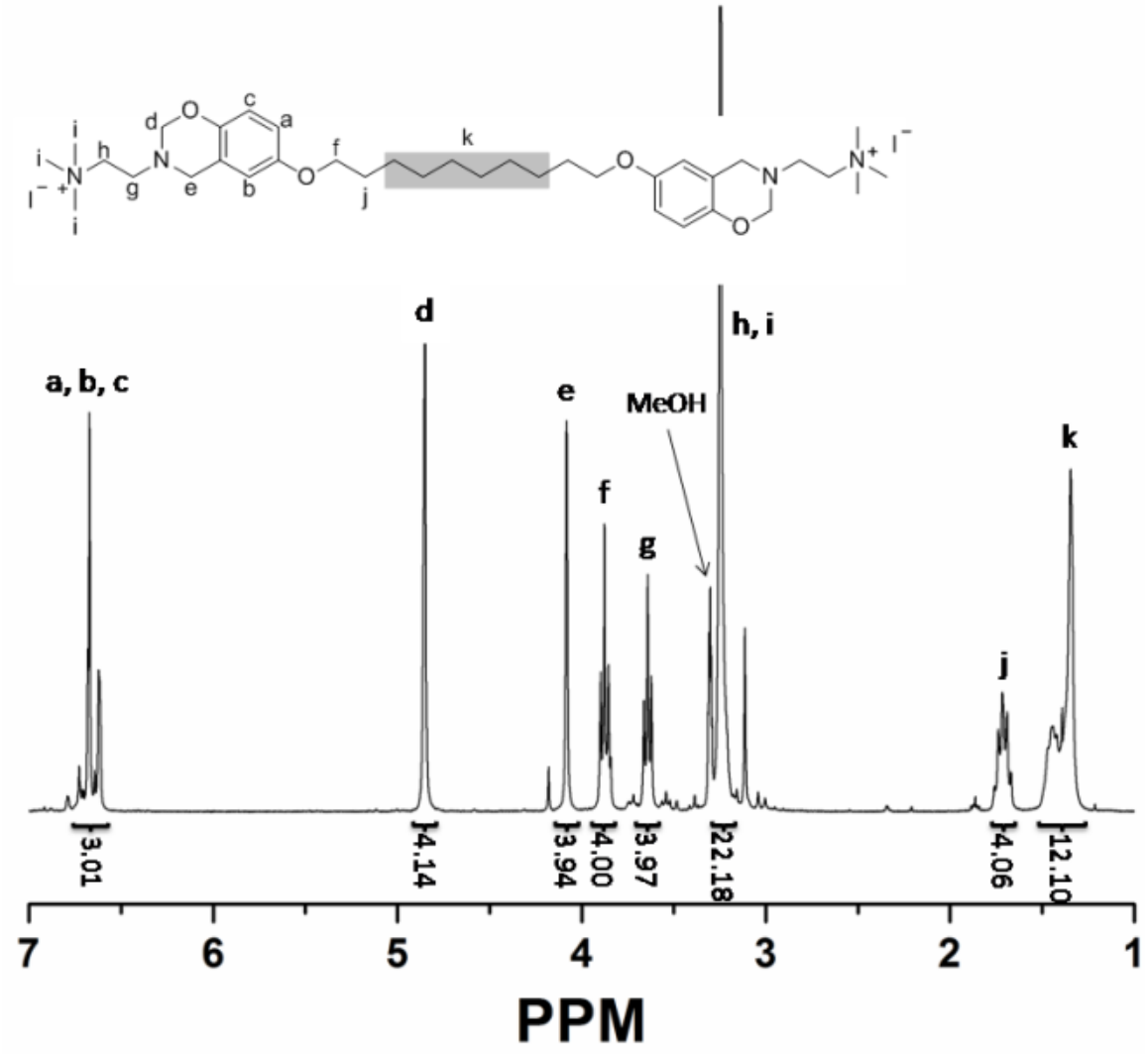


*Figure C4*. $^{1}$H NMR of quaternized BZ(10)DMEDA.

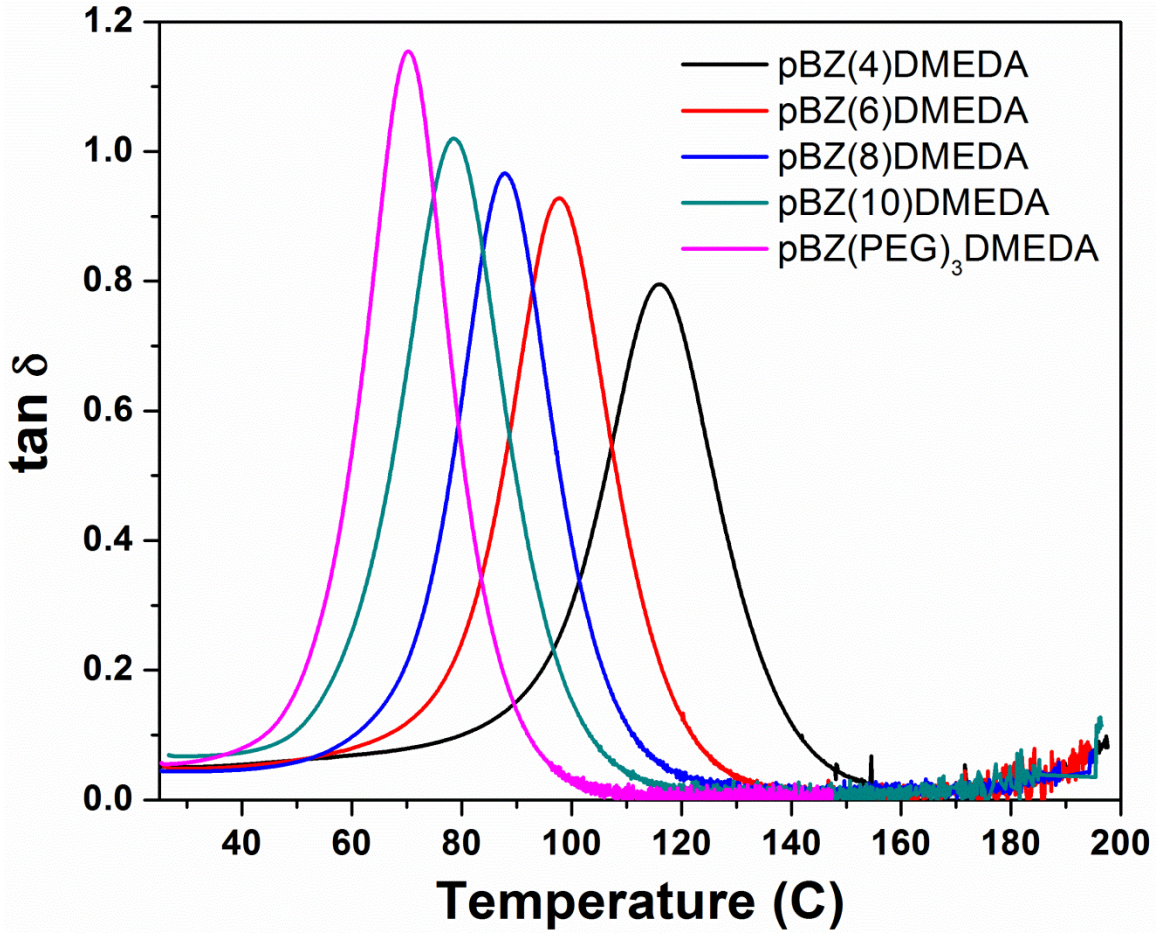


*Figure C5*. Representative DMA traces for BZ(R)DMEDA.